A SIMPLIFIED METHOD TO ESTIMATE NONLINEAR RESPONSE WITH AN APPROXIMATE LINEAR ANALYSIS FOR REINFORCED CONCRETE STURCTURES

By

Brandon Warden
JoAnn P. Browning
Adolfo Matamoros

A Report on Research Sponsored by

STRUCTURAL ENGINEERING AND MATERIALS LABORATORY
UNIVERSITY OF KANSAS

Structural Engineering and Engineering Materials
SM Report No. 83
April 2006

THE UNIVERSITY OF KANSAS CENTER FOR RESEARCH, INC.
2385 Irving Hill Road – Campus West, Lawrence, Kansas 66045

ACKNOWLEDGEMENTS

This report is based on a thesis submitted by Branden Warden in partial fulfillment of the requirements of the Masters of Science Degree in Civil Engineering. Funding for this research was provided by the Department of Civil, Environmental and Architectural Engineering Structural Engineering Materials Laboratories at the University of Kansas. Additional funding for the project was provided by the National Science Foundation under NSF Grant No. CMS – 0532084.

Table of Contents

LIST OF TABLES

LIST OF FIGURES

Abstract

A background on simple methods to estimate nonlinear response of multi-degree- of-freedom (MDOF) systems currently in use is presented as an introduction to development of a new method. A series of nonlinear analyses of 105 concrete building structures with varying number of stories and structural configurations evaluated to determine the maximum drift demands imposed by a suite of 10 ground motions. The ground motions were selected and scaled to represent a smooth displacement spectrum. The combination of damping and effective stiffness of equivalent single-degree-of-freedom (SDOF) linear systems that resulted in the most accurate estimates of the maximum nonlinear drift for high and moderate seismic demands is presented. The location and magnitude of the story drift ratio (SDR) for linear SDOF and nonlinear MDOF models of the building systems was also examined and compared. A primary conclusion of the study was that an equivalent SDOF system evaluated with an effective period of 2.3 and 2.0 times initial period in regions of high and moderate seismicity, respectively, and a 10% damped response spectrum produced the most consistent and accurate estimate of nonlinear building displacement for the frames and earthquakes considered. In general, the magnitude of SDR for the nonlinear MDOF systems were 1.5 time the SDR for linear SDOF systems.

Chapter 1: Introduction and Review of Literature

1.0. General

When designing earthquake resistant structures, an engineer must estimate the strength of the structure and the maximum lateral displacement that is likely to occur as a result of an earthquake. Because structural damage during earthquakes can be directly linked to lateral distortion (Algan 1982), engineers have devised and experimented with a wide assortment of methods to predict the displacement of building structures. "Displacement" in this text refers to the lateral movement of a structure relative to its initial position.

Most methods used to assess the inelastic response of a structure can be grouped into one of two categories: (1) force-based methods that examine the relationship between base shear forces and roof displacements based on the capacity of the structure; and (2) displacement-based methods that estimate displacement demand based on the inelastic or elastic displacement response spectrum. The driving force behind the creation of new methods is usually to determine a more accurate result or to create a simplified method for easier application by practicing engineers.

This chapter examines the various existing simplified methods for estimating lateral displacement caused by earthquakes. The methods are grouped according to the general type of procedure, and then on the progression of their development. This literature review is a preface to the development of an improved simple method to determine nonlinear displacement based on the response of a linear system.

1.1. Capacity Spectrum Method

The capacity spectrum method was developed to evaluate a structure by comparing the seismic capacity with the seismic demand in the context of earthquake spectra and nonlinear static analysis. A capacity curve is created by plotting the total lateral seismic shear applied to the structure at various increments of loading, versus the lateral displacement of a given portion of the building (generally the roof), under

that applied lateral force. The demand curve is generally represented as a modified form of an earthquake response spectrum. Many versions of the capacity spectrum method have been developed in the past and are described in the following six sections.

1.1.1. S.A. Freeman (1979)

The capacity spectrum method developed by S.A.Freeman (1979) is utilized as a "quick" procedure for evaluating the seismic vulnerability of buildings. This method employs the use of nonlinear static analysis to determine building capacity and an elastic response spectrum to represent the earthquake demand. Nonlinear static analysis is completed by subjecting a model of the building to a set of lateral loads applied at each story level. The loads are incrementally increased, and the corresponding displacement at a reference point, such as the roof, is determined. The capacity curve is then produced as the total lateral load at each increment versus the displacement at the reference node. The capacity and demand curves are superimposed, and the response of the structure is estimated at the intersection of the two curves as seen in Fig. 1.1. Damping is assumed to modify the elastic response spectrum to coincide with the effects of the nonlinear behavior of the structure.

1.1.2. ATC-40 (1996)

The capacity spectrum method adopted by ATC-40 (Applied Technology Council 1996) affixes some modifications to the approach proposed by Freeman. The ATC-40 method is based on idealistic hysteretic models for the structure, and spectra are modified based on various equivalent-damping ratios. To use the ATC-40 capacity spectrum method, the capacity curve (which relates base shear to roof displacements) and the demand response spectrum are converted into Acceleration-Displacement Response Spectra (ADRS) format. For this to be achieved, both curves are plotted as spectral acceleration vs. spectral displacement as shown in Fig 1.2. In Fig 1.2, the expected performance (performance point) is determined as the intersection of the capacity spectrum and the reduced seismic demand curve. ATC-

40 provides three different procedures to estimate the earthquake-induced deformation demands. Two of the methods are iterative and require direct calculations where as the third is an entirely graphical method.

Krawinkler (1995) noted two flaws associated with the ATC-40 capacity spectrum method. The first is that no physical principle justifies the existence of a stable relationship between the hysteretic energy dissipation and equivalent viscous damping. The second flaw is that the period associated with the intersection of the capacity curve with the highly-damped spectrum may have little to do with the dynamic response of the inelastic system.

1.1.3. Fajfar (1999)

Fajfar saw the need for a more direct approach to determine the seismic demand. Hoping to simplify the analysis associated with the capacity spectrum method and correct some flaws, Fajfar (1999) proposed the N2 method. The goal was to offer a method that might be acceptable for practical design and for development of future design guidelines. The N2 method is similar to the capacity spectrum method except that it employs an inelastic response spectrum. Fajfar followed five steps: (1) determine the base shear and roof displacement relationship by using a nonlinear static analysis, (2) transform the force-deformation relationship of the multi-degree of freedom (MDOF) system into that of an equivalent single degree of freedom (SDOF) system using a participation factor, (3) idealize the force-displacement relationship of an equivalent SDOF system into an elasto-plastic form, (4) determine the seismic demand (ductility demand) for the equivalent SDOF system, and (5) check the performance at the expected maximum displacement. This performance evaluation procedure, known as the N2 method, can be used to produce a direct deformation-based design by reversing the capacity spectrum method. For example, one can start with the target displacement and solve for the required structural period using either an assumed ductility or acceleration demand.

1.1.4. Chopra and Goel (1999)

Chopra and Goel (1999) found that the ATC-40 method greatly underestimated the deformation demands of systems for a wide range of periods when used for structures that have hysteretic behavior with stable, reasonably-full hysteresis loops. Similar to the N2 method, their proposal uses an inelastic design response spectrum as the demand curve in the capacity spectrum method. Unlike the ATC-40 methods, which do not always converge, the new procedure always gives a unique value of deformation, which also corresponds to the ATC-40 method when it converges.

1.1.5. Albanesi, Nuti, and Vanzi (2000)

A simplified capacity spectrum procedure to assess the seismic response of nonlinear structures was proposed by Albanesi et al. (2000). The impetus for reformulating the procedure was the belief that the capacity spectrum method, though conceptually simple, required time-consuming iterations. Albanesi et al. tested the assumption that nonlinear behavior can be linearized to obtain the structural response. To substantiate this theory, they compared the results from the capacity spectrum method (with the traditional equal energy - equal displacement assumption) with numerical step-by-step simulation either for a bilinear model or a degrading Takeda model (1970).

Albanesi et al. proposed that the capacity spectrum method can be made more explicit, and thus simplified, using the variable damping response spectra, in which the damping level increases as the ductility of the system increases. The conclusions are that, for elasto-plastic structures, response for a given elastic period lies on a single curve in the acceleration-displacement response plane. Therefore, the value of the acceleration reduction is known, given the displacement response. This procedure allows the engineer to obtain the structural displacement and acceleration demand on the basis of two diagrams: (1) the variable damping response spectrum and (2) the

variation of the equivalent period as a function of the ratio between yield acceleration and elastic acceleration.

To assess the accuracy of the procedure, studies were completed using SDOF elasto-plastic systems and degrading stiffness Takeda systems, as well as two existing frames. Albanesi et al. found that for both of the real structures, the procedure using the equivalent damping from the degrading Takeda model gives the best results.

1.1.6. Lin and Chang (2003)

The version of the capacity spectrum method proposed by Lin and Chang (2003) used the real acceleration response spectrum instead of the pseudo-acceleration response spectrum to determine the demand diagram. The method proposed by Lin and Chang was compared with six hysteretic systems that Chopra and Goel (1999) used in their study. Lin and Chang found their method to be more accurate than the model used in the ATC-40 method. The method was then evaluated using three equivalent viscous damping models to determine the equivalent viscous damping. For systems with damping ratios greater than 10% and periods longer than 0.15 seconds, the results more closely predict the actual displacements than does the ATC-40 method.

1.2. Equivalent Linear System Analysis

A simple method for estimating displacement response of inelastic systems is to analyze an equivalent linear system. This can be accomplished by either a substitute structure approach (the linear system contains modified properties to represent the ultimate response of a nonlinear system), or with response modification factors that are applied to linear analysis results to estimate nonlinear response. Several different methods that generally fit in one of these categories are described in this section.

1.2.1. Development of Substitute Structure Method

The substitute structure method evolved during several different studies of the nonlinear response of reinforced concrete systems. The primary contributors are described below.

Gulkan and Sozen (1974)

Gulkan and Sozen (1974) determined that the response of reinforced concrete structures to strong earthquake motion is influenced by two basic phenomena: a reduction in stiffness and an increase in energy-dissipation capacity. As displacements increase due to the earthquake motion, the stiffness of the structure decreases while the capacity to dissipate energy increases. The conclusion drawn from their study is that the maximum dynamic response of reinforced concrete structures, as represented by SDOF systems, can be approximated by linear response analysis using a reduced stiffness and a substitute damping that is related to the hysteretic properties of the concrete.

Shibata and Sozen (1976)

Shibata and Sozen (1976) proposed the substitute-structure method as a design tool that would allow engineers to estimate the minimum strengths required for each of the structural members, so as not to exceed the allowable displacements. The substitute structure method stems from the idea that an inelastic response can be represented by a linear response. Building on the work done by Gulkan and Sozen (1974) for SDOF systems, the substitute structure model can be used to determine the inelastic response of a MDOF system. The substitute structure method relates the flexural stiffness of a substitute frame element to the actual frame elements by a damage ratio:

$$(EI)_{si} = (EI)_{ai} / \mu_i \qquad (1\text{-}1)$$

where $(EI)_{si}$ and $(EI)_{ai}$ are the cross-sectional flexural stiffness for the substitute frame element i and the actual frame element respectively, and μ_i is the selected damage ratio for element i. The inelastic earthquake response of a SDOF system can

then be estimated by analyzing a linear model with reduced stiffness and a substitute-damping factor, which is related to the damage ratio as follows:

$$\beta_s = 0.2\left\{1-\left[\frac{1}{(\mu_i)^{0.5}}\right]\right\}+0.02 \qquad (1\text{-}2)$$

where β_s is the substitute-damping factor, and μ_i is damage ratio.

Shimazaki and Sozen (1984)

Shimazaki and Sozen (1984) found that the maximum nonlinear displacement is unaffected by the base shear strength for systems with a fundamental period greater than the characteristic period, T_g, the period defined on a response spectrum at which the nearly constant acceleration response region ends. An idealized linear acceleration response spectrum of a single degree of freedom oscillator may be described as:

$$S_a = PGA * g * A_a \quad \text{for } T < T_g \qquad (1\text{-}3)$$

$$S_a = PGA * g * A_a * (T_g/T) \quad \text{for } T > T_g \qquad (1\text{-}4)$$

where PGA is the peak ground acceleration normalized to the acceleration of gravity, g, and A_a is the amplification factor for the ground motion. Shimazaki found that a simple relationship between the maximum displacement response and the period of the linear system can be established using an idealized displacement response spectrum and a system with an effective period T_{eff}:

$$T_{eff} = \sqrt{2} * T_i \qquad (1\text{-}5)$$

where T_i is the first-mode period obtained using un-cracked sections. The nonlinear displacement response can then be calculated as the linear response of a system with period T_{eff}. This method provides a reasonable upper bound for displacement response of structures having periods that are longer than T_g.

1.2.2. Lepage (1997)

Lepage set out to find a procedure to simplify the estimate of nonlinear displacement response for structures that did not satisfy the work done by Shimazaki and Sozen (having $T_{eff} < T_g$). The proposal by Lepage uses a generalized displacement response spectrum that is linear with respect to building period. His equation is found to provide a reasonable upper bound to nonlinear displacements if a nominal amount of base shear strength is provided:

$$D_{max} = F_a * \alpha * g * T_g * \left(\frac{T}{(2\pi)^2} \right) \tag{1-6}$$

where D_{max} is the maximum displacement response, F_a is the acceleration amplification factor, g is the acceleration of gravity, α is the peak ground acceleration, T_g is the characteristic period for ground motion, and T is the period of vibration. This procedure gives good results when a threshold level of base shear strength is provided:

$$C_y = \alpha \ (1\text{-}TR) \geq \alpha/6 \tag{1-7}$$

where C_y represents the base shear strength coefficient, α is the peak ground acceleration, and TR is the period ratio:

$$TR = T_{eff} / T_g \tag{1-8}$$

1.2.3. Matamoros, Browning, and Luft (2003)

A procedure to roughly estimate building displacement based on the area of load-resisting elements was proposed by Matamoros, Browning, and Luft (2003). The work establishes an approximate relationship between the maximum displacement response of a system and the period (as represented by the ratio of the total weight to the total area of vertical elements) of the linear system, using an idealized displacement-response spectrum.

Using element proportions and generalized mass distributions, the drift demand of a structure was related to a "structural index" (SI):

$$SI = 100 * \left(\frac{A_{ce} + A_{wt}}{A_{ft}} \right) \tag{1-9}$$

where: A_{ce} = the effective cross-sectional area of columns at the base of the building,

$A_{ce} = \sum A_{col} / 2$

A_{col} is the total cross-sectional area of columns at the base

A_{wt} = the cross-sectional area of walls at the base of the building, and

$A_{wt} = \sum A_{cw} + \sum A_{mw} / 10$

A_{cw} = the total area of reinforced concrete walls at base of building.

A_{mw} is the total area of masonry filler walls at base of building, assuming the walls are continuous above the base

A_{ft} = the total floor area for all floors of the structure.

Based on the evaluation of shaking table tests and actual building responses, a rough estimate of mean drift ratio (MDR, the ratio of maximum lateral displacement to total building height) became:

$$MDR \cong \frac{PGA * g}{100 * SI} * \left(\frac{1}{N_{stories} * H} \right) \qquad \text{if } N_{stories} < N_{g\ limit} \tag{1-10}$$

$$MDR \cong \frac{PGA * g}{100 * SI} * \left(\frac{1}{N_{stories} * H} \right) * \left(\frac{N_{g\ limit}}{N_{stories}} \right) \qquad \text{if } N_{stories} > N_{g\ limit} \tag{1-11}$$

where PGA is the peak ground acceleration normalized to the acceleration of gravity, g, $N_{stories}$ is the number of stories, H is the average story height, and $N_{g\ limit}$ is the limit of the number of stories above which the displacement must be reduced. The story limit is defined as the characteristic period divided by 0.1, which relates to a six-story building, on firm soil. A correction factor CF_{wall} is defined for structures having walls with height-to-length ratios (H_w/l_w) exceeding 5:

$$CF_{wall} \cong \left(\frac{H_w}{15 l_w} \right)^2, \qquad \frac{H_w}{l_w} \geq 5 \tag{1-12}$$

Matamoros, et al. concluded that this method is best used to evaluate a large database of buildings or to determine if a more detailed analysis is needed.

1.2.4. Iwan and Gates (1979)

The importance of creating a generally accepted model for stiffness-degrading hysteretic behavior was examined by Iwan and Gates (1979). This study presented the results of an analysis of SDOF systems using six hysteretic models subjected to twelve earthquakes. The findings of Iwan and Gates verify that both the optimum effective period and damping are monotonically increasing functions of the ductility ratio. This follows that as a system degrades in stiffness and increases in total displacement, the increase in energy dissipation helps to limit the maximum total displacement. Their conclusion also demonstrates that the overall stiffness is strongly influenced by smaller amplitude oscillations, which then comprise a large portion of the overall response. Iwan and Gates found that knowing the precise details of the load displacement behavior of a structure may not be necessary in order to make a reasonably accurate estimate of its response. The conclusion drawn by Iwan and Gates is that the primary effect of material deterioration or stiffness degradation is to increase the effective period of the system. Deterioration and stiffness degradation appear to have much less effect on the effective damping of the system.

Iwan (1980)

In a subsequent study Iwan derived the empirical equations (1-16) and (1-17) to estimate the period shift and equivalent damping ratio:

$$(T_e/T_o) = 1+0.121(\mu-1)^{0.939} \quad (1\text{-}16)$$

$$\zeta_e = \zeta_o+0.0587(\mu-1)^{0.371} \quad (1\text{-}17)$$

where T_e/T_o represents a period shift ratio, ζ_e is the effective viscous damping, ζ_o is the initial damping ratio of system, and μ is the ductility ratio defined as the maximum amplitude of the response divided by the generalized yield displacement.

1.2.5. Newmark and Hall (1982)

Newmark and Hall devised a unique method to estimate the maximum deformation demand of a structure. Unlike previous studies, this method was derived using elasto-plastic behavior and a displacement modification factor. Using this method, the maximum response of the inelastic SDOF system is estimated as a product of the maximum deformation of a linear elastic system (with the same lateral stiffness and same damping coefficient as that of the inelastic system) and a displacement modification factor. The displacement modification factor, C, varies depending on the spectral region in which the initial period of vibration of the SDOF system is located:

$$C = \mu, \quad T<T_a=1/33 \text{ s}$$

$$C = \mu / (2\mu - 1)^{\beta}, \quad T_a<T<T_b=0.125 \text{ s}$$

$$C = \mu / (2\mu - 1)^{0.5}, \quad T_b<T<T_{c'}$$

(1-18)

$$C = T_c/ T, \quad T_{c'}<T<T_c$$

$$C = 1, \quad T > T_c$$

where, T_c is the corner period, μ is the ductility ratio, and T is the initial period of vibration. The remaining variables are defined as:

$$\beta=\frac{\log\left(\frac{T}{T_a}\right)}{2*\log\left(\frac{T_b}{T_a}\right)}$$

$$T_{c'} = T_c (2\mu - 1)^{0.5}/\mu .$$

The Newmark and Hall method is an early attempt to consider the affects of site conditions (in terms of the site response spectrum) on the response of the building.

1.2.6. FEMA 273 Coefficient Method (1997)

Another method that estimates nonlinear displacement using numerous coefficients to modify elastic SDOF response calculations is proposed by FEMA

(FEMA 273, 1997). According to FEMA-273, the target displacement δ_t can be determined by:

$$\delta_t = C_0 C_1 C_2 C_3 S_a T_e^2 / 4\pi^2 g \qquad (1\text{-}19)$$

In equation (1-19), T_e is the effective fundamental period of the building in the direction under consideration, C_0 accounts for the difference between the roof displacement of an MDOF building and the displacement of the equivalent SDOF system; the factor C_1 takes into account the observed difference in peak displacement response amplitude for nonlinear response as compared with linear response, as observed for buildings with rather short initial vibration periods. The modification factor, C_2, represents the effect of a pinched hysteretic shape, stiffness degradation, and strength deterioration on maximum displacement response. The fourth factor, C_3, takes into account the increase in displacements due to P-delta effects. The response spectrum acceleration (normalized to gravity) is represented by S_a, at the effective fundamental period and damping ratio of the building in the direction under consideration.

The advantage of the FEMA-273 method is that it is not an iterative method, but instead is a less numerically intensive model that requires various correction factors to adjust the linear displacement to represent an equivalent nonlinear displacement. One disadvantage, however, is that it may not account for P-delta effects accurately or the effects of soft soils (FEMA 440, 2005).

1.2.7. Iwan and Guyader (2002)

Modifying previous equations proposed by Iwan and Gates (1979), Iwan and Guyader (2002) developed new expressions to estimate the maximum deformation demands in inelastic SDOF systems. The new equations were based on the ductility ratio (μ) to estimate the period shift and equivalent damping ratio:

For $\mu < 4.0$

$$(T_{eq}/T) = 1 + 0.111(\mu\text{-}1)^2 - 0.0167(\mu\text{-}1)^3$$

$$\xi_{eq} = \xi_0 + 0.0319(\mu\text{-}1)^2 - 0.00666(\mu\text{-}1)^3$$

For $\mu > 4.0$ (1-20)

$$(T_{eq}/T) = 1.279 + 0.0892(\mu\text{-}1)$$

$$\xi_{eq} = \xi_0 + 0.106 - 0.00116(\mu\text{-}1)$$

Similar to Iwan (1980) T_e/T_o represents a period shift ratio, ξ_e is the effective viscous damping, ξ_o is the initial damping ratio of system, and μ is the ductility ratio defined as the maximum amplitude of the response divided by the generalized yield displacement.

The new method was developed to account for the effects of higher-level ductilities on the period and damping. The new method proved most successful for structures with periods longer than 0.5 seconds.

1.2.8. Ruiz-Garcia and Miranda (2003)

Noting that the Newmark and Hall (1982) method overcomplicated the displacement modification factor, Ruiz-Garcia and Miranda proposed a simplified displacement modification factor. The conclusions from the study established that the earthquake magnitude, distance to source, and average shear wave velocities do not have a significant affect on the ratio of maximum inelastic displacement demands to maximum elastic displacement demands. The method institutes a single expression for the displacement modification factor, C_R, instead of five different expressions. Their expression is given by:

$$C_R = 1 + \left[\frac{1}{a\left(\frac{T}{T_s}\right)^b} - \frac{1}{c} \right] \qquad (1\text{-}21)$$

where, T, is the vibration period of system; T_s is the characteristic period of the site; and *a*, *b*, and *c* are site dependent constants. In the method proposed by Ruiz-Garcia and Miranda, the corner period increases as the displacement ductility ratio increases.

1.3. Direct Displacement-Based Method

Direct displacement-based design is a procedure proposed to determine a more "rational" level of seismic design strength for the plastic hinge locations of structures than the level provided by current force-based procedures. This is accomplished by considering the specific force-deformation relationship of a structure when determining the periodicity of response to a particular ground motion. Normal capacity design procedures that emphasize avoiding undesirable hinge locations and shear failures must still be implemented. The development of the direct displacement based design method is described below.

1.3.1. Kowalsky (1994)

Kowalsky proposed determining the period of a system by implementing the secant stiffness, K_e, in an equivalent linear method. The period of vibration of the equivalent system, T_{eq}, is calculated at the maximum deformation using the equivalent stiffness as:

$$T_{eq} = T_0\sqrt{\frac{\mu}{1-\alpha+\alpha\mu}} \tag{1-22}$$

where α is equal to the post-yield to initial stiffness ratio T_0 is the initial period of the system, and μ is the ductility ratio.

The proposed direct-stiffness method uses a set of displacement response spectra in lieu of the traditional acceleration response spectra used in conventional design guides. Kowalsky also proposes a method to relate the equivalent viscous damping, ξ_{eq}, to the ductility ratio, μ. Kowalsky defines the equivalent damping ratio as the sum of the initial ductility ratio, ξ_0, and an equivalent hysterectic damping as follows:

$$\xi_{eq} = \xi_0 + \left(\frac{1}{\pi}\right)\left[1 - \left(\frac{1-\alpha}{\sqrt{\mu}}\right) - \alpha\sqrt{\mu}\right]. \quad (1\text{-}23)$$

1.3.2. Priestley and Kowalsky (2000)

A direct displacement approach was proposed by Priestley and Kowalsky (2000) to determine the required base shear strength for concrete buildings in order to limit displacement. Priestly and Kowalsky state that the force-based design approach, as used by representative building codes (UBC 1997, IBC 2000), makes two assumptions that lead to an increase in the error of its results: (1) the initial stiffness of a structure determines its displacement response, and (2) that a ductility capacity can be assigned to a structural system regardless of its geometry, member strength, and foundation conditions. Priestley and Kowalsky also state that displacement-based design is fundamentally more direct than force-based design because yield curvature is dependent only on yield strain and section depth. Consequently, strength and stiffness are linearly related. Priestley and Kowalsky propose a set of relationships that correlate stiffness to strength based on the geometry of the member. The procedure that Priestley and Kowalsky propose also considers the stiffness after yielding has occurred, unlike force-based methods. An important conclusion from the study is that the required base-shear strength is proportional to the square of seismic intensity (peak ground acceleration), whereas force-based design relates base-shear strength linearly to seismic intensity.

1.4. Comparisons of Simplified Methods

A number of studies have been performed to compare results of simplified analysis techniques. A discussion of these studies is provided in this section to complete the background information on simplified nonlinear analysis methods.

1.4.1. Iwan and Gates (1979)

Iwan and Gates (1979) saw the need for a single, accurate, analytical model that could be used for a nonlinear system. Although nonlinear problems can currently be solved numerically using digital computation techniques, effective linear models have the advantage of requiring less engineering hours to develop as well as being easier to understand and use. Iwan and Gates felt that the accuracy of these linear methods should be examined due to the popularity and frequency of their use. They considered a broad range of approximate methods including those based on harmonic response behavior as well as those based on stationary random response behavior. Iwan and Gates evaluated the following six different linearization methods based on harmonic response:

(1) Harmonic Equivalent Linearization (HEL), (Caughey, 1960)

(2) Resonant Amplitude Matching (RAM), (Jennings, 1968)

(3) Dynamic Mass (DM), (Jennings, 1968)

(4) Constant Critical Damping (CCD), (Jennings, 1968)

(5) Geometric Stiffness (GS), (Rosenblueth and Herrera, 1964) and

(6) Geometric Energy (GE), (Jacobsen 1960).

In the HEL method, the difference between the nonlinear equation of motion and the linear equation is minimized with respect to the period of oscillation. The RAM method ignores the shift in period of the hysteretic system. In the DM method, the stiffness of the linearized system is taken to be the nominal stiffness of the hysteretic system. The mass of the linearized system is varied, so that the resonant period of the linearized system agrees with the observed hysteretic system. The CCD method agrees with the HEL method in how the effective period is defined, and the damping is defined as per the RAM method. The CCD method differs from the RAM and HEL method due to the assumption that the critical damping factor is the same for both the hysteretic and linear systems. Thus, the effective viscous damping will be different than that of the RAM method. In the GS method, the stiffness of the

linearized system is determined directly from the geometry of the hysteresis loops rather than from a resonant period-matching condition. This is achieved by using the secant stiffness rather than the effective linear system stiffness. The GE method uses the geometry of both the skeleton curve (relationship between bending moment and curvature) and the first hysteresis loop to calculate the effective viscous damping.

Iwan and Gates (1979) also evaluated the three following methods based on random response:

(1) Stationary Random Equivalent Linearization (SREL), (Caughey, 1960)

(2) Average Period and Damping (ADP), (Newmark and Rosenblueth, 1971)

(3) Average Stiffness and Energy (ASE) (Gates, 1977).

The SREL method is similar to the HEL method except that minimization of the equation difference must be interpreted in a statistical sense. Furthermore, the response is assumed to be a narrow band process. The APD method is used for determining the earthquake response of any nonlinear SDOF system with a generalized force-displacement relationship that is symmetric about the origin and does not deteriorate. The ASE method is quite similar to the ADP method except that the parameters employed are the degrading stiffness and energy dissipation rather than the period of the structure and viscous damping.

Iwan and Gates found that all the approximate methods considered, except the RAM method, indicate that the effective period lengthens with increasing ductility. They also found that the methods based on harmonic response considerably over-estimate the lengthened period of the structure, because these methods do not take into account responses lower than the peak amplitude. The averaging methods do account in some manner for the lower amplitudes and, therefore, give realistic estimates of the effective period.

1.4.2. Miranda and Ruiz-Garcia (2002)

Miranda and Ruiz-Garcia (2002) added to the work of Iwan and Gates (1979) by also examining the results for short period structures and determining whether the

approximate method tended to overestimate or underestimate the displacements. Miranda was primarily interested in discovering which approximate methods produce better results for specific periods of vibration, or at least for specific spectral regions. Another objective of the study was to discover which methods will provide better results for specific levels of inelastic behavior that will be expected to occur in the structure.

Miranda and Ruiz-Garcia (2002) evaluated six approximate methods to estimate the maximum inelastic displacement demand of SDOF systems by using the maximum displacement demands of elastic SDOF systems. Miranda and Ruiz-Garcia chose to evaluate four methods that are based on equivalent linearization, and two methods in which the maximum inelastic displacement is estimated as the product of the maximum deformation of a linear elastic system and a modification factor. For consistency, these evaluations employ the same lateral stiffness and the same damping coefficient as those of the inelastic system for which the maximum displacement is being estimated. Miranda evaluated the following six methods:

(1) a harmonic loading method, (Rosenblueth and Herrera, 1964)

(2) a method developed using the Takeda (1970) hysteretic model, (Gulkan and Sozen, 1974)

(3) a period shift method, (Iwan, 1980)

(4) a displacement-based method, which uses the secant stiffness model, (Kowalsky, 1994)

(5) a method in which the displacement modification factor varies depending on the spectral region, (Newmark and Hall, 1982) and

(6) a method which has a modified displacement-modification factor as well (Miranda, 2000).

Miranda confirmed several conclusions based on this comparative study. First, the Rosenblueth and Herrera method underestimates the maximum inelastic displacement for all three types of hysteretic models (the elasto-plastic model, the modified Clough (1996) stiffness-degrading model, and the Takeda hysteretic model).

Second, the methods proposed by Gulkan and Sozen, Kowalsky, and Iwan all provide better estimates of displacements than the Rosenblueth and Herrera model for periods longer than 0.4 seconds. Finally, the Newmark and Hall method and the Miranda method fare equally well for periods longer than 0.5 seconds. The advantage associated with the methods proposed by Newmark & Hall and Miranda is the considerable ease of use in practical situations, because elastic analysis results can be used directly.

1.4.3. Ramirez, Constantinou, Gomez, Whitttaker, Chrysostomou (2002)

Ramirez et al. (2002) extended the work done by Tsopelas et al. (1997) to include non-linear viscous and hysteretic damping systems. The study was to determine the accuracy of the simplified analysis methods of the 2000 National Earthquake Hazard Reduction Program (NEHRP) Provisions. Ramirez et al. used twenty scaled-horizontal components of ten earthquakes to test this method (excluding earthquakes recorded in near field and soft soil types).

Ramirez et al. considered two types of structural behavior: smooth perfect bilinear hysteretic behavior (which did not take into account deterioration of strength, deterioration of stiffness, or P-Delta effects) and bilinear elastic behavior (which also did not account for deterioration of strength or stiffness.) Three types of systems were considered: linear viscous damping systems, nonlinear viscous damping systems, and nonlinear systems with smooth elasto-platic behavior.

Ramirez et al. found that although the 2000 NEHRP Provisions simplify the method of analysis, they do predict the accelerations and displacements of the structure reasonably well, though sometimes over-conservatively. However, the simplified methods under-predict the peak velocities of structures with effective periods exceeding 1.5 seconds and over-predict the peak velocities for structures with effective periods less than 1.0 second. Ramirez et al. recommend the use of a correction factor for velocity response estimates.

1.4.4. Lin, Chang, and Wang (2004)

Lin, Chang, and Wang (2004) tested the accuracy of both the coefficient method (FEMA-273, 1997) and the capacity spectrum method (ATC-40, 1996) by conducting pseudo-dynamic tests, cyclic loading tests, and tests on three reinforced concrete (RC) columns. The pseudo-dynamic test was used as the control in the study, with the maximum displacements at the roof used as a reference to compare the results of the other methods. The results of the tests show that the target displacements estimated using the FEMA-273 method, on average, over-estimate the peak deformations by 28%, while the ATC-40 capacity spectrum method underestimates the deformations by 20%. One reason cited for such differences was from an over-estimation of the hysteretic damping ratio in the capacity spectrum method. Thus, the study suggests using the Kowalsky (2000) hysteretic damping model, which performs significantly better in estimating the displacements. This method on average produces an error between the experimental and estimated displacements of -11% when ignoring the effects of stiffness degradation, and an error of –6.6% when the inelastic design spectrum is used instead of the elastic design spectrum.

1.4.5. Matamoros, Browning, and Luft (2003)

The focus of this work was to compare the results obtained from the floor-area method with the equivalent-period method (derived by Shimazaki and Sozen (1984) and later modified by Lepage (1997)), as well as with the target-displacement method (also know as the coefficient method or FEMA 273 (1997)). The coefficient method, as earlier noted, requires knowledge of how the structure is detailed in order to estimate the displacements, whereas the floor-area method and the equivalent-period method do not require such knowledge. The floor-area and equivalent-period methods are more conservative than the coefficient method, having a "safety index" of 0.8, 0.7, and 0.2 respectively. The safety index is defined as:

$$\text{Safety Index} = \text{std}\left[\frac{\Delta\text{meas.}}{\Delta\text{calc.}} - 1\right] * 100 \qquad (1\text{-}24)$$

where std is the standard deviation, Δmeas. is the measured drift, and Δcalc. is the calculated drift. Matamoros et al. conclude that the simplified methods do an adequate job of estimating the upper bound of the non-linear displacements. The study determined that the proposed simplified methods will work quite well in assessing the general expected performance of buildings in seismic zones and can determine if a more detailed analysis is needed.

1.4.6. Akkar and Miranda (2005)

Akkar and Miranda compared the results of five approximate methods. In a previous study, an evaluation of the Iwan (1980) equivalent period method, the Kowalsky (1994) secant stiffness method, and the Newmark and Hall (1982) displacement modification factor method was completed. These methods were re-examined with the addition of improved methods by Iwan and Guyader (2002) and Ruiz-Garcia and Miranda (2003).

The various methods were evaluated using 216 earthquake ground motions recorded in firm site conditions for 12 earthquakes. For periods longer than 1.0 second, all methods produce relatively accurate results with deviations of less than 15%. When the Takeda model is used, overestimations of 20% to 30% are found using the Kowalsky equivalent linear method. For short period ranges, all methods can lead to relatively large errors in the estimation of inelastic deformation demands; however, the Ruiz-Garcia and Miranda method lead to mean errors closer to one. The mean error is defined as:

$$E_{T,R} = \left[\frac{\Delta ap}{\Delta ex}\right]_{T,R} \qquad (1\text{-}25)$$

where $E_{T,R}$ is the ratio of approximate (Δap) to exact (Δex) maximum inelastic deformation at a given period of vibration, T, and for a given lateral strength ratio, R (ratio of the strength required to maintain the elastic system to the lateral yield

strength). The errors produced by any of these methods can be relatively large, particularly for lateral strength ratios larger than four.

1.4.7. FEMA 440 (2005)

FEMA 440 provides a brief overview of the capacity spectrum method, direct coefficient method, and displacement based approaches in addition to a relative comparison. Two advantages attributed to the capacity spectrum method are that the intersection of "capacity " and "demand" curves implies a sense of dynamic equilibrium, and that the influence of strength and stiffness on peak displacement is represented by the graphic nature of the procedure. As currently presented in ATC-40 (1996), the procedure equates viscous damping to hysteretic damping, providing a link to the actual characteristics of the structure. The interpretation of the graphic solution can provide insight for an effective retrofit strategy. The disadvantage of the capacity spectrum method is the awkward iterative procedure that may lead to no solution or multiple solutions. In addition, equating hysteretic energy dissipation to viscous damping energy dissipation provides a specious sense that the procedure is "theoretically" based on fundamental physical properties.

The principal advantage of the displacement coefficient method is that it is direct and simple to apply. This method is also based on the idea that a strength reduction factor is a function of the displacement ductility ratio and the period of vibration, which have been studied and generally accepted in the technical community for some time.

1.5. Summary of Previous Work

Over the past three decades engineers have researched, modified, and revised a plethora of methods and equations to accurately, yet simply, predict structural damage from earthquakes. Out of this research, force-based and displacement-based methods are the two predominant methods to have emerged.

The capacity spectrum method is a force-based method that was originally developed by Freeman (1979) as a graphical procedure to assess structural damage. The capacity spectrum method was adopted by the Applied Technology Council in 1996 as a way to relate base shear demands to roof displacements. This method has gained popularity due to its graphical nature and its ability to equate viscous damping to hysteretic damping. Unfortunately, there is no physical principle that justifies this relationship, and the true dynamic response of the inelastic system may have little to do with the period associated with the intersection of the capacity curve and the damped spectrum. The intricate calculations involved in this method detracts from its "simplicity" and may be perceived as providing an understanding of structural dynamics that may not exist.

The Equivalent Linear System is a displacement-based approach that estimates the displacements of an inelastic system by either converting that system into an equivalent linear system (equivalent damping and stiffness) or by using modification factors to adjust the response of the elastic system. This method finds its roots in the substitute structure method as proposed by Shibata and Sozen (1976) but has evolved into several methods including the coefficient method adopted by FEMA 273 (1997). The chief advantage of this method is its simplicity, in terms of calculations and interpretation of results. Another benefit of this method is that the underlying structural dynamics principles have been widely accepted.

The direct displacement-based method can be described as a companion to force-based methods in that it attempts to better estimate the strength requirements at the location of plastic hinge formation. Kowalsky stated that displacement-based design is fundamentally more direct than force-based design because strength and stiffness are linearly related. Therefore, he proposed a set of relationships that correlate stiffness to strength based on the geometry of the member, thus relating equivalent viscous damping to the ductility ratio. The clearest advantage associated with this method is that it is fundamentally more direct; however, with the gained

accuracy there is less simplicity and more required information regarding the detailing of the structure.

Many studies have been conducted to compare the accuracy of existing methods with proposed methods. Some comparative studies are based purely on the accuracy of the analytical results, while others attempt to also qualify the simplicity of the method. Researchers note however, that in one comparative study the displacement coefficient method (FEMA-273, 1997) tended to over-estimate the peak deformations by 28%, the capacity spectrum method (ATC-40, 1996) typically underestimated the deformation by 20%, and the direct displacement-based method by Kowalsky underestimated the displacements by 11% (Lin et al, 2004). These results indicate that a need still exists to develop a more accurate method for estimating building displacements.

In addition to improving accuracy, a primary focus of research has been to obtain a simple approach. An advantage of these simple methods is that they do not require expertise in structural dynamics, which may be advantageous in regions of lower seismicity and in some underdeveloped countries. As an initial analysis tool, these methods provide good estimates of structural response to generally qualify demands before a more detailed analysis is preformed. These advantages have been noted in comparative studies evaluated in this chapter (Akkar et al., 2005; Matamoros et al., 2003). The analysis of the comparative studies supports the need for a method that is both accurate and simple.

1.6. Objective & Scope

Most of the earlier work described above has been based on the response of SDOF systems. The primary goal of this research is to develop a displacement-based method from an assessment of SDOF system response and nonlinear MDOF system response based on maximum roof displacement and maximum story distortions. Despite the multitude of procedures that exist, the complexities of some methods and unknown precision associated with MDOF response have prevented any one method

from becoming accepted by all. By examining the responses of a suite of MDOF systems with respect to the response estimated using linear SDOF analysis, a simple procedure for estimating nonlinear MDOF displacement response can be proposed.

The scope of this study is to determine the correlations of the nonlinear dynamic response and linear SDOF response of 105 frames to a suite of ten earthquakes in two regions of seismicity. The optimum effective period factor and equivalent viscous damping are identified. In addition, the relationship between magnitude and location of story drift ratio in nonlinear MDOF and linear SDOF analysis is defined.

Chapter 2 of this document describes the analytical procedures used to complete the study. Using the methods described in Chapter 2, Chapter 3 presents a comparison of the calculated linear SDOF and nonlinear MDOF responses. An optimum effective period factor and equivalent viscous damping were developed to provide appropriate estimates of maximum structural displacement across a wide range of structures, ground motions, and two levels of seismicity. Chapter 4 presents the variations associated with maximum story distortions calculated from linear SDOF and nonlinear MDOF analyses. Chapter 5 compares the procedure developed in this study with the methods of Iwan and Gates (1979) and Lepage (1997). A summary and conclusion are included in Chapter 6.

Chapter 2: Analysis of RC Frames

2.0. General

In Chapter 1, various methods that provide simple estimates of building displacement were briefly outlined and explained along with comparative studies. The intent of this research is to develop a simple design and analysis procedure based on the displacement response of nonlinear MDOF systems. The advantage of the proposed method over previous methods is that the proposed method illustrates the optimum correlation between linear SDOF and nonlinear MDOF analysis of frames.

The study was performed using the ground motions from ten diverse earthquakes. The selected earthquakes have soil types that can be described as rock, stiff, or soft. Table 2.1 presents a description of each earthquake record, including location, peak ground acceleration, characteristic period, and record duration. The un-scaled ground acceleration records are presented in Fig 2.1. The properties of these sample earthquakes include varying peak ground acceleration, duration, corner period, and intensity. The records were selected and scaled to represent a smooth displacement spectrum deemed reasonable for a region of high semicity (S_d=10T in.) as shown in Fig 2.2. A suite of concrete frames originally proportioned for high and moderate seismic demands (Browning, 1998) were evaluated for linear and nonlinear response.

2.1. Frames Properties

The suite of frames considered was chosen because it encompassed a large range of stiffness configurations, initial periods, and varying dimensions. To match typical properties found in construction, the material properties for the concrete included a compressive strength f'_c equal to 4000 psi, an average modulus of elasticity of 4,000,000 psi, and a shear modulus of 1,600,000 psi. The yield stress of the reinforcing steel was assumed to be 60,000 psi.

Each frame had three bays and ranged in height from 5 to 17 stories. Bay widths were either 20 or 30 feet. The first floor story heights were 10, 12, and 16 feet,

with a uniform story height of either 10 feet or 12 feet for all the remaining stories. The girders varied in depth from one-tenth the total span length to one-twelfth the total span length (Browning, 1998). Fig 2.3 illustrates the dimensions associated with a typical interior frame having square bay dimensions. Both the foundation and the beam column joint cores were considered to be rigid. The gravity load (160 psf) was assumed to act over a tributary width equal to the bay length.

2.1.1. Proportioning Procedure

The reinforced concrete frames used in this study were proportioned based on a procedure to control the expected drift to be within 1.5% of the total building height during response to strong ground motion (Browning, 1998). The response of a building is a function of its mass and stiffness. The researcher controlled, the deflection using a target period criterion. Using the formula developed by Shimizaki(1984) and expanded by Lepage(1997), an acceptable upper bound for the displacement response of a building with an increase in damping and a lengthened period was estimated as:

$$D_b = PF * c * \sqrt{2} * T_i \tag{2-1}$$

where PF is the participation factor, c is the slope of the representative displacement response spectrum, and T_i is the initial period of the structure based on uncracked sections. Rearranging this equation and substituting the desired deflection (D_t) in for the displacement bound, the target period of the structure based on uncracked sections was defined as follows:

$$T_t = \frac{D_t}{PF * c * \sqrt{2}}. \tag{2-2}$$

To arrive at the target period, member proportions were adjusted, thus altering the stiffness of the structure. The members were first proportioned to resist gravity load demands, and then the period of the structure was compared with the target period to ensure compliance with drift demands. Gravity loads were defined as the loads acting

upon the frame during strong ground motion, and columns were dimensioned to limit the axial stress to 45% of the capacity.

Although the frames were initially proportioned based on an allowable period, the dimensions of the columns and girders were compared to existing frames that were designed using traditional methods and found to be representative of these structures. The procedure outlined in the study done by Browning (1998) requires that sufficient base shear strength is obtained, the columns and girders are of adequate strength, and that structural detailing is adequate to ensure ductile behavior. For these reasons, the frames used in this study are considered to be typical reinforced concrete frames.

2.1.2. High Seismicity

As described in Section 2.0, the high seismic demand was qualified by a spectrum defined as D=10T in. The frames evaluated for high seismic demand had columns with reinforcement ratios of 2.0%, while the girders had average reinforcement ratios of 0.75% (0.5% positive reinforcement and 1.0% negative reinforcement). The frames proportioned for high seismicity for the initial analysis were assumed to have girder depths of one-twelfth the bay width. These frames had initial periods ranging from 0.50 to 2.08 seconds, base shear strength coefficients of 0.04 to 0.23, and column height to overall depth ratios of 3 to 10 (Browning, 1998). The frames subjected to high seismic demands were proportioned for gravity loads and according to the stiffness requirements for limiting maximum building displacements. The second requirement (stiffness) was controlled for most frames except for frames having 13 or more stories and with thirty-foot bays. The selected columns were square and sized so that at the time of the earthquake the total axial stress in the columns would not exceed 45% of the capacity. Table 2.2a contains the member dimensions for the frames proportioned for regions of high seismicity. Two dimensions are provided for the columns (base and top) because for frames having

more than seven stories, a change in column stiffness was allowed at mid-height of the building.

2.1.3. Moderate Seismicity

To determine the accuracy of the proposed method, moderate seismic demands also were evaluated. The moderate seismic displacement demand was selected to represent the highest demand noted in the Central Eastern United States (S_d=5T in.) (Browning, 1998). The scaled displacement response spectra are shown in Fig 2.4 and appropriate scaled effective peak ground accelerations can be found in Table 2.1.

The frames evaluated using moderate seismic demand incorporated columns having reinforcement ratios of 1.0% and typical girder reinforcement ratios of 0.75% (having 0.5% positive reinforcement and 1.0% negative reinforcement). The moderate seismicity frames were assumed to have girder depths of one-twelfth the bay width. These frames had initial periods ranging from 0.6 to 2.6 seconds, base shear strength coefficients of 0.02 to 0.16, and column height to overall depth (using square columns) ratios of 3 to 12 (Browning, 1998). Initially all frames in the study were proportioned for gravity loads, calculated using 160 psf over a tributary width equal to the bay length. The columns proportioned to satisfy these gravity load demands were determined to also satisfy the stiffness requirements to control lateral displacements. Table 2.2b contains the member dimensions for the frames proportioned for regions of moderate seismicity. The column dimensions were allowed to be reduced at mid-height of the frames having more than seven stories.

2.1.4. Frames Proportioned for Additional Girder Stiffness

The column dimensions selected for frames in a region of high seismicity with 20-ft bays tended to be slightly larger than column dimensions in typical existing frames (Browning, 1998). This fact was in part due to the small proportions used for the girders, which led to a more flexible frame. To investigate frames with more

conventional column dimensions, frames with increased girder depth (one-tenth the span length) were evaluated. The frames with 30-ft bays were not re-evaluated using deeper girders, because the column dimensions of these frames were found to be representative of member proportions in existing structures. In addition, many of the frames had column dimensions limited by gravity-load requirements. Similarly, the frames proportioned for moderate seismic demands had column dimensions that were determined using the gravity load criterion and were found to also satisfy displacement limitations. Therefore, using deeper girder dimensions would not have been advantageous to the proportions required for the columns. Table 2.2c contains the member dimensions for the frames proportioned for additional girder stiffness in regions of high seismicity.

2.2. Linear Analysis

To accurately determine the impact of the nonlinear response on the frames, the linear response was first calculated as a means for comparison. Significant nonlinear action is noted only for the frames proportioned for high seismicity; therefore, frame behavior (story drift ratios and displaced shapes) will only be compared for frames proportioned for high seismicity. The linear estimates of maximum roof displacements, deflected shapes, periods, and participation factors were calculated using a modal analysis for the first three modes of vibration. Table 2.3 lists the participation factors and periods associated with the first three modes for frames subjected to high seismicity. The stiffness of the elements was based on uncracked section properties, and the contribution of the slab was assumed to benefit the stiffness of the girders in the frames. The slab stiffness contribution depends upon the effective slab width. For the girders in the study, a factor of two was determined to be appropriate (Browning, 1998).

For the linear analysis the maximum roof displacement was calculated using 1-10,15, and 20 percent damped spectra for each earthquake; representative damped spectra can be found in Figs. 2.5a-j for high seismicity. As shown by the associated

participation factors in Table 2.3, the first mode was the dominant mode in all cases. The linear response of the frames was calculated using the response spectra (for the first mode response) for comparison with nonlinear response (as described in Section 2.3).

Two common methods exist for determining the maximum linear displaced shape for a structure from a combination of the mode shapes. The "square root sum of the squares" (SRSS) rule developed by E. Rosenblueth for modal combination is:

$$r_e = (r_1^2 + r_2^2 + \ldots + r_n^2)^{1/2} \tag{2-3}$$

where the peak response of each mode (r_n) is squared, then those values are summed, and the square root of the sum provides an estimate of the total peak response (deflected shape). Another rule is the complete quadratic combination (CQC):

$$r_e = \left(\sum_{i=1}^{N} \sum_{n=1}^{N} \rho_{in} r_{io} r_{no} \right)^{1/2} \tag{2-4}$$

where ρ_{in} is the correlation coefficient between the peak responses, r_{io} and r_{no}, for the *i*th and *n*th mode respectively. The CQC rule may provide a more accurate estimate for the total peak response and can be either larger or smaller than the SRSS method (Chopra 1995). The additional accuracy of the CQC rule becomes important in the calculation of forces in members (Lopez 2001); in contrast, for this study modal combinations are only used to calculate the deflected shape. Therefore, the SRSS method for the first three modes was used for simplicity in this study.

Figures 2.6a-g show the (SRSS) maximum linear displacement response for each frame and the corresponding earthquake that produced this response. Notably for a given number of stories, the earthquake that produced the maximum displacement for the thirty-foot bay frames was also responsible for the maximum displacement in the twenty-foot bay frames. The displaced shape associated with maximum response for each frame closely resembles a first mode response. Figures 2.6a-g clearly illustrate that the period of the frame (a function of the frame's height and stiffness) is directly related to the period of the earthquake that causes the maximum deformations. For frames having seven stories or less, the maximum

deformations are predominately associated with the earthquake Tarzana. A greater variation is seen in the frames having between nine and eleven stories with Seattle, Sendai, and Santa Barbara quakes each causing maximum deformations. The Sendai and Santa Barbara earthquakes dominate the response of frames having more than thirteen stories. Table 2.4 contains the tabulated maximum linear displacements, and its companion Table 2.5 lists the maximum mean drift ratios (MDR) for 2% damping for each frame.

The maximum deflected shape was used to calculate the maximum story drift ratio for the linear response. The story drift ratio (SDR) is a function of the differential displacement per story and sheds light on the location of the maximum distortion in the frame in its response to strong ground motion:

$$SDR(\%) = \frac{(d_n - d_{n-1})}{h_{story}} * 100 \qquad (2\text{-}5)$$

where d_n is the displacement at the top of the story being investigated, d_{n-1} is the displacement at the bottom of the story being investigated, and h_{story} is the height of the story. Table 2.6 contains the maximum SDR for every frame and each earthquake. Figures 2.7a-g illustrate the maximum story drift ratios for each frame and the corresponding earthquakes. Similar to maximum displacement, the maximum SDR was associated with the same earthquake for a given story height for both the twenty and thirty-foot bay frames. The corresponding locations of maximum story drift for every frame and each earthquake can be found in Table 2.7. The location where maximum story drift occurs is important in understanding the location in the structure where the largest deformations will occur. For the suite of frames subjected to linear analysis, on average the maximum SDR occurred at the third floor. One noticeable trend is that the maximum story drift for frames taller than seven stories is likely to occur above mid-height. This can be attributed to the proportioning of the frames and the column dimensions decreasing at mid-height for frames taller than seven stories. Thus, the stiffness at this location decreases as well. In general, the maximum story drift occurs at one-third the height of the frame. For each frame the

earthquake that produced the maximum SDR also was responsible for the maximum MDR; additional relationships are noted and discussed in Section 3.5.

2.3. Nonlinear Analysis

The nonlinear analysis for the frames proportioned for strong earthquake motion was conducted by Browning (1998) using a program called LARZ, developed by Otani (1974) and later modified by Saiidi (1979a, 1979b) and Lopez (1988). The program has been used in several studies and has proven to be a reliable tool in representing the displacement response of reinforced concrete structures during strong ground motions (Saiidi, 1979b; Eberhard, 1989; Lopez, 1988; Lepage, 1997; Browning et al., 1997).

The numerical model adopted by LARZ includes several simplifying assumptions:

1. Ground motion and lateral forces are in the horizontal direction.
2. The structure, loads, and response are defined in one vertical plane.
3. The members are defined as massless line elements having (a) rigid ends, (b) nonlinear flexural springs attached to the rigid ends, and (c) a linear elastic middle that connects the two springs. The centroidal axis of the members coincides with their positions.
4. Masses are lumped at defined horizontal degrees of freedom.
5. The beam-column joint cores are considered to be rigid.
6. The foundation is considered to be rigid.
7. Numerical integration of the differential equation of motion is completed using the constant average-acceleration method (Newmark, 1959).
8. The nonlinear response of the members is in flexure with hysteresis rules defined by Takeda (1970).
9. Slip of the reinforcement at the beam-to-column connections is included as additional rotation in the flexural response of the elements.
10. Second order gravity effect (P-Δ) can be included in the analysis.

11. Axial deformations are neglected in all members.

The nonlinear response of beams and columns was calculated for flexure only, in accordance with hysteresis rules defined by Takeda (1970). Flexural deformations were defined for all members by an idealized moment-curvature relationship represented by a tri-linear curve. The tri-linear curve shown in Fig 2.8 is characterized by three distinct regions: first the uncracked section, then the cracked section, and finally the yielded section. Moment-curvature values were calculated to represent initial cracking of the concrete and yielding of the reinforcement. A third pair of coordinates defined the post yield stiffness of the member.

The initial stiffness of the systems was defined by the gross sectional properties. The contribution of the slab was assumed to augment the stiffness of the girders in the frames. As in the linear analysis, the stiffness of the girders was factored by two.

The yield strength of the members was defined as the nominal ultimate moment capacities. Member dimensions can be found in Table 2.2a-c. The concrete stress-strain relationship defined by Hognestad (1951) was used, with a limiting compressive strain of 0.004. A minimum value of post-yield stiffness (0.01% of secant stiffness) was defined. Hysteresis in the elements followed the rules defined by Takeda (1970) with an unloading-slope of 0.4, and a coefficient of damping equal to 2% was used to account for the effects of viscous damping. The analysis also took into account slip rotations at joints and second order (P-Δ) effects. The results for maximum nonlinear roof displacement (calculated using LARZ) are found in Tables 2.8a-c. Tables 2.9a-c list these maximum roof displacements converted into maximum MDR. The maximum SDR is tabulated in Tables 2.10a-c, and the locations are in Table 2.11a-b. Additional figures for maximum SDR from nonlinear analysis can be found in the referenced study (Browning 1998).

Chapter 3: Comparison of Linear and Nonlinear Response

3.0. General

Previous research has focused on determining the optimum relationship between linear SDOF and nonlinear MDOF displacement response through the use of an effective period and equivalent damping (Iwan 1980). The effective period can be defined as a multiple of the initial period, which corresponds to an estimated linear displacement using a linear response spectrum at the effective period (yielding the same magnitude as the nonlinear displacement). This multiple is defined as the modification factor for the initial period.

An initial comparative analysis was made for each individual frame to determine the correct modification factor. Fig. 3.1 shows the results of this type of comparison for all frames with girder depth equal to one-twelfth the span length subjected to the Taft earthquake scaled to represent a region of high seismicity. The maximum nonlinear displacement is plotted versus the initial frame period (represented as diamonds) as well as the 5%-damped displacement response spectrum. In addition, the effective periods were determined and are plotted as crosses on the response spectrum. The average modification factor was found to be 1.8 for this record, leading to the assumption that an effective period is approximately twice the initial period. Although this spectral shape tended to produce reasonably successful results, other spectral shapes were not as successful. For example, Fig 3.2 shows the results for Kobe scaled for high seismicity. Unlike Taft, an effective period could not be determined for all of the frames because several frames had displacements that were larger than any point on the displacement response spectrum. Those frames are represented by symbols located at an effective period of zero.

Rather than analyzing the frames individually, the suite of frames was examined as a whole to determine an optimum level of damping to estimate the maximum displacements for the entire suite of frames for a particular earthquake. A least-squares method was used to determine the optimum combination of a period

modification factor and effective linear spectrum damping to estimate displacement of all frames when analyzed as a single data set. This process is two dimensional in nature. First, the modification factor is determined that provides the best fit for the data set to a spectrum with a given effective damping. Then the effective damping that provides a best fit to the displacement responses in the data set must be selected. This process is described in Section 3.1.

3.1. Selection of Optimum Damping

The determination of an optimum level of damping and period modification factor required an analysis of the linear and nonlinear response of each set of frames (those proportioned for high seismicity, moderate seismicity, and high seismicity with stiff girders) for each earthquake. For each level of damping, the difference between the maximum adjusted nonlinear displacement (maximum displacement calculated from nonlinear analysis and divided, or adjusted, by the first mode participation factor) at the calculated effective period and the spectral response value at that effective period was determined. This maximum adjusted nonlinear displacement plotted with respect to the effective period is referred to as the effective nonlinear displacement in this study. A least-squares method was used to evaluate the difference and select the best-fit equivalent damping and period modification factor. The spectral curve having the least deviation (minimized differences) from the set of effective nonlinear displacement data is called the least-squares regression curve (Spiegel 1975) and for this study corresponds to the "idealized" damping level for a particular earthquake.

The "ideal" level of damping varied by both the earthquake and the level of seismicity associated with the suite of frames. Because the same level of damping did not produce the response spectrum for all earthquakes with the minimum deviation from the "real" displacements, the "optimum" damping and associated period modification factor were determined as the response spectrum that on average provided the least deviation for all frames and earthquakes.

The least-squares method does an adequate job of determining which level of damping best corresponds to the effective nonlinear displacements; on the other hand, this method does not lend any information as to the error associated with the predicted displacements. To qualify which damping level produced the least deviation for all frames and earthquakes, the percent difference between the effective nonlinear displacement, $d_{eff,}$ and the estimated effective displacement, d_{est}, was calculated for each frame as:

$$percent\_difference = \frac{(d_{eff} - d_{est})}{d_{eff}} * 100 \qquad (3\text{-}1)$$

Figures 3.3a-c, illustrate the average percent difference for all frames as a function of viscous damping per earthquake for frames proportioned for high seismicity (L/12), high seismicity with stiff girders (L/10), and moderate seismicity, respectively. The accuracy of using a linear response spectrum to estimate nonlinear displacement depends on the level of viscous damping (as indicated by the percent difference). Overall, the most accurate level of damping (lowest percent difference) occurs close to 10% for both moderate and high seismicity and at 11% for deep girders in high seismic zones. For the Hachinohe record scaled to represent high sesimicity, the most accurate level of damping occurs at 12%, whereas for every other earthquake, the minimum occurs at less than 9% damping. A similar trait is apparent for records scaled to represent moderate seismicity. Figures 3.3a-c illustrate that the least percent difference for Santa Barbara and Hachinohe occurs at higher damping levels than the 10% damping level that on average produces a minimum percent difference for all earthquakes. This trend may indicate that structural responses to earthquakes with longer characteristic periods have increased ideal damping levels, as can be seen by the more rapidly decreasing slope of the Santa Barbara and Hachinohe curves.

Tables 3.1a-c illustrate the method used to qualify the optimum damping level for the suite of ground motions by the minimum percent difference (EQ 3-1). The tables show the minimum percent difference for each level of damping (from 2% to 12%) for each earthquake, separated into the frames proportioned for high seismicity

with two girder depths (L/12, L/10), as well as those proportioned for moderate seismicity. The average percent difference associated with each damping level is calculated in the right hand column of the table, and the ideal damping level (with the minimum percent difference for each earthquake) is in bold. For the frames proportioned for a level of high seismicity with girder depths equal to one-twelfth the span length and for the frames proportioned for moderate seismicity, the optimum levels of damping are 8% and 10%, respectively (as shown in Fig. 3.3a and 3.3c). For the frames proportioned for a level of high seismicity with stiff girders, the optimum level of damping is 11%. These values are averaged at the bottom of the table based on the number of frames in each set; the minimum percent difference is selected as the optimum level of damping for all the frames subjected to all earthquakes. The optimum level of damping for all frames was determined to be 10% damping. Figure 3.4 illustrates this by presenting the average percent differences for all frames subjected to strong and moderate ground motions found in Table 3.1a-c plotted with respect to the corresponding damping levels. The error associated with estimated displacements calculated using elastic spectra is interesting to note because it decreases dramatically as the equivalent viscous damping is increased from 2% to 6% (Fig 3.4). The percent difference associated with each level of damping can be estimated by the polynomial equation in Fig. 3.4.

Tables 3.2a-c list the period modification factors that produced the least percent differences for each level of damping. The average period modification factors associated with the 10% damped spectra are shown in bold. These optimum period modification factors for each type of frame and spectrum are calculated using different viscous damping coefficients are shown in Fig 3.5. Interestingly, Fig 3.5 shows that the optimal period modification factor is nearly constant for nonlinear analyses conducted using spectra with damping of 6% or greater. In addition, a clear separation exists between the response of frames to high and moderate seismic demand. This is expected due to the level of nonlinear response (and thus increased period) being greater for the frames subjected to high seismic demands. Similarly,

the period adjustment factor was most influenced for frames subjected to high seismic demands and lower damping levels. The period adjustment factor for moderate seismic demands remained nearly constant for all damping levels. The period modification factor for moderate seismicity was calculated to be approximately 1.9, and the period modification factor for high seismicity (the average for frames subjected to high seismicity with girder depth L/10 and L/12) was calculated to be approximately 2.3. Equations to estimate the optimum period adjustment factor are presented in Fig 3.5 for various damping levels.

Figures 3.6a-j and 3.7a-j show the optimum damped (10%) spectra for high seismicity (including girders of depths of both one-tenth and one-twelfth the span length) and moderate seismicity, respectively. The adjusted nonlinear displacements at effective periods are plotted in the figures for comparison. Curves representing one and two standard deviations from the optimum spectrum are also shown and will be examined in Section 3.7.

3.2. Effect of Earthquake Properties on Optimum Response

The characteristic properties of each earthquake were examined to determine their relation to the selected optimum level of damping (10%). The characteristic properties of each earthquake that was examined are listed in Table 2.1, including peak ground acceleration (PGA), corner period (T_g), duration, and the one-second spectral acceleration (S_{a1}).

Each property was analyzed with respect to the idealized damping level associated with each earthquake. Figures 3.8a-d show the characteristic property for each earthquake, plotted with respect to percent error for both the ideal damping level for each earthquake and the optimum damping (10%). The percent error in these plots is the average percent difference from the adjusted nonlinear displacement to the chosen response spectrum for each earthquake. The solid data points correspond to the percent difference associated with the ideal level of damping calculated for each

earthquake; the hollow data points correspond to the percent difference when using the optimum10% damping.

Few trends are evident to associate the earthquake properties with percent difference. The characteristic period and PGA appear to have some effect with respect to error for the frames proportioned with deep girders. From the plotted trend lines, the earthquakes with a characteristic period larger than 1.0 second and a short PGA (less than approximately 0.3g) have an increase in error associated with this method, as show in Fig 3.8a-b. No discernable trend for duration and S_{a1} (Fig. 3.8c-d) was evident. For each characteristic property, only a slight increase in the percent difference associated with using the optimum 10% damping (for all earthquakes) as compared to the ideal damping level (associated with each earthquake) was evident. Of additional interest is the fact that the frames with stiff girders had the lowest percentage difference at approximately 10% on average. These frames were less sensitive to the ground motions with long T_g and short PGA.

3.3. Effect of Period on Optimum Response

When the percent difference was calculated from the idealized response spectrum and the adjusted nonlinear displacement, the least variance was found to be associated with the frames having shorter periods. The data was then separated and evaluated in terms of the initial frame periods. The frames in this study with initial periods less than one second were considered to have "short" periods. Figures 3.9a-j illustrate the benefit of using the proposed method to estimate displacements for short-period frames as compared to frames having longer periods. Frames proportioned for a region of high seismicity (with girder depths of L/12) are shown to illustrate this trend. By separating the data based on initial frame periods, the optimum period adjustment factor (based on the minimum percent difference between the estimated response and the adjusted nonlinear response) for the short period frames was found to be 2.4; for the frames with longer periods the factor was 2.6. Figures 3.9a-j show that the frames having periods less than one second tend to have

less deviation from the idealized response curve. For the frames with an initial period longer than one second, two distinct bands of data can be seen for all earthquakes. The factors attributed to this phenomenon are discussed in Section 3.4.

3.4. Effect of Frame Geometry on Optimum Response

Figs 3.9a-j show evidence of a separation of data points from frames with initial periods longer than 1.0 second. Further investigation determined that the separation was directly related to the bay length of the frame. Figures 3.10a-j show the 10% response spectrum (for high seismicity) plotted with the effective nonlinear displacements with the twenty-foot and thirty-foot bays delineated to illustrate the impact of the bay length. The response spectrum tended, for nearly all the earthquakes, to more accurately estimate displacements for the thirty-foot bays than for the twenty-foot bays.

The twenty-foot and thirty-foot bays were proportioned with girder depths equal to one-twelfth their span length (L/12). To determine if the story stiffness of the frames was responsible for the separation of data points seen in Fig 3.10a-j, an estimate of the lateral stiffness per story was calculated as (Schultz 1992):

$$k_i = \frac{24E}{h^2} \frac{1}{\left(\frac{2}{\sum k_c} + \frac{1}{\sum k_{gb}} + \frac{1}{\sum k_{ga}} \right)} \qquad (3\text{-}2)$$

$$k_c = \frac{I_c}{h} \qquad k_g = \frac{I_g}{L}$$

where k is the stiffness, h is the height of story, and L is the length of span. The stiffness subscripts are k_i for story stiffness, k_c for column stiffness, k_{gb} for the stiffness of the girder below the story, and k_{gb} for stiffness of the girder above the story. Tables 3.3a-c list the tabulated story stiffness values ranging from a minimum of 241 kips/in to a maximum of 3314 kips/in. In Tables 3.3a-c the stiffness data is divided into three categories: the stiffness of the stories at the base of the structure (Base), the stiffness of the stories at the top of the structure (Top), and the stiffness of

the first floor for the frames that have tall first stories (Tall). Table 3.3a-c clearly illustrates that the stories with thirty-foot bays are significantly stiffer (average of 2244 kips/in) than the stories with twenty-foot bays (average of 918 kips/in). The twenty-foot bay frames with deep girders had moderate story stiffness (average of 925 kips/in). The proposed method was found to be more accurate for the frames with stiffer stories (twenty-foot bay frames with deep girders and thirty-foot bay frames) when subjected to high seismicity ground motions. The distinction between "stiffer" and "softer" story frames did not evidence any correlation between effective nonlinear displacement and the optimum damped spectral response as shown in Fig. 3.7a-j for the frames proportioned for moderate seismicity.

3.5. Story Drift Ratio (SDR) and Mean Drift Ratio (MDR)

The SDR was calculated as defined in Chapter 2 to gain insight on the location of greatest distortions in the building. The mean drift ratio (MDR, a simpler way to estimate distortions) is the average displacement per story, calculated as the roof displacement divided by the total height of the building. The question arises as to whether a large SDR or large MDR leads to an increase in error in predicting the effective nonlinear displacement using the proposed method. Figure 3.11 shows that the calculated average percent difference is not dependent on the maximum SDR. The most significant impact on the percent difference calculated for the proposed method is the associated earthquake. As seen in Fig 3.11, the grouping of data points is somewhat associated with a particular earthquake and not the maximum SDR.

One way to examine the behavior of a frame is to determine the coefficient of distortion, which is the ratio of the SDR to the MDR. Figures 3.12a-b plot the coefficient of distortion versus MDR for all of the frames subjected to high seismicity (L/12). Figure 3.12a illustrates that for linear analysis of a SDOF systems, the average coefficient of distortion is 1.8. The coefficient only slightly decreases as the MDR is increased. Figure 3.12b shows a much more pronounced trend associated with MDR for nonlinear analysis (MDOF system); as the MDR increases, the

coefficient of distortion rapidly decreases. Consequently, for SDOF systems, the coefficient of distortion is nearly constant; but for MDOF systems, the coefficient of distortion tends to decrease as a function of the overall drift.

3.6. Predicting Displacements from any Damping Level

To determine the accuracy associated with each damping level and corresponding period adjustment factor to estimate the linear displacement of a frame, the following procedure was performed. The accuracy associated with each damping level at estimating the nonlinear displacement using a linear response spectrum was determined by comparing the ratio of the calculated nonlinear displacement to the displacement predicted using a linear analysis. The displacement predicted by the linear analysis was determined by using the period adjustment factors from Tables 3.2a-c associated with the corresponding damping level and earthquake. The ratio of calculated nonlinear displacement to predicted linear displacement ideally should equal one for all results. Table 3.4a-c shows the average is nearly one for all damping levels, with 8% damping having the average closest to one. The standard of deviation gives a good indication of how accurately displacement was predicted for a data set. Estimations made using 10% damping had the lowest standard deviation. The coefficient of variation (COV) provides further insight into how much variation exists between the average and the standard of deviation. Estimations made using 12% damping had the minimum COV. Although, COV is not the best indicator for this analysis because it is too largely influenced by the average. To accurately determine the best damping level for estimating nonlinear displacements using a linear response spectrum all of these factors must be considered. Estimations made using a 10% damped spectrum were selected as "optimum" because 10% damping produced for the data set:

1. the least percent difference (Section 3.2),
2. the lowest standard deviation as seen from Table 3.4a-c, and
3. an average close to 1.0.

3.7. Proposed Method to Estimate Maximum Roof Displacement

Based on the analysis in this chapter, the optimum use of an effective period method can be defined. The response spectrum with 10% viscous damping was selected as the ideal damping level to use with the effective period of the building to estimate displacement. The initial period of the frame is modified using the modification factor to produce the effective period. An estimate of the maximum nonlinear displacement for the frame ($D_{NL\text{-}EST}$) is then obtained by using an effective period (T_{eff}), 10%-damped displacement response spectrum (S_d), and finally the calculated participation factor (P.F.) for the frame:

$$D_{NL\text{-}EST} = \text{P.F.} * S_d\left(T_{eff},\ 10\%\ \text{Damping}\right). \tag{3-3}$$

The average period adjustment factor (the factor used to convert the initial period to an effective period) was calculated as 2.4 for all frames subjected to high seismicity ground motion and 2.1 for all frames subjected to moderate seismicity ground motion.

As a design method, a level of safety may be desired when estimating nonlinear response. The linear displacement response is modified to obtain an upper bound to estimate the effective nonlinear displacement. A "safety" modification factor (γ_i) was calculated as the ratio of the effective nonlinear displacement (E.NL.D) to linear displacement [S_d (T_{eff}, 10%)] for the suite of frames:

$$\frac{\text{E. NL. D.}}{S_d * \left(T_{eff},\ 10\%\right)} = \gamma_i \text{ (initial safety modification factor)}. \tag{3-4}$$

Note, this requires providing a design response spectrum with 10% damping. Table 3.5 contains the average safety modification factor, standard deviation, and coefficient of variation for each earthquake and each suite of frames at 10% damping. An average safety modification factor (γ_i) and standard deviation were calculated for all the frames and all the earthquakes. On average, the optimum γ_i is equal to one. The safety modification factor was 1.2 for all earthquakes and frames to predict displacements within one standard deviation and was approximately 1.3 to predict displacements within two standard deviations.

In Figs 3.6a-j the response spectra are plotted with curves denoting the first two standard deviations of data. For the proposed design procedure, the variance associated with two standard deviations was used to ensure that the maximum displacement response of 98 percent of the studied frames was represented. Therefore, an equation to conservatively predict displacement is:

$$D_{NL\text{-}EST} = P.F.* S_d\left(T_{eff},\ 10\%\ \text{Damping}\right)* \gamma_f \qquad (3\text{-}5)$$

where γ_f is the safety modification factor equal to 1.4.

Chapter 4: Relationship between Magnitude and Location of Maximum SDR for Nonlinear and Linear Analysis

4.0. General

Because the damage associated with an earthquake can be largely attributed to the displacements caused in the building, the distortions and the location of these distortions was investigated. One way to qualify these distortions is by story drift ratio (SDR), which is the ratio of interstory drift to story height. The location of the maximum SDR is an indicator of the story most affected by the earthquake. When the maximum SDR occurs at lower floors, the impact on the structure can be more critical due to higher axial loads on the columns and increased p-delta effects. The SDR values calculated using nonlinear dynamic analysis and linear analysis (calculated using the SRSS method) were investigated to determine if a relationship exists between the nonlinear and linear responses. A general relationship was established between the location and magnitude of maximum nonlinear SDR and maximum linear SDR The relationship (as defined by equation 4.1) describes how the location of maximum SDR moved higher in the structure. This relationship is important to our study, because in order to fully develop a relationship between linear and nonlinear analysis not only is a method to estimate the total roof displacement needed (as determined in Chapter 3), but also needed is an understanding of the magnitude and location of maximum distortion are affected.

4.1. Comparison of Nonlinear and Linear Analysis for Location of Maximum SDR

The ability to estimate the location where the maximum story drift is likely to occur provides information about possible locations of damage during response to seismic ground motion. Interpreting how the results of a linear analysis compare with the nonlinear response is necessary to evaluate building behavior. To determine if a relationship exists between the location of maximum SDR for a building analyzed

using nonlinear analysis versus linear analysis; the maximum SDR location was divided by the height of the building and plotted versus the period of the building in Fig 4.1a. The maximum SDR location is defined at the top of the story that has the maximum distortion. The analysis was completed for frames proportioned using girder depths equal to L/ 12 and for a region of high seismicity.

Two best-fit lines are plotted in Fig. 4.1a for all frames subjected to high seismicity with one line for the nonlinear results and one line for the linear results. In general, the ratio of maximum SDR location to total building height decreased as the period increased. This trend was more pronounced for the linear analysis than nonlinear analysis results. For the nonlinear analysis, the location of maximum SDR on average occurred between 34% and 48% of the total building height, for all ranges of period. The large range of scatter for the nonlinear results creates difficulty in defining a more exact relationship.

Figure 4.1b shows the same SDR location ratios plotted vs. maximum MDR as opposed to periods (Fig. 4.1a). The trends for linear and nonlinear analysis are quite similar and generally increase with an increasing MDR. The trendline associated with nonlinear analysis has a more pronounced slope than the trendline for linear analysis which is nearly constant.

The nonlinear SDR location divided by the linear SDR location was plotted versus period to determine if a relationship exists (Fig 4.2a-b). Both the average (solid line) and the average plus two standard deviations (dashed line) are plotted in Fig 4.2a. The plot in Fig 4.2a shows that the location of maximum SDR for nonlinear analysis varies on average from approximately 1.1 to1.7 times that of the linear analysis as the period increases. On average, buildings with relatively short periods have similar locations of SDR for linear analysis and nonlinear analysis; however, for buildings with longer periods, the location of SDR rises in the structure.

In Fig 4.2b each earthquake is distinguished by a best-fit line; this was done to determine the impact of the earthquake. One noticeable trend was that, in general, the earthquakes having high one-second spectral acceleration had either no change in

story location from nonlinear to linear analysis or, in some cases, even a drop in story location. On the other hand, the earthquakes with low one-second accelerations were the most sensitive to a change in period. The only exception to this rule was the response associated with Taft, which had the greatest shift in location due to period despite having a median one-second spectral acceleration of 441 ft/s^2.

4.2. Comparison of the Magnitude of SDR for Nonlinear and Linear Analysis

Also of interest is determining the relationship for magnitude of maximum SDR between nonlinear and linear analysis. To determine how the type of analysis affected the calculated magnitude of the maximum SDR, the maximum nonlinear SDR divided by the maximum linear SDR was plotted for all earthquakes verses the initial period, as seen in Fig 4.3a. One noticeable trend was the decrease in scatter as the period of the frames increased.

Due to the large range of scatter seen for most periods in Fig 4.3a, trend lines were plotted for each earthquake to determine if the earthquake characteristic properties impacted this scatter. For most earthquakes, the maximum nonlinear SDR was approximately 1.5 times that of the maximum linear SDR (on average). One exception was the responses to the Hachinohe earthquake, where the ratio of nonlinear to linear maximum SDR ranged from 2.75 to 0.75, depending on the period of the frame. The three trend lines in Fig 4.3a that have a significant negative slope correspond to the earthquakes having T_g greater than approximately 1.0 and a PGA < 0.3 g (Sendai, Santa Barbara, and Hachinohe). Further statistical analysis was performed after removing the Hachinohe, Santa Barbara, and Sendai data from Fig 4.3a. This new analysis is shown in Fig 4.3b. After the removal of the three sets of data the standard deviation and average value for the remaining data was reduced from 0.51 to 0.42 and 1.46 to 1.40, respectively, as can be seen by the dashed lines in Fig 4.3b.

Because of the disparity of trend lines demonstrated by three of the shown earthquake responses (plotted in Fig 4.3a), various earthquake properties were

investigated to determine if these earthquakes could be distinguished from the other seven. In Section 3.2, the characteristic properties were investigated as to their impact on the estimates of nonlinear displacement. These same characteristic properties were re-examined to determine if they directly contributed to the relationships seen in the magnitude ratios of maximum SDR. Figures 4.4a-d show the ratio of nonlinear to linear maximum SDR plotted versus the characteristic properties. As was previously seen for displacement estimates, the corner period (T_g, Fig 4.4a) and the peak ground acceleration (PGA, Fig 4.4b) produced the clearest trend with respect to the scatter associated with the maximum SDR. In general, as the corner period increased, the magnitude of the ratio between nonlinear SDR to linear SDR increased. Responses associated with Sendai, Santa Barbara, and Hachinohe are found at the highest end of the corner period ($Tg > 0.9$ sec.) and the lowest range of PGA ($PGA < 0.3$ g) where the SDR tends to increase. Similarly, this ratio can be seen to decrease as the peak ground acceleration increases. Neither the duration nor the S_{a1} of the earthquakes provided any clear trends as to the effect each had on the ratio of nonlinear to linear maximum SDR.

4.3. Proposed Method to Estimate Location and Magnitude of Maximum SDR

The following method is proposed to estimate the location and magnitude of the maximum SDR for nonlinear analysis using the results of a linear analysis. A general estimate of maximum SDR location based on the frame responses analyzed in this study as shown by the average trend line in Fig 4.5a & 4.5b may be represented as:

$$\text{Max SDR}_{\text{NL-Loc}} = \left(\frac{3}{7} * T_i + 1\right) * \text{Max SDR}_{\text{L-Loc}} \qquad (4.1)$$

where the T_i is the initial period based on gross uncracked sections. There is more scatter associated with the calculation of maximum SDR than with the maximum roof displacement calculated in Chapter 3. The ratio of location is defined in terms of both

story to story and feet to feet in Figures 4.5a & 4.5b, respectively. The scatter of data in Fig 4.5a (story/story) is greater than the scatter of data in Fig 4.5b (ft/ft)

The ratio of the nonlinear maximum SDR location to linear maximum SDR location was also plotted versus the linear maximum MDR to determine if a more pronounced relationship exists for MDR than did for frame period. This estimate of maximum SDR location based on the frames responses can be shown by the average trend line in Fig 4.5c represented as:

$$\text{Max SDR}_{\text{NL-Loc}} = (-\text{MDR} + 2) * \text{Max SDR}_{\text{L-Loc}} \qquad (4.2)$$

The deviation associated with plotting the ratio of nonlinear and linear SDR location versus linear maximum MDR did not provide any additional accuracy. On average, the location of maximum SDR for nonlinear analysis is approximately 1.3 times that calculated using linear SDOF analysis (Fig 4.5a-c)

The relationship that exists between SDR for nonlinear and linear analyses is presented in Table 4.1 where both the magnitude and location of maximum SDR are compared. The table presents the average ratio of nonlinear to linear maximum SDR in terms of location and magnitude, one standard deviation, and a coefficient of variation for each of the ten earthquakes. The average magnitude ratios ranged from 1.18 to 1.85 for Llolleo and Hachinohe respectively, and the average location ratios ranged from 0.98 to 1.78 for Seattle and Taft respectively. When all earthquakes were considered, the average magnitude ratio was found to be 1.46 with one standard deviation and coefficient of variation of .51 and .35, respectively. For location ratios for all earthquakes, the average, standard deviation, and coefficient of variation were 1.34, 0.86, and .64, respectively. From Table 4.1, the average ratio of nonlinear location to linear location was found to be 1.34, with a standard deviation of 0.86 and a coefficient of variation of 0.64.

Because the maximum roof displacement for the frames appeared to be affected differently by properties associated with Sendai, Santa Barbara, and Hachinohe records (Section 3.2), the data in Table 4.1 was re-examined with only the remaining seven records. The coefficient of variation calculated for the magnitude

ratios had only a slight decrease, whereas the location ratio coefficient of variation was nearly identical. The location and magnitude of SDR seem to be less affected by the earthquake properties than maximum roof displacement.

As can be seen in Fig 4.5d, the magnitude of the maximum SDR for a nonlinear MDOF system can be roughly estimated from a linear SDOF analysis using:

$$\text{Max SDR}_{\text{NL-Magnitude}} = 1.5 * \text{Max SDR}_{\text{L-Magnitude}} \quad (4.3)$$

As shown in Table 4.1, the average ratio of nonlinear SDR to linear SDR magnitude was found to be 1.46, with a standard deviation of 0.51 and a coefficient of variation of 0.35. If two standard deviations of the data are to be encompassed, then a ratio of 2.5 is used. The average nonlinear SDR location can be estimated as 1.4 times the height calculated using linear analysis, or a factor of 3.1 to encompass two standard deviations of the data.

The magnitude of the maximum SDR for a nonlinear system was plotted versus MDR as shown Fig 4.5e, and can be roughly estimated from a linear analysis using:

$$\text{Max SDR}_{\text{NL-Loc}} = (-1.2 * \text{MDR} + 2) * \text{Max SDR}_{\text{L-Loc}} \quad (4.4)$$

The plot using MDR appears to have a better trend with maximum SDR than period had, but a large deviation is associated with MDR as well. Interestingly, as the calculated maximum linear MDR increases, the calculated maximum linear SDR tends to over-estimate the magnitude of SDR from linear MDOF analysis.

Chapter 5: Comparison of Proposed Method with Existing Methods

5.0. General

To evaluate the ability of the proposed method to predict displacements, this method was compared with several other simplified methods. The methods were considered simplified based on three determiners: (1) limited amount of information required to perform the analysis regarding the frames proportioning, (2) limited knowledge of the earthquake, and (3) minimal calculation requirements. The method proposed by Iwan and Guyader (2002) demanded the most knowledge, requiring information regarding the ductility of the girders and columns. Both the method proposed by this study (hence know as the Warden method) and the Lepage method require only information pertaining to the earthquake response and initial period of the frame. These "simplified" methods were compared using the frames proportioned for high seismicity with girder depths of L/12. Comparisons will be drawn based on the accuracy of each method to predict the maximum nonlinear roof displacements of the frames in relation to the actual displacements as determined by nonlinear analysis.

5.1 Lepage (1997)

The method proposed by Lepage (as described in section 1.2.2.) was used to evaluate the suite of frames considered. This simple method utilizes a generalized displacement response spectrum for all of the earthquakes in the study:

$$D_{max} = F_a * \alpha * g * T_g * \left(\frac{T}{(2\pi)^2} \right) \qquad (1\text{-}6)$$

For this study, two percent damping was assumed so that F_a is equal to 3.66, g = 386 in/sec^2, α is the participation factor that can be found in Table 2.3, T_g can be found in Table 2.1 for each earthquake, and T is the effective period of each frame. The method proposed by Lepage provided an upper bound for nonlinear displacements with limited calculations.

5.2 Iwan & Guyader (2002)

The method proposed by Iwan and Guyader in 2002 was evaluated for the suite of frames, subjected to high seismicity, which were considered in this study. Results were compared with the maximum nonlinear displacements calculated by computer analysis. The method proposed by Iwan and Guyader required the calculation of a maximum ductility ratio for each frame considered. Their method was based on a SDOF system; however, because the frames investigated in this study were MDOF systems, both the maximum girder ductility ratio and maximum column ductility ratio were considered. The girder ductility was larger in all cases than the column ductility ratio. All frames in this study had a ductility ratio which was less than four, and all frames were analyzed using equation (1-20) from section 1.2.7 as described below.

For $\mu < 4.0$

$$(T_{eq}/T) = 1 + 0.111(\mu-1)^2 - 0.0167(\mu-1)^3$$
$$\xi_{eq} = \xi_0 + 0.0319(\mu-1)^2 - 0.00666(\mu-1)^3 \qquad (1\text{-}20)$$

To determine if an obvious relationship exists between maximum displacement and maximum ductility ratio, several graphs were constructed. Figures 5.1a-b present the pertinent information in this relationship. These figures show very little data to support any relationship existing between maximum roof displacement and ductility. Any slight relationship that might exist would be associated with the girder ductility. Therefore, at this time no conclusive relationship between the maximum displacement and maximum ductility ratio was found.

Another difficulty associated with the method proposed by Iwan and Guyader is that the calculated equivalent damping changes with each frame, as well as with the equivalent period. In contrast, the Warden method and the Lepage method implement one damping ratio and one period adjustment factor for all frames.

The maximum displacement calculated using the method proposed by Iwan is described in the following equation:

$$D_{max,Iwan} = P.F.*S_d\,(T_{eq}, \xi_{eq}) \qquad (5\text{-}1)$$

where an equivalent displacement, S_d, is calculated using the linear response associated with T_{eq} and ξ_{eq}, the equivalent period and damping respectively as calculated by (1-20).

5.3. Warden Method

The Warden method, as described in Section 3.7, uses the response spectrum associated with 10% viscous damping (determined to be the optimum damping level) and an effective building period (estimated as the initial period of the frame modified by a period adjustment factor associated with the appropriate level of seismicity) to produce an estimated maximum roof displacement. The frames used in this comparison of methods were subjected to high seismicity ground motion and had a period adjustment factor of 2.4. This calculation is described by the equation:

$$D_{NL\text{-}EST} = P.F.*S_d\,(T_{eff}, 10\%\ \text{Damping}) \qquad (3\text{-}3)$$

where the estimated maximum nonlinear roof displacement for the frame ($D_{NL\text{-}EST}$) is obtained by using an effective period (T_{eff}), 10%-damped displacement response spectrum (S_d), and the calculated participation factor (P.F.) for the frame.

5.4. Numerical Evaluation of Methods

Equations 1-6, 5-1, and 3-3 were used to calculate the maximum displacement for the frames proportioned for high seismicity. The estimated displacements were compared with results from nonlinear analysis. Figures 5.2a-j show how each method fared for each earthquake. The displacements calculated using both the maximum column ductility (Iwan, col.) and the maximum girder ductility (Iwan, gir.) are both

presented. Figures 5.2a-j provide a concise overall summary for how each method performed for each earthquake. The figures demonstrate that estimates calculated using the method proposed by Iwan experience some difficulty with periods longer than 1.5 seconds in response to the Taft earthquake. In addition, using maximum girder ductility provided a better estimate of maximum roof drift with the Iwan method than maximum column ductility. This can be attributed to the maximum girder ductility being larger than the maximum column ductility. Only the Warden method provides reasonable results in response to the Seattle earthquake. Yet despite the wealth of information these graphs provide, results are not immediately clear as to how well each method accurately predicts displacement for all structures in all earthquakes.

In order to better interpret this data, Figs 5.3a-j show the estimated maximum displacement divided by the calculated maximum nonlinear displacement for each method for each earthquake. Each method can be evaluated based on its variance from one, where a value larger than one is a conservative estimate. Figs 5.3a-j clearly illustrate that, in general, the method proposed by Lepage provides an upper bound, but does not have the accuracy associated with the other two methods. The results associated with the method proposed by Iwan, shown in Figs 5.3a-j, are for girder ductility only. The Iwan method is more likely to underestimate the results than either of the other methods. The Warden method is the most accurate at estimating the displacements based on these frames and earthquakes, but is not always conservative.

In order to better qualify the deviation of each method from the actual displacement, Table 5.1 shows the average percent difference for all frames and each earthquake when each method is compared to the actual response. Figure 5.4 was plotted from this table. One interesting observation came in the comparison of displacements calculated using girder ductility as compared with column ductility. The percent difference was found to be nearly the same no matter which ductility was used. This conclusion could be attributed to the similarities between column and

girder ductility found in this study. The Warden method was the only method to have a percent difference consistently under 20 percent. In Section 3.2 a relationship was seen to exist between the percent difference and T_g. Figure 5.4 clearly shows an increase in error associated with earthquakes of higher T_g for the Iwan and Lepage methods.

Chapter 6: Summary & Conclusion

6.0 General

This study first examines the various existing simplified methods for estimating lateral displacement caused by earthquakes, as well as examines several studies that compare the accuracy of these methods. The literature review is a preface to the development of an improved, simple method to determine nonlinear displacement based on the response of a linear system. Thus, the primary goal of this research is to develop a displacement-based method from an assessment of SDOF system response and nonlinear MDOF system response based on maximum roof displacement and maximum story distortions.

6.1 Summary of Investigation

The focus of this study was to determine the correlation of the nonlinear dynamic response and linear SDOF response of 105 frames to a suite of ten earthquakes in two regions of seismicity. The frames were proportioned in a previous study (Browning, 1998), and the proportioning method is presented in Chapter 2 of this document, as well as a description of the analytical procedures used to complete this study.

Through a comparison of the calculated linear SDOF and nonlinear MDOF responses, an optimum period modification factor and equivalent viscous damping were developed to provide appropriate estimates of maximum structural displacement across a wide range of structures, a wide range of ground motions, and two levels of seismicity.

In light of the fact that the damage associated with an earthquake can be largely attributed to the displacements caused in a building, both the distortions and the locations of these distortions were investigated. The distortions can be characterized by the SDR values calculated using nonlinear dynamic analysis and linear analysis (calculated using the SRSS method). In addition, variations associated

with maximum story distortions calculated from linear SDOF and nonlinear MDOF analyses and the relationship between magnitude and location of story drift ratio in nonlinear MDOF and linear SDOF analysis are defined.

The ability of the proposed Warden method to predict displacements is compared with the methods of Iwan and Gates (1979) and Lepage (1997). These two methods were considered "simplified" based on the limited amount of information required to perform the analysis regarding the frames proportioning, limited knowledge of the earthquake, and minimal calculation requirements. All three methods were compared using the frames proportioned for high seismicity with girder depths of L/12.

6.2 Results of Investigation

Several relationships were established during the course of this study:

1. Overall, the most accurate level of damping (lowest percent difference) occurs with 8%, 10%, and 11% for moderate, high seismicity, and deep girders in high seismicity, respectively. The damping level found to be most accurate for all levels of sesimicity was 10%.
2. A period adjustment factor for 10% damping and moderate seismicity was calculated as 2.0, and a period adjustment factor for high seismicity (the average for frames subjected to high seismicity with girder depth L/10 and L/12) was found to be 2.3.
3. Accordingly, the proposed Warden method estimates maximum nonlinear displacement as:

$$D_{NL\text{-}EST} = P.F. * S_d\left(T_{eff},\ 10\%\ \text{Damping}\right). \qquad (3\text{-}3)$$

where the maximum nonlinear displacement of the frame ($D_{NL\text{-}EST}$) is obtained by using an effective period (T_{eff}, the initial period of the frame modified by the adjustment factor), a 10%-damped displacement response spectrum (S_d), and finally the calculated participation factor (P.F.) for the frame.

$$D_{NL\text{-}EST} = P.F. * S_d\left(T_{eff},\ 10\%\ \text{Damping}\right). \qquad (3\text{-}3)$$

4. For a design procedure, an equation to conservatively predict displacement is:

$$D_{NL\text{-}EST} = P.F.^{*}S_d\left(T_{eff},\ 10\%\ \text{Damping}\right)^{*}\gamma_f \qquad (3\text{-}5)$$

   where γ_f is the safety modification factor equal to 1.4. A design spectrum of 10% damping is required.

5. Several other characteristics were seen to have a large impact on the accuracy of the proposed method, including properties of the earthquake as well as properties of the frames. Earthquakes having characteristic periods longer than one second were seen to have increasing error associated with estimated displacements.

6. The stiffness of the frame was seen to affect the accuracy of the method. Frames proportioned for higher stiffness provided more accurate estimates.

7. Another property of the frame that impacted the overall accuracy of the method was the initial period of the frame. The displacements of frames having relatively short periods (less than one) more closely corresponded to the displacements predicted by nonlinear analysis than to those with longer periods.

8. A relationship between the magnitude and location of maximum distortion from linear to nonlinear analysis was observed. On average, the magnitude of nonlinear SDR was determined to be nearly 1.5 times the linear SDR, and the location of maximum SDR moved higher in the structure by a factor of approximately 1.4. More detailed equations are provided in Section 4.3, which represent average trends with a large amount of scatter.

9. The proposed Warden method was found to more accurately predict the displacements associated with nonlinear response than other methods that required a similar amount of information regarding the frame and earthquake. The Warden method was found to predict the nonlinear displacement within 20% of the calculated displacement.

6.3 Conclusions

This paper presents a simplified method to estimate the nonlinear displacement of a MDOF system using a linear response spectrum with an optimum damping level and period adjustment factor. The research determined that both the properties of the earthquake and the properties of the frames impacted the accuracy of the method. Relationships were also developed relating the location and magnitude of SDR from linear analysis to nonlinear analysis. The proposed Warden method was determined to provide reasonable results for the regular frames and earthquakes considered, as compared with other "simplified" methods requiring limited information. While no current method is 100 percent accurate in predicting damage to any structure subjected to any earthquake, this method and relationships developed in this study can allow for a general estimate of displacements and locations of maximum distortion in buildings subjected to seismic events.

WORKS CITED

Akkar S. D., and E Miranda. "Statistical Evaluation of Approximate Methods for Estimating Maximum Deformation Demands on Existing Structures." *Journal of Structural Engineering (ASCE)* 2005. Vol. 131:160-172.

Albanesi, T., C. Nuti., and I. Vanzi. "A Simplified Procedure to Asses the Seismic Response of Nonlinear Structures." *Earthquake Spectra*, 2000. Vol.16: 715-734.

Algan, B.B. *Drift and Damage Considerations in Earthquake-Resistant Design of Reinforced Concrete Building*. Ph.D. Thesis, Graduate College of the University of Illinois, Urbana, Illinois. 1982.

Applied Technology Council, 1996. *Seismic evaluation and Retrofit of Concrete Buildings, ATC-40 Report*. Redwood City, California. Vols. 1 and 2, 1996.

Browning, J. *Proportioning of Earthquake Resistant Reinforced Concrete Building Structures.* Ph.D. Thesis, School of Civil Engineering, Purdue University, West Lafayette, Indiana. 1998.

Caughey, T.K., "Random Excitation of a System with Bilinear Hysteresis." *Journal of Applied Mechanics, American Society of Mechanical Engineers, Dec., 1960.* Vol. 27, No. 4: 649-652.

Chopra, A.K. *Dynamics of Structures: Theory and Applications to Earthquake Engineering.* Prentice-Hall: New Jersey, 1995.

Chopra, A.K., and R.K Goel. "Capacity-demand-diagram methods for estimating seismic deformations on inelastic structures: SDF systems." *Report No. PEER-1999/02*. Pacific Earthquake Engineering Research Center, University of California, Berkeley, California, 1999.

Chopra, A.K., and R.K Goel. "Evaluation of NSP to estimate seismic deformation: SDF system." *Journal of Structural Engineering (ASCE),* 2000. Vol.126: 482-490.

Clough, R.W., and S.B. Johnston. "Effect of Stiffness Degradation on Earthquake Ductility Requirements." *Proceedings of Japan Earthquake Engineering Symposium.* Tokyo, Japan, 1996: 227-231.

Eberhard, M.O., and M.A. Sozen. "Experiments and Analyses to Study the Seismic Response of Reinforced Concrete Frame-Wall Structures with Yielding Columns." *Civil Engineering Studies, Structural Research Series No. 548.* University of Illinois, Urbana, Illinois, 1989.

Fajfar P. "Capacity Spectrum Method Based on Inelastic Demand Spectra." *Earthquake Engineering and Structural Dynamics,* 1999. Vol. 28: 979-993.

FEMA 273. *NEHRP Guidelines for the Seismic Rehabilitation of Buildings.* Applied Technology Council (ATC-33 Project). Redwood City, California. October, 1997.

FEMA 440. *Improvement of Nonlinear Static Seismis Analysis Procedures.* Applied Technology Council (ATC-55 Project). Redwood City, California, December, 2004.

Freeman, S.A. "Prediction of response of concrete buildings to severe earthquake motion." *American Concrete Institute, Publication SP-55.* Detroit, 1979: 589-605.

Freeman, S.A., J.P Nicoletti, and J.V Tyrell, "Evaluation of Existing Buildings for Seismic Risk-A case study of Puget Sound Naval Shipyard, Bremerton, Washington." *Proceedings of the First U.S. National Conference of Earthquake Engineering.* EERI, Berkley, California. 1975:113-122.

Hogenstad, E. "A study of Combined Bending and Axial Load in Reinforced Concrete Members." *Bulletin Series,* No.399. University of Illinois Engineering Experiment Station, Urbana, Illinois.

Gulkan P., and M. Sozen. "Inelastic Response of Reinforced Concrete Structures to Earthquake Motions." *American Concrete Institute Journal*, 1974. Vol.71: 604-610.

Iwan, W.D., and N.C Gates. "Estimating Earthquake Response of Simple Hysteretic Structures." *Journal of the Engineering Mechanics Division* (ASCE) 1979: 391-405.

Iwan, W.D., and N.C Gates. "The Effective Period and Damping of a Class of Hysteretic Structures *Earthquake Engineering and Structural Dynamics*, 1979b. Vol. 8:199-211.

Iwan, W.D. "Estimating inelastic response spectra from elastic spectra." *Earthquake Engineering and Structural Dynamics, 1980.* Vol. 8: 375-388.

Iwan, W.D., and A.C. Guyader. "A study of the accuracy of the capacity spectrum method in engineering analysis." *Proceedings of the Third U.S.- Japan Workshop on Performance-based Earthquake Eng. Methodology for Reinforced Concrete Building Structures.* Pacific Earthquake Engineering Research Center, Aug. 2002, Seattle, Washington: 86-102.

Jacobsen, L. S. "Damping in Composite Structures," *Proceedings of the Second World Conference on Earthquake Engineering.* Tokyo and Kyoto, Japan, 1960. Vol. 2: 1029-1044.

Jennings, P.C. "Equivalent Viscous Damping for Yielding Structures." *Journal of the Engineering Mechanics Division, Proc. Paper 5793.* ASCE, Feb.,1968. Vol. 94, EM1: 103-116.

Kowalsky, M.J., M.N. Priestly, and G.A. MacRae. "Displacement-based design, a methodology for seismic design applied to sdof reinforced concrete structures." *Structural system Research Project*, Report SSRP-94/16, University of California, San Diego and La Jolla, California, 1994.

Krawinkler, H. "New trends in seismic design methodology." *Proceedings of the Tenth European Conference on Earthquake Engineering.* Vienna, Balkema, Rotterdam, 1994. Vol. 2: 821-830.

Lepage, A. *A Method for Drift-Control in Earthquake-Resistant Design of RC Building Structures.* Ph.D. Thesis. University of Illinois, Urbana-Champaign, Illinois, 1997.

Lin, Y.Y., and K.C. Chang. "An Improved Capacity Spectrum Method for ATC-40. *Earthquake Engineering and Structural Dynamics,* 2003. Vol.32: 2013-2025.

Lin, Y.Y., K.C Chang, and Y.L Wang. "Comparison of Displacement Coefficient Method and Capacity Spectrum Method with Experimental Results of RC Columns." *Earthquake Engineering and Structural Dynamics,* 2004. Vol. 33: 35-48.

Lopez, R. R. "Numerical Model for Nonlinear Response of R/C Frame-Wall Structures." Ph.D. Thesis. Graduate College of the University of Illinois, Urbana, Illinois, 1988.

Lopez, O.A., A.K. Chopra, and J. J. Hernandez. "Evaluation of combination rules for maximum response calculation in multi-component seismic analysis." *Earthquake Engineering and Structural Dynamics*, 2001. Vol.30: 1379-1396.

Matamoros, A., J. Browning, and M. Luft. "Evaluation of Simple Methods for Estimating Drift of Reinforced Concrete Buildings Subjected to Earthquakes. *Earthquake Spectra*, 2003. Vol.19: 839-861.

Miranda, E. "Inelastic displacement ratios for structures on firm sites." *Journal of Structural Engineering,* 2000. Vol.126: 1150-1159.

Miranda, E., and J. Ruiz-Garcia. "Evaluation of Approximate Methods to Estimate Maximum Inelastic Displacement Demands." *Earthquake Engineering and Structural Dynamics,* 2002. Vol.31: 539-560.

Newmark,N.M., and W.J. Hall. *Earthquake Spectra and Design.* Macmillan, New York, 1959.

Newmark, N.M., and W.J. Hall. "Earthquake Spectra and Design." *Earthquake Engineering Research Monograph Series*. EERI Institute, Oakland, California, 1982.

Otani, S. "SAKE: A Computer Program for Inelastic Response of R/C Frames to Earthquakes." *Structural Research Series,* No. 413. Civil Engineering Studies, University of Illinois, Urbana, Illinois, 1974.

Priestley, M.J., and M.J.Kowalsky. "Direct Displacement-Based Seismic Design of Concrete Buildings." *Bulletin of the New Zealand Society for Earthquake Engineering*, 2000. Vol.33: 421-444.

Ramirez, O.M., et al. "Evaluation of Simplified Methods of Analysis of Yielding Structures with Damping Systems. *Earthquake Spectra,* 2002. Vol.18: 501-530.

Rosenblueth E., and I. Herrera. "One kind of hysteretic damping." *Journal of Engineering Mechanics Division.* ASCE, 1964. Vol.90:37-48.

Ruiz-Garcia, J., and E. Miranda, E. "Inelastic displacement ratios for evaluation of existing structures." *Earthquake Engineering Structural Dynamics.* Vol.31:1237-1258

Saiidi, M., and M .A. Sozen. "Simple and Complex Models for Nonlinear Seismic Response of Reinforced Concrete Structures." *Structural Research Series,* No. 465. Civil Engineering Studies, University of Illinois, Urbana, Illinois, 1979.

Saiidi, M., and M.A. Sozen. "User's Manual for the LARZ Family: Computer Programs for Nonlinear Seismic Analysis of Reinforced Concrete Planar Structures." *Structural Research Series,* No. 466. Civil Engineering Studies, University of Illinois, Urbana, Illinois, 1979.

Shibata A., and M. Sozen. "Substitute-Structure Method for Seismic Design in R/C." *Journal of Structural Division.* ASCE, 1976. Vol.102:1-18.

Shimazaki K., and M. Sozen. "Seismic Drift of Reinforced Concrete Structures" *Technical Research Report of Hazama-Gumi, Ltd.* 1976: 145-166.

Spiegel, M.R. *Probability and Statistics.* St. Louis: McGraw-Hill, 1975. pp.259-265.
Takeda, T., M.A. Sozen, and N.N Nielson. "Reinforced concrete response to simulated earthquakes." *Journal of Structural Division.* ASCE, 1970. Vol.96: 2557-2573.

Tsopelas, P., et al. "Evaluation of Simplified Methods of Analysis for Yielding Structures." *National Center for Earthquake Engineering Research Report 97-00012.* State University of New York, Buffalo, New York, 1997

TABLES

Table 2.1 Properties of Ground Motions Considered in this Study

Earthquake	Station	Source	Record Duration (sec)	Peak Ground Acceleration (g)	Characteristic Period T_g (sec)	One-Second Acceleration S_{a1}	Scaled Peak Ground Acceleration (Moderate) (g)	Scaled Peak Ground Acceleration (High) (g)
San Fernando 02-09-1971	Castaic, (CAS) Old Ridge Route, CA	CALTECH (1973b)	30	0.32	0.35	327	0.39	0.78
Northridge 01-17-1994	Tarzana, (TAR) Cedar Hill Nursery, CA	CSMIP (1994)	30	0.99	0.44	175	0.31	0.62
Chile 03-03-1985	Llolleo, (LLO) D.I.C., Chile	Saragoni et al (1985)	75	0.71	0.50	247	0.28	0.55
Imperial Valley 05-18-1940	El Centro, (ELC) Irrigation Distric, CA	CALTECH (1971)	45	0.35	0.55	138	0.25	0.50
Hyogo-Ken-Nanbu 01-17-1995	Kobe, (KOB) KMMO, Japan	JMA (1995)	30[a]	0.83	0.70	450	0.20	0.39
Kern County 07-21-1952	Taft, (TAF) Lincoln School Tunnel, CA	CALTECH (1971)	45	0.16	0.72	441	0.19	0.38
Western Washington 04-13-1949	Seattle, (SEA) Army Base, WA	CALTECH (1973a)	65	0.07	0.89	595	0.15	0.31
Miyagi-Ken-Oki 04-13-1949	Sendai, (SEN) Tohoku University, Japan	Mori and Crouse (1981)	40	0.26	0.95	668	0.14	0.29
Kern County 07-21-1952	Santa Barbara, (SAB) Courthous, CA	CALTECH (1971)	60	0.13	1.03	516	0.13	0.27
Tokachi-Oki 05-16-1968	Hachinohe, (HAC) Harbor, Japan	Mori and Crouse (1981)	35	0.19	1.14	456	0.12	0.24

Notes:
[a] Cut from original record at 25 sec.

Table 2.2a Member Proportions for High Seismicity, Girder Depth =

No. of Stories	Bay Width (ft.)	Story Height (ft.)	Column Base (in.)	Column Top (in.)	Girders Depth (in.)	Girders Width (in.)	Ic Base ($in.^4$)	Ic Top ($in.^4$)	Ig ($in.^4$)
5	20	10	28	28	20	10	51221	51221	6667
	20	12	28	28	20	10	51221	51221	6667
	20	10*	30	30	20	10	67500	67500	6667
	30	10	26	26	30	16	38081	38081	36000
	30	12	28	28	30	16	51221	51221	36000
	30	10*	30	30	30	16	67500	67500	36000
7	20	10	28	28	20	10	51221	51221	6667
	20	12	30	30	20	10	67500	67500	6667
	20	10*	30	30	20	10	67500	67500	6667
	30	10	26	26	30	16	38081	38081	36000
	30	12	28	28	30	16	51221	51221	36000
	30	10*	30	30	30	16	67500	67500	36000
9	20	10	30	28	20	10	67500	51221	6667
	20	12	32	28	20	10	87381	51221	6667
	20	10*	32	28	20	10	87381	51221	6667
	30	10	30	22	30	16	67500	19521	36000
	30	12	30	24	30	16	67500	27648	36000
	30	10*	32	24	30	16	87381	27648	36000
11	20	10	32	28	20	10	87381	51221	6667
	20	12	32	30	20	10	87381	67500	6667
	20	10*	32	30	20	10	87381	67500	6667
	30	10	30	22	30	16	67500	19521	36000
	30	12	32	24	30	16	87381	27648	36000
	30	10*	32	24	30	16	87381	27648	36000
13	20	10	32	30	20	10	87381	67500	6667
	20	12	34	30	20	10	111361	67500	6667
	20	10*	34	30	20	10	111361	67500	6667
	30	10	32	24	30	16	87381	27648	36000
	30	12	32	24	30	16	87381	27648	36000
	30	10*	32	24	30	16	87381	27648	36000
15	20	10	34	30	20	10	111361	67500	6667
	20	12	34	32	20	10	111361	87381	6667
	20	10*	34	32	20	10	111361	87381	6667
	30	10	34	24	30	16	111361	27648	36000
	30	12	34	24	30	16	111361	27648	36000
	30	10*	34	24	30	16	111361	27648	36000
17	20	10	34	32	20	10	111361	87381	6667
	20	12	34	34	20	10	111361	111361	6667
	20	10*	34	34	20	10	111361	111361	6667
	30	10	36	26	30	16	139968	38081	36000
	30	12	36	26	30	16	139968	38081	36000
	30	10*	36	26	30	16	139968	38081	36000

* Tall 1st story (16ft.) with 10-ft. stories above

Table 2.2b Member Proportions for Moderate Seismicity, Girder

No. of Stories	Bay Width (ft.)	Story Height (ft.)	Column Base (in.)	Column Top (in.)	Girders Depth (in.)	Girders Width (in.)	Ic Base ($in.^4$)	Ic Top ($in.^4$)	Ig ($in.^4$)
5	20	10	16	16	20	10	5461	5461	6667
	20	12	16	16	20	10	5461	5461	6667
	20	10*	16	16	20	10	5461	5461	6667
	30	10	22	22	30	16	19521	19521	36000
	30	12	22	22	30	16	19521	19521	36000
	30	10*	22	22	30	16	19521	19521	36000
7	20	10	16	16	20	10	5461	5461	6667
	20	12	16	16	20	10	5461	5461	6667
	20	10*	16	16	20	10	5461	5461	6667
	30	10	24	24	30	16	27648	27648	36000
	30	12	24	24	30	16	27648	27648	36000
	30	10*	24	24	30	16	27648	27648	36000
9	20	10	18	16	20	10	8748	5461	6667
	20	12	18	16	20	10	8748	5461	6667
	20	10*	18	16	20	10	8748	5461	6667
	30	10	28	22	30	16	51221	19521	36000
	30	12	28	22	30	16	51221	19521	36000
	30	10*	28	22	30	16	51221	19521	36000
11	20	10	20	16	20	10	13333	5461	6667
	20	12	20	16	20	10	13333	5461	6667
	20	10*	20	16	20	10	13333	5461	6667
	30	10	30	24	30	16	67500	27648	36000
	30	12	30	24	30	16	67500	27648	36000
	30	10*	30	24	30	16	67500	27648	36000
13	20	10	22	16	20	10	19521	5461	6667
	20	12	22	16	20	10	19521	5461	6667
	20	10*	22	16	20	10	19521	5461	6667
	30	10	34	24	30	16	111361	27648	36000
	30	12	34	24	30	16	111361	27648	36000
	30	10*	34	24	30	16	111361	27648	36000
15	20	10	24	18	20	10	27648	8748	6667
	20	12	24	18	20	10	27648	8748	6667
	20	10*	24	18	20	10	27648	8748	6667
	30	10	36	26	30	16	139968	38081	36000
	30	12	36	26	30	16	139968	38081	36000
	30	10*	36	26	30	16	139968	38081	36000
17	20	10	26	18	20	10	38081	8748	6667
	20	12	26	18	20	10	38081	8748	6667
	20	10*	26	18	20	10	38081	8748	6667
	30	10	38	28	30	16	173761	51221	36000
	30	12	38	28	30	16	173761	51221	36000
	30	10*	38	28	30	16	173761	51221	36000

* Tall 1st story (16ft.) with 10-ft. stories above

Table 2.2c Member Proportions for High Seismicity, Girder Depth = L/10

No. of Stories	Bay Width (ft.)	Story Height (ft.)	Column Base (in.)	Column Top (in.)	Girders Depth (in.)	Girders Width (in.)	Ic Base ($in.^4$)	Ic Top ($in.^4$)	Ig ($in.^4$)
5	20	10	20	20	24	12	13333	13333	13824
	20	12	22	22	24	12	19521	19521	13824
	20	10*	24	24	24	12	27648	27648	13824
7	20	10	20	20	24	12	13333	13333	13824
	20	12	22	22	24	12	19521	19521	13824
	20	10*	24	24	24	12	27648	27648	13824
9	20	10	20	20	24	12	13333	13333	13824
	20	12	22	20	24	12	19521	13333	13824
	20	10*	24	18	24	12	27648	8748	13824
11	20	10	20	20	24	12	13333	13333	13824
	20	12	22	20	24	12	19521	13333	13824
	20	10*	24	18	24	12	27648	8748	13824
13	20	10	22	18	24	12	19521	13333	13824
	20	12	22	22	24	12	19521	13333	13824
	20	10*	26	18	24	12	38081	8748	13824
15	20	10	22	18	24	12	19521	8748	13824
	20	12	26	18	24	12	38081	8748	13824
	20	10*	24	18	24	12	27648	8748	13824
17	20	10	24	18	24	12	27648	8748	13824
	20	12	26	18	24	12	38081	8748	13824
	20	10*	24	18	24	12	27648	8748	13824

* Tall 1st story (16ft.) with 10-ft. stories above

Table 2.3 Period and Participation Factors for the First Three Modes

No. of Stories	Mode	30 ft. Bays						20 ft. Bays					
		10 ft.*		12 ft.*		16 ft.*		10 ft.*		12 ft.*		16 ft.*	
		T	PF	T	PF	T	PF	T	PF	T	PF	T	PF
5	1	0.51	1.28	0.60	1.28	0.57	1.24	0.50	1.30	0.61	1.30	0.56	1.28
	2	0.16	0.41	0.19	0.41	0.17	0.33	0.14	0.45	0.18	0.44	0.16	0.40
	3	0.09	0.19	0.10	0.20	0.09	0.12	0.07	0.21	0.09	0.21	0.07	0.15
7	1	0.68	1.28	0.85	1.28	0.76	1.26	0.69	1.31	0.88	1.30	0.74	1.30
	2	0.22	0.43	0.27	0.43	0.24	0.37	0.21	0.48	0.27	0.46	0.22	0.45
	3	0.12	0.24	0.15	0.24	0.13	0.17	0.10	0.26	0.14	0.26	0.11	0.22
9	1	0.92	1.31	1.11	1.31	0.97	1.29	0.92	1.30	1.10	1.31	0.99	1.30
	2	0.31	0.47	0.38	0.47	0.33	0.43	0.29	0.48	0.35	0.48	0.31	0.46
	3	0.18	0.27	0.22	0.26	0.18	0.22	0.15	0.29	0.19	0.29	0.16	0.26
11	1	1.13	1.32	1.34	1.32	1.18	1.30	1.12	1.31	1.35	1.30	1.19	1.30
	2	0.39	0.48	0.46	0.48	0.40	0.44	0.35	0.48	0.43	0.48	0.37	0.46
	3	0.22	0.27	0.26	0.27	0.22	0.23	0.19	0.30	0.23	0.29	0.20	0.27
13	1	1.30	1.31	1.62	1.32	1.40	1.31	1.32	1.31	1.60	1.31	1.39	1.30
	2	0.44	0.48	0.55	0.49	0.47	0.46	0.42	0.48	0.51	0.48	0.44	0.47
	3	0.25	0.28	0.32	0.28	0.27	0.24	0.23	0.30	0.28	0.30	0.24	0.28
15	1	1.47	1.32	1.82	1.33	1.56	1.32	1.52	1.31	1.83	1.31	1.59	1.31
	2	0.50	0.49	0.63	0.50	0.53	0.47	0.49	0.49	0.58	0.48	0.50	0.48
	3	0.29	0.28	0.36	0.28	0.30	0.26	0.27	0.31	0.32	0.30	0.28	0.29
17	1	1.62	1.30	2.00	1.33	1.71	1.32	1.72	1.31	2.07	1.31	1.78	1.31
	2	0.55	0.43	0.68	0.50	0.58	0.48	0.55	0.49	0.66	0.49	0.57	0.48
	3	0.31	0.20	0.39	0.28	0.33	0.26	0.31	0.31	0.37	0.30	0.31	0.29

T = Period, sec
P.F. = Participation Factor
* Story Height of First Floor

Table 2.4 Maximum Roof Displacement (in.) from Linear Analysis for High Seismicity, Girder Depth = L/12

No. of Stories	Bay Width (ft.)	Total Height (ft.)	Castaic	Tarzana	Llolleo	ElCentro	Kobe	Taft	Seattle	Sendai	Santa Barabara	Hachinohe
5	30	50	6.32	4.45	5.59	4.79	4.02	3.86	3.66	3.52	2.33	3.65
	30	56	4.11	8.73	5.45	5.85	3.63	3.04	3.09	3.06	2.77	3.27
	30	60	3.27	8.90	6.15	6.27	4.29	6.20	2.81	3.84	2.60	3.89
	20	50	6.66	4.48	5.32	4.57	4.23	3.91	2.88	2.67	2.31	3.96
	20	56	4.51	7.63	5.82	6.39	4.19	2.79	3.35	3.26	2.85	3.17
	20	60	3.36	7.85	6.46	6.40	4.64	6.17	2.98	4.21	2.50	4.18
7	30	70	3.90	10.47	4.49	7.69	9.05	6.91	6.14	4.64	2.93	3.54
	30	76	5.91	11.29	8.18	6.88	7.32	7.67	8.58	9.62	4.40	7.79
	30	84	6.48	6.56	9.24	11.50	9.27	8.59	15.15	9.19	7.80	9.27
	20	70	4.00	11.24	4.51	8.28	9.31	7.55	6.61	4.77	3.08	3.65
	20	76	5.80	12.22	7.69	6.94	7.05	7.73	9.99	8.83	4.14	6.72
	20	84	6.92	5.78	8.34	11.83	9.84	8.82	17.25	10.82	9.32	10.15
9	30	90	7.08	5.21	7.83	11.80	10.93	9.08	18.46	16.78	10.49	10.86
	30	96	6.56	4.81	7.51	12.30	10.20	6.52	17.10	20.67	12.09	11.23
	30	108	9.45	5.54	10.62	10.64	9.88	7.74	7.74	14.31	8.80	17.01
	20	90	6.96	5.13	7.80	11.70	10.86	9.01	18.35	16.52	10.38	10.79
	20	96	6.91	4.87	7.28	12.23	10.86	6.30	16.79	19.25	12.16	11.30
	20	108	9.67	5.04	9.71	10.77	9.98	7.74	15.00	14.21	9.62	16.39
11	30	110	9.20	5.89	11.54	11.12	9.86	7.54	13.13	15.15	8.62	17.56
	30	116	8.22	6.73	9.90	11.86	9.54	8.62	14.27	18.19	9.03	17.89
	30	132	6.53	6.54	9.77	7.46	13.17	9.93	17.20	15.90	9.40	13.26
	20	110	9.44	5.54	11.03	10.71	9.85	7.73	13.51	14.36	8.51	17.22
	20	116	8.15	6.85	9.77	11.75	9.55	8.81	14.36	18.22	9.14	17.97
	20	132	6.77	6.57	9.62	7.10	13.13	9.74	16.67	15.38	9.27	12.84
13	30	130	6.38	6.38	10.11	8.34	12.48	9.94	17.79	17.28	9.55	14.63
	30	136	8.17	6.61	10.29	8.64	13.49	9.28	13.51	14.45	11.51	11.28
	30	156	6.30	11.22	8.90	12.14	12.55	9.30	8.08	17.26	15.81	7.75
	20	130	6.22	6.36	9.78	7.49	12.68	9.97	17.95	16.49	9.40	13.68
	20	136	7.92	6.77	10.14	8.34	13.43	9.16	14.11	14.38	10.74	11.45
	20	156	6.59	11.13	8.83	11.43	12.97	9.25	7.54	16.77	15.31	7.85
15	30	150	11.48	8.71	10.13	9.09	14.19	9.28	10.47	15.29	14.55	9.73
	30	156	8.67	11.37	9.16	10.99	13.76	9.18	8.34	15.98	14.69	7.99
	30	180	6.27	10.10	11.07	14.15	11.59	9.41	6.59	19.96	21.32	7.84
	20	150	10.59	10.41	9.29	9.91	14.08	8.98	8.72	14.19	13.47	8.15
	20	156	11.19	11.21	8.84	11.19	13.16	9.21	7.59	16.53	15.12	7.90
	20	180	6.19	10.23	10.44	13.94	11.26	9.13	6.04	19.54	22.08	7.87
17	30	170	6.29	11.25	8.92	12.21	12.53	9.34	8.19	17.34	15.90	7.77
	30	176	6.03	10.31	9.16	13.63	11.89	9.41	7.86	18.43	16.56	7.41
	30	204	6.50	14.22	13.16	17.10	10.78	9.95	7.05	15.78	27.05	13.47
	20	170	6.05	9.97	9.62	13.72	11.84	9.29	7.52	18.62	16.50	7.27
	20	176	5.94	10.39	11.34	13.95	11.56	9.19	8.02	19.51	17.22	7.22
	20	204	6.15	16.93	12.89	17.26	10.06	9.38	6.46	14.30	24.98	17.28

Table 2.5 Maximum Mean Drift Ratio (%) from Linear Analysis for High Seismicity, Girder Depth = L/12

No. of Stories	Bay Width (ft.)	Total Height (ft.)	Castaic	Tarzana	Llolleo	ElCentro	Kobe	Taft	Seattle	Sendai	Santa Barabara	Hachinohe
5	30	50	1.05	0.74	0.93	0.80	0.67	0.64	0.61	0.59	0.39	0.61
	30	56	0.61	1.30	0.81	0.87	0.54	0.45	0.46	0.46	0.41	0.49
	30	60	0.45	1.24	0.85	0.87	0.60	0.86	0.39	0.53	0.36	0.54
	20	50	1.11	0.75	0.89	0.76	0.70	0.65	0.48	0.44	0.38	0.66
	20	56	0.67	1.13	0.87	0.95	0.62	0.41	0.50	0.48	0.42	0.47
	20	60	0.47	1.09	0.90	0.89	0.64	0.86	0.41	0.59	0.35	0.58
7	30	70	0.46	1.25	0.53	0.92	1.08	0.82	0.73	0.55	0.35	0.42
	30	76	0.65	1.24	0.90	0.75	0.80	0.84	0.94	1.06	0.48	0.85
	30	84	0.64	0.65	0.92	1.14	0.92	0.85	1.50	0.91	0.77	0.92
	20	70	0.48	1.34	0.54	0.99	1.11	0.90	0.79	0.57	0.37	0.43
	20	76	0.64	1.34	0.84	0.76	0.77	0.85	1.10	0.97	0.45	0.74
	20	84	0.69	0.57	0.83	1.17	0.98	0.88	1.71	1.07	0.92	1.01
9	30	90	0.66	0.48	0.72	1.09	1.01	0.84	1.71	1.55	0.97	1.01
	30	96	0.57	0.42	0.65	1.07	0.89	0.57	1.48	1.79	1.05	0.97
	30	108	0.73	0.43	0.82	0.82	0.76	0.60	0.60	1.10	0.68	1.31
	20	90	0.64	0.47	0.72	1.08	1.01	0.83	1.70	1.53	0.96	1.00
	20	96	0.60	0.42	0.63	1.06	0.94	0.55	1.46	1.67	1.06	0.98
	20	108	0.75	0.39	0.75	0.83	0.77	0.60	1.16	1.10	0.74	1.26
11	30	110	0.70	0.45	0.87	0.84	0.75	0.57	0.99	1.15	0.65	1.33
	30	116	0.59	0.48	0.71	0.85	0.69	0.62	1.03	1.31	0.65	1.29
	30	132	0.41	0.41	0.62	0.47	0.83	0.63	1.09	1.00	0.59	0.84
	20	110	0.72	0.42	0.84	0.81	0.75	0.59	1.02	1.09	0.64	1.30
	20	116	0.59	0.49	0.70	0.84	0.69	0.63	1.03	1.31	0.66	1.29
	20	132	0.43	0.41	0.61	0.45	0.83	0.61	1.05	0.97	0.59	0.81
13	30	130	0.41	0.41	0.65	0.53	0.80	0.64	1.14	1.11	0.61	0.94
	30	136	0.50	0.40	0.63	0.53	0.83	0.57	0.83	0.89	0.71	0.69
	30	156	0.34	0.60	0.48	0.65	0.67	0.50	0.43	0.92	0.84	0.41
	20	130	0.40	0.41	0.63	0.48	0.81	0.64	1.15	1.06	0.60	0.88
	20	136	0.49	0.41	0.62	0.51	0.82	0.56	0.86	0.88	0.66	0.70
	20	156	0.35	0.59	0.47	0.61	0.69	0.49	0.40	0.90	0.82	0.42
15	30	150	0.64	0.48	0.56	0.51	0.79	0.52	0.58	0.85	0.81	0.54
	30	156	0.46	0.61	0.49	0.59	0.74	0.49	0.45	0.85	0.78	0.43
	30	180	0.29	0.47	0.51	0.66	0.54	0.44	0.31	0.92	0.99	0.36
	20	150	0.59	0.58	0.52	0.55	0.78	0.50	0.48	0.79	0.75	0.45
	20	156	0.60	0.60	0.47	0.60	0.70	0.49	0.41	0.88	0.81	0.42
	20	180	0.29	0.47	0.48	0.65	0.52	0.42	0.28	0.90	1.02	0.36
17	30	170	0.31	0.55	0.44	0.60	0.61	0.46	0.40	0.85	0.78	0.38
	30	176	0.29	0.49	0.43	0.65	0.56	0.45	0.37	0.87	0.78	0.35
	30	204	0.27	0.58	0.54	0.70	0.44	0.41	0.29	0.64	1.10	0.55
	20	170	0.30	0.49	0.47	0.67	0.58	0.46	0.37	0.91	0.81	0.36
	20	176	0.28	0.49	0.54	0.66	0.55	0.43	0.38	0.92	0.82	0.34
	20	204	0.25	0.69	0.53	0.70	0.41	0.38	0.26	0.58	1.02	0.71

Table 2.6 Maximum SDR (%) from Linear Analysis for High Seismicity, Girder Depth = L/12

No. of Stories	Bay Width (ft.)	Total Height (ft.)	Castaic	Tarzana	Llolleo	ElCentro	Kobe	Taft	Seattle	Sendai	Santa Barabara	Hachinohe
5	30	50	1.43	1.01	1.27	1.09	0.91	0.88	0.83	0.80	0.53	0.83
	30	56	0.82	1.74	1.09	1.17	0.73	0.61	0.62	0.61	0.55	0.65
	30	60	0.61	1.69	1.16	1.19	0.81	1.18	0.53	0.73	0.49	0.74
	20	50	1.41	0.95	1.13	0.97	0.90	0.83	0.61	0.56	0.49	0.84
	20	56	0.87	1.48	1.13	1.24	0.82	0.54	0.65	0.63	0.55	0.62
	20	60	0.60	1.41	1.16	1.15	0.84	1.11	0.54	0.76	0.45	0.75
7	30	70	0.66	1.73	0.77	1.27	1.50	1.15	1.02	0.77	0.48	0.59
	30	76	0.91	1.72	1.25	1.05	1.11	1.17	1.31	1.46	0.67	1.19
	30	84	0.91	0.92	1.29	1.60	1.29	1.19	2.10	1.28	1.08	1.29
	20	70	0.63	1.82	0.72	1.34	1.51	1.22	1.07	0.77	0.50	0.59
	20	76	0.86	1.80	1.14	1.03	1.04	1.14	1.48	1.30	0.61	0.99
	20	84	0.94	0.78	1.14	1.62	1.35	1.20	2.36	1.48	1.28	1.39
9	30	90	0.85	0.67	0.99	1.52	1.41	1.17	2.39	2.19	1.36	1.41
	30	96	0.80	0.58	0.86	1.40	1.16	0.75	1.94	2.34	1.37	1.27
	30	108	0.97	0.69	1.08	1.08	1.00	0.78	0.78	1.49	0.91	1.77
	20	90	0.89	0.67	1.00	1.50	1.39	1.15	2.35	2.11	1.33	1.38
	20	96	0.83	0.61	0.86	1.45	1.39	0.74	1.99	2.29	1.44	1.34
	20	108	1.05	0.56	1.02	1.13	1.06	0.83	1.58	1.49	1.01	1.72
11	30	110	0.90	0.70	1.19	1.14	1.00	0.75	1.37	1.59	0.90	1.85
	30	116	0.81	0.76	0.95	1.13	0.92	0.83	1.36	1.72	0.86	1.69
	30	132	0.64	0.70	0.81	0.67	1.09	0.85	1.49	1.37	0.81	1.15
	20	110	1.03	0.62	1.16	1.13	1.04	0.83	1.42	1.52	0.90	1.82
	20	116	0.85	0.77	0.98	1.18	0.96	0.89	1.44	1.83	0.92	1.80
	20	132	0.62	0.71	0.87	0.63	1.16	0.86	1.48	1.36	0.82	1.14
13	30	130	0.59	0.59	0.87	0.72	1.10	0.89	1.61	1.56	0.86	1.33
	30	136	0.77	0.67	0.85	0.76	1.10	0.76	1.09	1.17	0.93	0.91
	30	156	0.57	0.82	0.71	0.89	0.91	0.69	0.57	1.30	1.20	0.57
	20	130	0.60	0.70	0.89	0.68	1.15	0.91	1.63	1.50	0.85	1.24
	20	136	0.71	0.74	0.88	0.73	1.15	0.78	1.20	1.23	0.92	0.98
	20	156	0.60	0.84	0.71	0.87	0.98	0.70	0.58	1.25	1.14	0.60
15	30	150	0.91	0.67	0.80	0.71	1.03	0.70	0.76	1.14	1.09	0.73
	30	156	0.71	0.87	0.77	0.85	0.98	0.66	0.62	1.13	1.02	0.57
	30	180	0.44	0.70	0.71	0.88	0.72	0.62	0.43	1.25	1.37	0.51
	20	150	0.88	0.85	0.75	0.79	1.11	0.72	0.68	1.11	1.05	0.65
	20	156	0.87	0.86	0.72	0.87	1.00	0.71	0.59	1.24	1.14	0.62
	20	180	0.47	0.87	0.71	0.94	0.75	0.62	0.41	1.28	1.44	0.53
17	30	170	0.52	0.81	0.69	0.87	0.84	0.61	0.56	1.13	1.03	0.51
	30	176	0.48	0.88	0.65	0.91	0.76	0.62	0.52	1.15	1.03	0.50
	30	204	0.40	0.91	0.71	0.95	0.73	0.62	0.48	0.84	1.48	0.71
	20	170	0.49	0.74	0.72	0.98	0.82	0.64	0.53	1.28	1.13	0.50
	20	176	0.46	0.82	0.79	0.95	0.78	0.61	0.54	1.29	1.14	0.49
	20	204	0.42	1.02	0.75	1.01	0.67	0.60	0.46	0.83	1.43	0.99

Table 2.7 Location (story) of Maximum SDR from Linear Analysis for High Seismicity, Girder Depth = L/12

No. of Stories	Bay Width (ft.)	Total Height (ft.)	Castaic	Tarzana	Llolleo	ElCentro	Kobe	Taft	Seattle	Sendai	Santa Barabara	Hachinohe
5	30	50	2	2	2	2	2	2	2	2	2	2
	30	56	1	1	1	1	1	1	1	1	1	1
	30	60	2	2	2	2	2	2	2	2	2	2
	20	50	3	3	3	3	3	3	3	3	3	3
	20	56	2	2	2	2	2	2	2	2	2	2
	20	60	3	3	3	3	3	3	3	3	3	3
7	30	70	2	2	2	2	2	2	2	2	2	2
	30	76	1	1	1	1	1	1	1	1	1	1
	30	84	2	2	2	2	2	2	2	2	2	2
	20	70	3	3	3	3	3	3	3	3	3	3
	20	76	2	2	2	2	2	2	2	2	2	2
	20	84	3	3	3	3	3	3	3	3	3	3
9	30	90	2	2	5	5	5	5	5	5	5	5
	30	96	2	2	2	2	2	2	2	2	2	2
	30	108	2	2	5	5	5	2	2	5	5	5
	20	90	3	3	3	3	3	3	3	3	3	3
	20	96	2	2	3	3	3	3	3	3	3	3
	20	108	3	3	3	3	3	3	3	4	4	3
11	30	110	3	2	6	6	6	6	6	6	6	6
	30	116	2	2	2	2	2	2	2	2	2	2
	30	132	2	2	3	2	6	6	6	6	6	6
	20	110	3	3	4	4	4	3	4	4	4	4
	20	116	2	2	3	3	3	3	3	3	3	3
	20	132	3	3	3	3	4	4	4	4	4	4
13	30	130	3	3	3	6	6	6	6	6	6	6
	30	136	2	2	2	2	2	2	6	6	6	2
	30	156	2	3	2	3	6	6	6	6	6	6
	20	130	3	3	4	4	4	4	4	4	4	4
	20	136	3	2	3	3	3	3	4	4	4	4
	20	156	3	4	3	4	4	4	3	4	4	4
15	30	150	3	3	3	3	3	3	3	8	8	3
	30	156	2	2	2	2	2	2	2	2	2	2
	30	180	2	3	3	3	3	3	3	8	8	3
	20	150	4	4	4	4	4	4	4	5	5	4
	20	156	3	3	3	3	3	3	3	4	4	3
	20	180	3	3	4	4	4	3	3	4	4	4
17	30	170	3	3	3	3	4	4	3	4	4	4
	30	176	2	2	2	2	2	2	2	3	3	2
	30	204	3	3	3	3	3	3	3	4	9	4
	20	170	3	4	4	4	4	5	4	5	5	5
	20	176	2	3	3	3	4	4	3	4	4	3
	20	204	3	4	4	4	3	3	3	4	5	5

Table 2.8a Maximum Roof Displacement (in.) from Non-Linear Analysis for High Seismicity, Girder Depth = L/12

No. of Stories	Bay Width (ft.)	Total Height (ft.)	Castaic	Tarzana	Llolleo	ElCentro	Kobe	Taft	Seattle	Sendai	Santa Barabara	Hachinohe
5	30	50	4.20	3.48	4.47	6.42	6.82	4.67	8.32	7.99	7.44	6.29
	30	56	4.74	4.45	5.35	6.50	7.48	5.65	7.44	8.63	7.35	6.73
	30	60	5.06	5.24	6.25	6.08	8.10	6.69	6.22	9.36	7.00	7.70
	20	50	5.53	3.92	5.07	7.15	7.38	4.92	8.82	8.67	7.99	6.63
	20	56	5.35	4.59	5.63	7.03	8.25	6.24	7.18	9.23	7.82	7.62
	20	60	5.75	5.85	7.40	7.15	7.97	7.58	6.00	12.56	7.22	10.32
7	30	70	4.73	6.62	6.61	9.46	7.72	8.58	4.63	9.62	9.55	12.66
	30	76	4.94	6.76	7.18	9.98	7.86	8.79	4.56	10.29	10.47	12.81
	30	84	5.06	8.60	6.77	13.38	7.29	8.41	4.63	9.34	13.44	10.51
	20	70	5.64	7.89	7.21	10.80	8.26	9.39	5.04	10.47	10.69	14.74
	20	76	5.68	8.90	8.24	12.19	8.12	9.27	5.04	11.06	12.29	14.19
	20	84	5.91	10.61	7.97	14.41	7.32	8.75	4.94	10.02	15.73	11.28
9	30	90	5.29	8.86	6.87	13.45	6.87	8.71	5.97	8.27	14.51	9.38
	30	96	5.34	9.12	7.50	13.54	6.79	8.53	6.24	8.16	13.46	9.27
	30	108	5.72	7.68	6.39	15.21	8.33	7.89	6.45	9.46	13.84	9.19
	20	90	6.06	8.96	8.32	14.29	7.02	8.44	5.71	8.67	15.41	9.86
	20	96	6.17	8.86	8.36	13.94	6.81	8.37	6.91	9.39	16.22	9.46
	20	108	6.62	8.29	7.46	13.34	8.21	8.46	7.44	11.05	15.11	9.69
11	30	110	5.75	7.59	6.59	15.08	7.73	8.27	6.12	11.64	15.08	8.91
	30	116	5.77	7.33	6.78	15.63	7.84	9.02	6.04	12.33	16.02	9.38
	30	132	6.48	8.34	9.55	13.20	8.50	11.80	5.55	14.59	13.96	8.31
	20	110	6.82	8.13	7.96	14.09	8.14	10.16	6.96	10.70	13.28	9.05
	20	116	7.24	7.95	9.08	14.41	7.85	11.39	7.38	12.34	14.59	9.72
	20	132	8.38	12.64	10.76	14.84	8.47	11.21	7.88	14.28	15.70	9.83
13	30	130	6.24	7.87	9.08	12.96	8.39	11.64	5.34	14.63	13.85	8.08
	30	136	6.52	9.27	9.63	13.44	8.61	11.02	5.31	14.14	13.98	8.73
	30	156	6.96	13.70	8.07	13.68	8.57	11.92	6.79	11.09	13.81	9.23
	20	130	8.33	12.44	10.58	14.69	8.39	11.23	8.32	14.03	15.37	9.99
	20	136	8.53	12.17	10.56	15.09	8.57	11.16	8.40	14.28	16.17	10.97
	20	156	9.26	15.13	8.15	13.62	8.78	15.51	9.19	12.96	14.00	11.48
15	30	150	6.74	12.23	8.97	14.01	8.70	11.14	5.62	12.94	14.15	9.33
	30	156	6.87	12.93	8.46	14.01	8.52	11.54	6.43	11.55	14.03	9.11
	30	180	7.34	14.24	5.77	11.92	8.38	15.78	9.18	11.31	11.67	12.16
	20	150	9.13	14.70	8.74	14.30	8.85	13.87	8.56	12.46	14.74	11.23
	20	156	9.22	15.17	8.17	14.30	9.05	15.70	9.48	13.08	14.14	11.63
	20	180	9.66	15.70	7.26	11.59	8.51	20.98	7.74	12.40	12.42	13.83
17	30	170	7.11	13.93	7.73	13.27	8.48	13.13	7.83	11.27	13.41	9.92
	30	176	7.21	13.73	6.71	12.64	8.35	14.67	8.71	11.21	12.71	10.90
	30	204	7.86	13.72	6.83	13.35	8.25	19.56	7.85	10.83	14.15	12.63
	20	170	9.51	16.17	7.97	11.89	8.78	17.56	8.61	12.82	11.75	13.20
	20	176	9.48	15.99	7.75	11.62	8.68	20.51	7.88	12.69	12.33	13.64
	20	204	9.55	12.90	6.86	14.62	7.48	18.81	7.37	10.53	14.70	14.47

Table 2.8b Maximum Roof Displacement (in.) from Non-Linear Analysis for Moderate Seismicity, Girder Depth = L/12

No. of Stories	Bay Width (ft.)	Total Height (ft.)	Castaic	Tarzana	Llolleo	ElCentro	Kobe	Taft	Seattle	Sendai	Santa Barabara	Hachinohe
5	30	50	2.19	1.70	2.22	3.03	3.83	2.15	4.30	5.07	3.04	4.33
	30	56	2.14	2.75	3.52	3.38	4.12	3.51	2.27	5.28	4.95	3.00
	30	60	2.12	3.11	3.54	3.47	4.32	3.27	2.69	4.81	4.52	3.28
	20	50	2.14	3.13	3.47	4.19	4.09	3.88	2.21	6.14	6.09	3.80
	20	56	2.25	4.12	3.22	6.71	2.84	3.46	2.03	3.89	4.96	7.02
	20	60	2.33	4.02	3.19	6.82	3.47	3.92	2.31	4.66	5.35	7.36
7	30	70	2.08	3.16	3.58	3.68	4.15	3.61	2.28	5.68	5.65	3.44
	30	76	2.09	3.40	3.17	5.29	3.53	3.85	1.96	4.73	6.03	5.60
	30	84	2.19	3.64	3.12	6.25	3.43	3.92	2.20	4.92	5.49	7.24
	20	70	2.50	4.49	3.41	7.41	3.19	3.72	3.18	4.43	4.26	7.56
	20	76	2.67	3.25	2.65	7.28	3.63	4.67	3.01	4.55	3.59	7.43
	20	84	2.77	3.74	3.52	8.11	3.40	4.98	2.52	6.22	3.99	6.91
9	30	90	2.24	3.43	3.28	6.32	3.80	4.08	2.34	5.15	5.78	7.06
	30	96	2.41	4.64	3.34	7.08	2.99	3.94	2.76	4.08	4.85	8.82
	30	108	2.62	4.21	3.28	7.56	3.75	3.86	3.25	4.29	4.74	9.12
	20	90	2.78	3.78	3.46	8.33	3.31	4.79	2.61	6.39	4.14	7.33
	20	96	2.79	4.35	4.10	7.46	3.16	5.21	2.38	5.96	3.70	6.04
	20	108	3.02	6.11	3.91	6.25	3.80	5.41	2.70	5.52	4.22	6.65
11	30	110	2.47	4.65	3.34	7.19	3.11	3.96	3.06	4.19	4.44	9.04
	30	116	2.60	4.26	3.40	7.33	3.58	3.65	3.27	4.37	4.47	8.37
	30	132	2.71	3.60	3.04	8.17	3.70	4.30	2.89	5.94	3.98	7.85
	20	110	2.98	5.70	4.11	6.44	3.97	5.34	2.71	5.97	4.18	6.72
	20	116	3.14	5.93	3.77	6.47	3.73	5.57	2.93	5.12	4.38	6.41
	20	132	3.40	6.79	3.04	6.14	3.88	7.24	3.95	5.37	4.99	5.99
13	30	130	2.69	3.72	3.22	7.09	3.90	3.79	3.22	4.63	4.53	8.29
	30	136	2.71	3.52	3.10	8.47	3.75	4.20	2.95	5.87	4.05	8.07
	30	156	2.81	4.78	4.26	7.58	3.68	5.41	2.59	6.51	3.95	6.54
	20	130	3.32	6.70	3.55	6.40	4.00	6.23	3.82	5.20	4.62	6.46
	20	136	3.44	6.65	3.08	6.30	3.88	7.04	3.74	5.38	0.00	6.07
	20	156	3.49	6.85	3.07	5.81	3.84	9.43	3.80	5.11	5.88	6.33
15	30	150	2.78	3.97	3.55	8.58	3.23	4.75	2.63	6.60	4.22	7.45
	30	156	2.80	4.45	4.04	8.24	3.45	5.26	2.47	6.57	3.83	6.71
	30	180	3.09	6.36	4.11	6.42	3.93	5.36	2.82	5.91	4.37	6.74
	20	150	3.56	7.02	3.26	5.85	3.96	7.39	4.00	5.43	5.21	5.93
	20	156	3.59	6.91	2.95	5.68	3.88	7.71	3.66	5.60	5.61	5.73
	20	180	3.85	6.68	3.44	5.96	3.71	9.60	3.02	5.52	5.79	6.84
17	30	170	2.87	5.11	4.30	7.42	3.77	5.39	2.76	6.39	4.00	6.57
	30	176	3.00	5.41	4.29	6.56	3.77	5.30	2.90	6.06	4.08	6.81
	30	204	3.34	7.16	3.82	6.37	4.05	6.18	3.44	5.37	4.56	6.54
	20	170	3.66	6.99	3.01	6.36	3.97	9.33	3.81	5.49	5.84	6.48
	20	176	3.71	6.84	3.30	6.24	3.86	10.27	3.29	5.05	5.96	6.67
	20	204	4.40	7.13	3.84	6.61	3.41	8.50	3.22	5.66	6.08	7.28

Table 2.8c Maximum Roof Displacement (in.) from Non-Linear Analysis for High Seismicity, Girder Depth = L/10

No. of Stories	Bay Width (ft.)	Total Height (ft.)	Castaic	Tarzana	Llolleo	ElCentro	Kobe	Taft	Seattle	Sendai	Santa Barabara	Hachinohe
5	20	50	4.00	3.22	4.39	6.13	6.64	4.41	7.91	7.57	6.01	7.01
	20	56	4.22	3.01	3.85	5.99	6.17	4.87	6.78	7.27	5.67	6.34
	20	60	4.62	4.48	5.49	6.09	7.83	6.07	6.72	8.44	6.97	6.80
7	20	70	4.63	6.04	6.34	8.87	7.39	8.16	4.59	8.93	12.32	9.05
	20	76	4.43	5.84	6.15	7.74	7.53	8.47	4.28	8.97	12.31	8.10
	20	84	4.87	7.39	6.78	12.03	7.27	8.44	4.42	9.33	10.74	12.60
9	20	90	5.06	8.56	6.58	12.41	6.33	8.24	5.23	7.77	8.81	12.49
	20	96	5.14	8.35	6.91	12.21	6.60	8.42	5.61	8.11	8.43	13.10
	20	108	5.43	7.77	6.30	13.46	8.05	7.81	6.78	8.86	8.96	13.02
11	20	110	5.41	7.19	6.08	13.78	8.18	7.43	5.95	9.45	8.52	12.58
	20	116	5.57	6.99	6.10	14.34	7.30	7.81	5.34	11.62	8.95	15.26
	20	132	5.86	8.22	8.94	12.70	7.92	8.88	5.12	13.08	8.07	12.78
13	20	130	5.69	8.03	8.70	12.47	7.98	8.71	5.10	12.94	8.49	12.72
	20	136	5.82	8.13	8.60	12.00	7.55	9.31	4.93	13.25	8.56	12.90
	20	156	6.42	12.37	8.27	12.17	8.25	11.13	5.77	10.82	8.64	13.52
15	20	150	6.15	12.26	8.94	12.09	8.43	11.26	5.98	11.54	8.72	13.20
	20	156	6.36	11.80	8.44	12.56	7.90	11.50	5.69	10.40	8.80	13.43
	20	180	6.95	13.43	5.89	12.81	8.42	11.02	9.03	11.23	11.16	11.85
17	20	170	6.60	13.11	6.73	12.12	8.48	10.65	7.69	10.82	10.10	12.63
	20	176	6.79	12.87	5.88	12.03	7.86	10.85	7.97	10.91	11.23	11.77
	20	204	7.13	14.07	7.18	12.03	8.15	13.15	8.78	10.54	12.67	13.00

Table 2.9a Maximum MDR (%) from Non-Linear Analysis for High Seismicity, Girder Depth = L/12

No. of Stories	Bay Width (ft.)	Total Height (ft.)	Castaic	Tarzana	Llolleo	ElCentro	Kobe	Taft	Seattle	Sendai	Santa Barabara	Hachinohe
5	30	50	0.70	0.58	0.75	1.07	1.14	0.78	1.39	1.33	1.05	1.24
	30	56	0.71	0.66	0.80	0.97	1.11	0.84	1.11	1.28	1.00	1.09
	30	60	0.70	0.73	0.87	0.84	1.12	0.93	0.86	1.30	1.07	0.97
	20	50	0.92	0.65	0.84	1.19	1.23	0.82	1.47	1.45	1.11	1.33
	20	56	0.80	0.68	0.84	1.05	1.23	0.93	1.07	1.37	1.13	1.16
	20	60	0.80	0.81	1.03	0.99	1.11	1.05	0.83	1.74	1.43	1.00
7	30	70	0.56	0.79	0.79	1.13	0.92	1.02	0.55	1.15	1.51	1.14
	30	76	0.54	0.74	0.79	1.09	0.86	0.96	0.50	1.13	1.40	1.15
	30	84	0.50	0.85	0.67	1.33	0.72	0.83	0.46	0.93	1.04	1.33
	20	70	0.67	0.94	0.86	1.29	0.98	1.12	0.60	1.25	1.75	1.27
	20	76	0.62	0.98	0.90	1.34	0.89	1.02	0.55	1.21	1.56	1.35
	20	84	0.59	1.05	0.79	1.43	0.73	0.87	0.49	0.99	1.12	1.56
9	30	90	0.49	0.82	0.64	1.25	0.64	0.81	0.55	0.77	0.87	1.34
	30	96	0.46	0.79	0.65	1.18	0.59	0.74	0.54	0.71	0.80	1.17
	30	108	0.44	0.59	0.49	1.17	0.64	0.61	0.50	0.73	0.71	1.07
	20	90	0.56	0.83	0.77	1.32	0.65	0.78	0.53	0.80	0.91	1.43
	20	96	0.54	0.77	0.73	1.21	0.59	0.73	0.60	0.82	0.82	1.41
	20	108	0.51	0.64	0.58	1.03	0.63	0.65	0.57	0.85	0.75	1.17
11	30	110	0.44	0.57	0.50	1.14	0.59	0.63	0.46	0.88	0.67	1.14
	30	116	0.41	0.53	0.49	1.12	0.56	0.65	0.43	0.89	0.67	1.15
	30	132	0.41	0.53	0.60	0.83	0.54	0.74	0.35	0.92	0.52	0.88
	20	110	0.52	0.62	0.60	1.07	0.62	0.77	0.53	0.81	0.69	1.01
	20	116	0.52	0.57	0.65	1.03	0.56	0.82	0.53	0.89	0.70	1.05
	20	132	0.53	0.80	0.68	0.94	0.53	0.71	0.50	0.90	0.62	0.99
13	30	130	0.40	0.50	0.58	0.83	0.54	0.75	0.34	0.94	0.52	0.89
	30	136	0.40	0.57	0.59	0.82	0.53	0.68	0.33	0.87	0.53	0.86
	30	156	0.37	0.73	0.43	0.73	0.46	0.64	0.36	0.59	0.49	0.74
	20	130	0.53	0.80	0.68	0.94	0.54	0.72	0.53	0.90	0.64	0.99
	20	136	0.52	0.75	0.65	0.92	0.53	0.68	0.51	0.87	0.67	0.99
	20	156	0.49	0.81	0.44	0.73	0.47	0.83	0.49	0.69	0.61	0.75
15	30	150	0.37	0.68	0.50	0.78	0.48	0.62	0.31	0.72	0.52	0.79
	30	156	0.37	0.69	0.45	0.75	0.45	0.62	0.34	0.62	0.49	0.75
	30	180	0.34	0.66	0.27	0.55	0.39	0.73	0.43	0.52	0.56	0.54
	20	150	0.51	0.82	0.49	0.79	0.49	0.77	0.48	0.69	0.62	0.82
	20	156	0.49	0.81	0.44	0.76	0.48	0.84	0.51	0.70	0.62	0.76
	20	180	0.45	0.73	0.34	0.54	0.39	0.97	0.36	0.57	0.64	0.57
17	30	170	0.35	0.68	0.38	0.65	0.42	0.64	0.38	0.55	0.49	0.66
	30	176	0.34	0.65	0.32	0.60	0.40	0.69	0.41	0.53	0.52	0.60
	30	204	0.32	0.56	0.28	0.55	0.34	0.80	0.32	0.44	0.52	0.58
	20	170	0.47	0.79	0.39	0.58	0.43	0.86	0.42	0.63	0.65	0.58
	20	176	0.45	0.76	0.37	0.55	0.41	0.97	0.37	0.60	0.65	0.58
	20	204	0.39	0.53	0.28	0.60	0.31	0.77	0.30	0.43	0.59	0.60

Table 2.9b Maximum MDR (%) from Non-Linear Analysis for Moderate Seismicity, Girder Depth = L/12

No. of Stories	Bay Width (ft.)	Total Height (ft.)	Castaic	Tarzana	Llolleo	ElCentro	Kobe	Taft	Seattle	Sendai	Santa Barabara	Hachinohe
5	30	50	0.37	0.28	0.37	0.51	0.64	0.36	0.72	0.84	0.72	0.51
	30	56	0.32	0.41	0.52	0.50	0.61	0.52	0.34	0.79	0.45	0.74
	30	60	0.29	0.43	0.49	0.48	0.60	0.45	0.37	0.67	0.46	0.63
	20	50	0.36	0.52	0.58	0.70	0.68	0.65	0.37	1.02	0.63	1.02
	20	56	0.33	0.61	0.48	1.00	0.42	0.51	0.30	0.58	1.05	0.74
	20	60	0.32	0.56	0.44	0.95	0.48	0.55	0.32	0.65	1.02	0.74
7	30	70	0.25	0.38	0.43	0.44	0.49	0.43	0.27	0.68	0.41	0.67
	30	76	0.23	0.37	0.35	0.58	0.39	0.42	0.22	0.52	0.61	0.66
	30	84	0.22	0.36	0.31	0.62	0.34	0.39	0.22	0.49	0.72	0.54
	20	70	0.30	0.53	0.41	0.88	0.38	0.44	0.38	0.53	0.90	0.51
	20	76	0.29	0.36	0.29	0.80	0.40	0.51	0.33	0.50	0.82	0.39
	20	84	0.27	0.37	0.35	0.80	0.34	0.49	0.25	0.62	0.69	0.40
9	30	90	0.21	0.32	0.30	0.58	0.35	0.38	0.22	0.48	0.65	0.54
	30	96	0.21	0.40	0.29	0.61	0.26	0.34	0.24	0.35	0.77	0.42
	30	108	0.20	0.32	0.25	0.58	0.29	0.30	0.25	0.33	0.70	0.37
	20	90	0.26	0.35	0.32	0.77	0.31	0.44	0.24	0.59	0.68	0.38
	20	96	0.24	0.38	0.36	0.65	0.27	0.45	0.21	0.52	0.52	0.32
	20	108	0.23	0.47	0.30	0.48	0.29	0.42	0.21	0.43	0.51	0.33
11	30	110	0.19	0.35	0.25	0.54	0.24	0.30	0.23	0.32	0.68	0.34
	30	116	0.19	0.31	0.24	0.53	0.26	0.26	0.24	0.31	0.60	0.32
	30	132	0.17	0.23	0.19	0.52	0.23	0.27	0.18	0.37	0.50	0.25
	20	110	0.23	0.43	0.31	0.49	0.30	0.40	0.21	0.45	0.51	0.32
	20	116	0.23	0.43	0.27	0.47	0.27	0.40	0.21	0.37	0.46	0.31
	20	132	0.21	0.43	0.19	0.39	0.24	0.46	0.25	0.34	0.38	0.32
13	30	130	0.17	0.24	0.21	0.45	0.25	0.24	0.21	0.30	0.53	0.29
	30	136	0.17	0.22	0.19	0.52	0.23	0.26	0.18	0.36	0.49	0.25
	30	156	0.15	0.26	0.23	0.40	0.20	0.29	0.14	0.35	0.35	0.21
	20	130	0.21	0.43	0.23	0.41	0.26	0.40	0.24	0.33	0.41	0.30
	20	136	0.21	0.41	0.19	0.39	0.24	0.43	0.23	0.33	0.37	0.00
	20	156	0.19	0.37	0.16	0.31	0.20	0.50	0.20	0.27	0.34	0.31
15	30	150	0.15	0.22	0.20	0.48	0.18	0.26	0.15	0.37	0.41	0.23
	30	156	0.15	0.24	0.22	0.44	0.18	0.28	0.13	0.35	0.36	0.20
	30	180	0.14	0.29	0.19	0.30	0.18	0.25	0.13	0.27	0.31	0.20
	20	150	0.20	0.39	0.18	0.33	0.22	0.41	0.22	0.30	0.33	0.29
	20	156	0.19	0.37	0.16	0.30	0.21	0.41	0.20	0.30	0.31	0.30
	20	180	0.18	0.31	0.16	0.28	0.17	0.44	0.14	0.26	0.32	0.27
17	30	170	0.14	0.25	0.21	0.36	0.18	0.26	0.14	0.31	0.32	0.20
	30	176	0.14	0.26	0.20	0.31	0.18	0.25	0.14	0.29	0.32	0.19
	30	204	0.14	0.29	0.16	0.26	0.17	0.25	0.14	0.22	0.27	0.19
	20	170	0.18	0.34	0.15	0.31	0.19	0.46	0.19	0.27	0.32	0.29
	20	176	0.18	0.32	0.16	0.30	0.18	0.49	0.16	0.24	0.32	0.28
	20	204	0.18	0.29	0.16	0.27	0.14	0.35	0.13	0.23	0.30	0.25

Table 2.9c Maximum MDR (%) from Non-Linear Analysis for High Seismicity, Girder Depth =L/10

No. of Stories	Bay Width (ft.)	Total Height (ft.)	Castaic	Tarzana	Llolleo	ElCentro	Kobe	Taft	Seattle	Sendai	Santa Barabara	Hachinohe
5	20	50	0.67	0.54	0.73	1.02	1.11	0.74	1.32	1.26	1.00	1.17
	20	56	0.63	0.45	0.57	0.89	0.92	0.72	1.01	1.08	0.84	0.94
	20	60	0.64	0.62	0.76	0.85	1.09	0.84	0.93	1.17	0.97	0.94
7	20	70	0.55	0.72	0.75	1.06	0.88	0.97	0.55	1.06	1.47	1.08
	20	76	0.49	0.64	0.67	0.85	0.83	0.93	0.47	0.98	1.35	0.89
	20	84	0.48	0.73	0.67	1.19	0.72	0.84	0.44	0.93	1.07	1.25
9	20	90	0.47	0.79	0.61	1.15	0.59	0.76	0.48	0.72	0.82	1.16
	20	96	0.45	0.72	0.60	1.06	0.57	0.73	0.49	0.70	0.73	1.14
	20	108	0.42	0.60	0.49	1.04	0.62	0.60	0.52	0.68	0.69	1.00
11	20	110	0.41	0.54	0.46	1.04	0.62	0.56	0.45	0.72	0.65	0.95
	20	116	0.40	0.50	0.44	1.03	0.52	0.56	0.38	0.83	0.64	1.10
	20	132	0.37	0.52	0.56	0.80	0.50	0.56	0.32	0.83	0.51	0.81
13	20	130	0.36	0.51	0.56	0.80	0.51	0.56	0.33	0.83	0.54	0.82
	20	136	0.36	0.50	0.53	0.74	0.46	0.57	0.30	0.81	0.52	0.79
	20	156	0.34	0.66	0.44	0.65	0.44	0.59	0.31	0.58	0.46	0.72
15	20	150	0.34	0.68	0.50	0.67	0.47	0.63	0.33	0.64	0.48	0.73
	20	156	0.34	0.63	0.45	0.67	0.42	0.61	0.30	0.56	0.47	0.72
	20	180	0.32	0.62	0.27	0.59	0.39	0.51	0.42	0.52	0.52	0.55
17	20	170	0.32	0.64	0.33	0.59	0.42	0.52	0.38	0.53	0.50	0.62
	20	176	0.32	0.61	0.28	0.57	0.37	0.51	0.38	0.52	0.53	0.56
	20	204	0.29	0.57	0.29	0.49	0.33	0.54	0.36	0.43	0.52	0.53

Table 2.10a Maximum SDR (%) from Non-Linear Analysis for High Seismicity, Girder Depth = L/12

No. of Stories	Bay Width (ft.)	Total Height (ft.)	Castaic	Tarzana	Llolleo	ElCentro	Kobe	Taft	Seattle	Sendai	Santa Barabara	Hachinohe
5	30	50	1.14	0.87	1.09	1.52	1.52	1.07	1.79	1.75	1.61	1.38
	30	56	1.07	0.85	1.05	1.28	1.38	1.05	1.36	1.63	1.33	1.29
	30	60	1.07	1.11	1.25	1.26	1.46	1.24	1.20	1.75	1.32	1.41
	20	50	1.27	1.11	1.03	1.58	1.65	1.02	1.84	1.85	1.79	1.39
	20	56	1.12	0.99	1.04	1.38	1.58	1.20	1.40	1.73	1.58	1.39
	20	60	1.39	1.50	1.34	1.30	1.63	1.32	1.08	2.25	1.41	1.83
7	30	70	1.09	1.18	1.22	1.67	1.47	1.51	0.80	1.72	1.66	2.21
	30	76	0.87	1.05	1.03	1.49	1.28	1.34	0.65	1.67	1.58	1.95
	30	84	0.90	1.54	1.00	2.00	1.11	1.29	0.69	1.47	2.00	1.53
	20	70	1.12	1.55	1.19	1.66	1.33	1.39	0.76	1.63	1.58	2.28
	20	76	1.11	1.63	1.28	1.74	1.14	1.26	0.73	1.61	1.72	2.02
	20	84	1.20	2.13	1.17	2.08	0.97	1.13	0.67	1.37	2.08	1.52
9	30	90	1.01	1.52	1.02	2.29	1.53	1.41	1.19	1.47	2.11	1.36
	30	96	0.87	1.57	0.95	2.01	1.18	1.21	1.07	1.27	1.92	1.29
	30	108	0.95	1.39	1.07	2.11	1.07	1.15	1.41	1.40	1.76	1.31
	20	90	0.91	1.48	1.35	2.07	0.99	1.33	0.78	1.25	1.85	1.22
	20	96	0.89	1.73	1.22	2.05	0.99	1.24	1.00	1.41	1.82	1.14
	20	108	1.15	1.34	1.02	1.61	1.15	1.01	1.65	1.46	1.68	1.15
11	30	110	1.02	1.34	1.07	2.03	1.33	1.24	1.53	2.22	1.88	1.33
	30	116	0.89	1.12	1.07	1.86	1.20	1.12	1.36	2.21	1.76	1.28
	30	132	0.99	1.21	1.02	1.67	1.17	1.06	1.27	2.07	1.69	1.24
	20	110	0.99	1.17	1.13	1.88	1.27	1.08	1.53	1.29	1.46	1.24
	20	116	0.98	0.99	1.23	1.73	1.25	1.13	1.57	1.66	1.46	1.17
	20	132	1.05	1.53	1.30	1.61	1.18	0.90	1.67	2.33	1.71	1.18
13	30	130	0.97	1.14	1.15	1.69	1.27	1.06	1.26	2.20	1.62	1.31
	30	136	0.91	1.29	0.90	1.65	1.09	0.97	1.23	1.91	1.74	1.12
	30	156	0.95	1.78	1.10	1.35	1.10	1.00	1.08	1.61	1.56	0.91
	20	130	1.00	1.42	1.21	1.64	1.21	0.89	1.64	2.23	1.71	1.17
	20	136	1.01	1.28	1.19	1.64	1.26	0.89	1.62	2.18	1.91	1.28
	20	156	1.21	1.33	0.97	1.39	1.15	0.82	1.22	1.54	1.47	1.02
15	30	150	0.96	1.95	1.10	1.62	1.15	1.03	1.20	1.74	1.67	0.97
	30	156	0.90	1.83	1.10	1.43	1.14	1.01	1.12	1.72	1.60	0.92
	30	180	0.92	1.29	0.83	1.15	1.15	0.86	1.02	1.11	1.15	1.24
	20	150	1.19	1.40	1.03	1.47	1.17	0.88	1.28	1.66	1.59	1.03
	20	156	1.03	1.31	0.91	1.40	1.05	0.84	1.18	1.37	1.43	1.03
	20	180	0.84	1.15	0.80	1.20	1.14	0.99	0.98	1.10	1.06	0.99
17	30	170	0.89	1.64	1.02	1.18	1.09	0.91	1.04	1.46	1.45	0.92
	30	176	0.83	1.38	0.86	0.99	1.07	0.77	0.97	1.28	1.25	0.99
	30	204	0.87	1.12	0.83	1.18	1.04	0.85	0.81	1.04	1.16	1.12
	20	170	0.84	1.34	0.83	1.18	0.99	0.95	0.99	1.16	1.11	0.98
	20	176	0.76	1.20	0.76	1.19	0.99	1.01	0.87	1.14	1.03	0.96
	20	204	0.76	1.05	0.82	1.23	0.97	0.88	0.81	1.00	1.01	1.09

Table 2.10b Maximum SDR (%) from Non-Linear Analysis for Moderate Seismicity, Girder Depth = L/12

No. of Stories	Bay Width (ft.)	Total Height (ft.)	Castaic	Tarzana	Llolleo	ElCentro	Kobe	Taft	Seattle	Sendai	Santa Barabara	Hachinohe
5	30	50	0.62	0.45	0.56	0.80	0.84	0.52	0.98	1.22	1.05	0.72
	30	56	0.64	0.71	0.82	0.91	1.13	0.85	0.63	1.44	0.84	1.42
	30	60	0.54	0.62	0.72	0.74	0.76	0.62	0.56	1.02	0.71	0.92
	20	50	0.66	0.83	0.82	0.96	0.98	0.88	0.54	1.52	0.93	1.51
	20	56	0.72	1.23	0.82	1.47	0.76	0.92	0.52	1.11	2.12	1.22
	20	60	0.63	1.10	0.67	1.38	0.81	0.78	0.47	1.03	1.60	1.04
7	30	70	0.51	0.58	0.64	0.71	0.72	0.61	0.45	1.06	0.63	1.03
	30	76	0.51	0.72	0.53	0.78	0.62	0.68	0.39	0.93	1.09	1.07
	30	84	0.46	0.73	0.50	0.91	0.53	0.63	0.38	0.82	1.08	0.86
	20	70	0.63	1.00	0.62	1.46	0.69	0.74	0.72	0.86	1.64	0.77
	20	76	0.65	0.87	0.64	1.45	0.64	0.90	0.64	0.78	1.34	0.83
	20	84	0.69	0.75	0.64	1.07	0.53	0.77	0.69	1.19	1.11	0.78
9	30	90	0.41	0.67	0.55	0.94	0.64	0.63	0.39	0.77	0.99	0.86
	30	96	0.38	0.66	0.47	0.98	0.58	0.53	0.48	0.56	1.09	0.62
	30	108	0.48	0.72	0.52	1.13	0.46	0.58	0.67	0.61	1.03	0.64
	20	90	0.61	0.76	0.66	1.15	0.63	0.70	0.76	1.26	1.09	0.72
	20	96	0.54	0.65	0.54	0.90	0.50	0.57	0.57	0.99	0.83	0.66
	20	108	0.59	1.03	0.61	0.90	0.52	0.59	0.67	0.93	0.99	0.60
11	30	110	0.39	0.73	0.44	0.98	0.52	0.52	0.49	0.63	1.06	0.57
	30	116	0.38	0.56	0.45	0.91	0.40	0.47	0.57	0.56	1.01	0.54
	30	132	0.44	0.53	0.42	0.89	0.42	0.49	0.54	0.84	0.78	0.51
	20	110	0.61	1.03	0.60	0.99	0.59	0.60	0.73	0.94	1.05	0.64
	20	116	0.49	0.94	0.56	0.85	0.55	0.55	0.58	0.86	0.85	0.54
	20	132	0.63	0.85	0.56	0.74	0.60	0.53	0.57	0.78	0.76	0.65
13	30	130	0.44	0.58	0.41	0.90	0.44	0.52	0.61	0.67	0.86	0.57
	30	136	0.40	0.49	0.44	0.91	0.43	0.49	0.55	0.83	0.75	0.52
	30	156	0.44	0.64	0.39	0.71	0.44	0.49	0.53	0.81	0.69	0.52
	20	130	0.63	0.97	0.61	0.72	0.62	0.52	0.66	0.89	0.91	0.61
	20	136	0.55	0.82	0.50	0.67	0.63	0.48	0.56	0.73	0.75	0.65
	20	156	0.58	0.82	0.50	0.81	0.66	0.59	0.49	0.78	0.74	0.78
15	30	150	0.41	0.51	0.46	0.72	0.43	0.47	0.50	0.88	0.67	0.51
	30	156	0.38	0.51	0.43	0.69	0.41	0.44	0.45	0.80	0.62	0.50
	30	180	0.40	0.76	0.41	0.60	0.37	0.37	0.48	0.64	0.66	0.41
	20	150	0.55	0.77	0.51	0.63	0.59	0.48	0.55	0.66	0.68	0.60
	20	156	0.49	0.65	0.43	0.60	0.59	0.49	0.46	0.62	0.59	0.63
	20	180	0.47	0.64	0.41	0.67	0.54	0.48	0.43	0.70	0.62	0.67
17	30	170	0.38	0.56	0.37	0.63	0.39	0.40	0.45	0.70	0.60	0.46
	30	176	0.35	0.56	0.36	0.59	0.36	0.37	0.45	0.63	0.65	0.42
	30	204	0.38	0.65	0.41	0.48	0.39	0.34	0.41	0.55	0.58	0.34
	20	170	0.54	0.70	0.49	0.71	0.60	0.52	0.49	0.64	0.65	0.66
	20	176	0.49	0.64	0.46	0.66	0.58	0.49	0.43	0.63	0.64	0.64
	20	204	0.50	0.66	0.44	0.78	0.46	0.46	0.47	0.64	0.77	0.80

Table 2.10c Maximum SDR (%) from Non-Linear Analysis for High Seismicity, Girder Depth=L/10

No. of Stories	Bay Width (ft.)	Total Height (ft.)	Castaic	Tarzana	Llolleo	ElCentro	Kobe	Taft	Seattle	Sendai	Santa Barabara	Hachinohe
5	20	50	1.14	0.78	1.14	1.54	1.53	1.05	1.83	1.82	1.66	1.38
	20	56	1.06	0.94	1.18	1.29	1.48	1.14	1.34	1.68	1.37	1.34
	20	60	0.97	0.72	0.86	1.33	1.35	0.96	1.46	1.59	1.36	1.24
7	20	70	1.00	1.18	1.28	1.63	1.56	1.54	0.81	1.73	1.66	2.33
	20	76	0.88	1.01	1.07	1.28	1.34	1.34	0.68	1.58	1.33	2.03
	20	84	0.91	1.40	1.03	1.91	1.20	1.33	0.68	1.57	1.95	1.72
9	20	90	0.96	1.52	1.16	1.98	1.24	1.27	0.82	1.25	2.12	1.27
	20	96	0.85	1.47	1.20	2.10	1.09	1.25	1.12	1.54	1.84	1.27
	20	108	0.87	1.31	1.04	1.92	0.91	1.10	1.34	1.23	1.86	1.19
11	20	110	0.96	1.25	0.88	1.91	0.89	1.31	1.12	1.41	1.67	1.12
	20	116	0.88	1.16	0.97	1.77	1.12	1.14	1.40	2.21	1.91	1.23
	20	132	0.91	1.15	0.95	1.46	1.03	1.12	1.06	1.81	1.41	1.15
13	20	130	0.93	1.28	1.01	1.66	1.09	1.06	1.17	1.99	1.54	1.19
	20	136	0.89	1.26	0.89	1.68	1.05	1.02	1.14	1.85	1.61	1.12
	20	156	0.88	1.42	0.91	1.16	0.79	0.97	0.94	1.46	1.42	1.04
15	20	150	0.87	1.50	1.17	1.31	0.95	0.98	1.02	1.58	1.52	1.00
	20	156	0.83	1.50	1.09	1.30	0.97	0.93	0.99	1.54	1.41	0.92
	20	180	0.99	1.37	0.85	1.15	1.11	1.10	1.03	1.22	1.10	1.11
17	20	170	0.90	1.41	0.93	1.02	1.03	1.10	0.95	1.31	1.33	0.94
	20	176	0.80	1.21	0.78	0.96	1.01	1.23	0.88	1.11	1.23	1.07
	20	204	0.94	1.24	0.91	1.25	1.12	1.36	0.80	1.25	1.05	1.30

Table 2.11a Location (story) of Maximum SDR from Non-Linear Analysis for High Seismicity, Girder Depth = L/12

No. of Stories	Bay Width (ft.)	Total Height (ft.)	Castaic	Tarzana	Llolleo	ElCentro	Kobe	Taft	Seattle	Sendai	Santa Barbara	Hachinohe
5	30	50	1	2	4	4	3	3	3	3	3	3
	30	56	2	2	4	4	4	4	4	4	3	4
	30	60	4	1	4	4	3	3	3	4	3	3
	20	50	2	1	2	2	2	2	2	2	2	2
	20	56	1	1	2	2	1	2	2	2	1	2
	20	60	1	1	2	1	1	2	2	2	1	2
7	30	70	2	3	5	4	5	5	4	5	5	5
	30	76	2	3	4	5	5	5	5	6	5	5
	30	84	5	5	6	4	4	4	4	5	5	5
	20	70	1	1	2	2	2	3	4	2	3	3
	20	76	1	1	2	2	3	3	2	2	3	3
	20	84	1	1	2	2	1	4	3	2	2	2
9	30	90	1	5	7	4	4	3	3	4	5	5
	30	96	3	6	6	6	6	7	5	6	7	7
	30	108	5	5	4	4	2	4	3	4	5	4
	20	90	2	3	1	3	4	2	3	3	5	3
	20	96	2	1	2	2	7	3	2	2	4	4
	20	108	1	1	2	3	2	3	1	2	3	2
11	30	110	6	4	4	6	3	5	3	4	6	5
	30	116	6	5	4	6	3	9	3	4	6	4
	30	132	6	6	3	4	3	4	3	4	4	3
	20	110	2	2	4	1	2	2	2	3	2	2
	20	116	2	2	2	4	2	3	2	2	6	3
	20	132	1	1	1	3	1	5	1	1	3	2
13	30	130	6	6	4	5	3	5	4	4	6	4
	30	136	9	9	6	8	5	7	6	7	6	6
	30	156	7	6	6	5	5	7	3	3	6	4
	20	130	2	1	1	4	2	7	2	2	4	3
	20	136	1	8	1	4	2	6	2	2	4	3
	20	156	1	7	6	2	2	7	2	1	5	7
15	30	150	8	7	7	6	6	9	4	4	6	5
	30	156	8	7	7	6	6	8	4	4	6	5
	30	180	8	6	7	8	6	4	3	6	8	6
	20	150	1	8	7	2	2	8	3	2	6	3
	20	156	1	9	8	2	2	9	3	2	6	9
	20	180	2	7	2	9	2	10	3	5	4	6
17	30	170	9	7	8	7	7	8	4	4	7	9
	30	176	9	7	8	9	7	13	4	4	7	9
	30	204	9	7	7	8	7	12	3	12	8	9
	20	170	1	9	2	11	7	11	3	6	3	8
	20	176	2	9	2	11	2	12	3	13	4	8
	20	204	2	1	12	10	2	12	2	13	10	5

Note: Location one is equal to base

Table 2.11b Location (story) of Maximum SDR from Non-Linear Analysis for High Seismicity, Girder Depth = L/10

No. of Stories	Bay Width (ft.)	Total Height (ft.)	Castaic	Tarzana	Llolleo	ElCentro	Kobe	Taft	Seattle	Sendai	Santa Barbara	Hachinohe
5	20	50	4	3	2	2	3	3	2	2	2	2
	20	56	1	2	1	1	1	1	1	1	1	1
	20	60	2	5	2	2	3	3	3	2	2	3
7	20	70	2	2	3	4	3	3	3	2	3	3
	20	76	2	4	2	3	3	3	3	2	3	3
	20	84	3	2	3	4	3	3	3	3	3	3
9	20	90	3	4	2	5	2	4	6	4	3	4
	20	96	5	6	6	5	5	5	7	6	5	5
	20	108	4	6	6	5	7	2	7	5	5	6
11	20	110	4	3	7	5	9	3	8	5	3	3
	20	116	6	7	8	7	9	3	8	7	6	7
	20	132	4	6	8	7	9	4	8	8	6	3
13	20	130	7	7	3	8	11	5	9	9	7	9
	20	136	7	7	2	8	10	4	9	9	9	9
	20	156	3	7	6	4	8	4	3	4	3	3
15	20	150	3	9	8	10	10	6	11	11	3	3
	20	156	8	9	8	9	10	4	11	11	3	3
	20	180	8	10	9	8	10	6	13	10	9	10
17	20	170	9	11	9	4	11	5	13	14	4	9
	20	176	9	11	9	12	11	4	13	11	3	10
	20	204	10	12	10	9	12	6	14	9	9	9

Note: Location one is equal to base

Table 3.1a Minimum Percent Difference (%) to Select Optimum Damping

	Damping Level (%)	Castaic	Tarzana	Llolleo	ElCentro	Kobe	Taft	Seattle	Sendai	Santa Barabara	Hachinohe	Avg. % Diff.
High Seismicity (Girder Depth L/12)	2	19.10	28.90	17.61	21.08	27.57	17.08	40.34	34.63	47.61	49.59	30.351
	3	16.11	22.50	16.23	24.26	20.57	14.06	29.67	25.35	35.89	42.39	24.704
	4	15.29	18.31	15.66	21.27	16.49	14.68	21.47	19.42	27.48	35.34	20.540
	5	14.82	16.33	16.49	17.40	13.65	14.18	19.06	18.34	21.11	29.87	18.124
	6	**14.81**	**15.32**	14.79	14.66	12.37	12.31	16.50	15.98	16.13	25.20	15.807
	7	15.14	15.35	12.00	12.47	9.06	**11.95**	13.83	14.94	12.70	21.14	13.856
	8	15.66	16.48	**11.28**	11.05	**8.00**	12.38	**12.85**	14.16	10.97	17.91	**13.072**
	9	16.33	17.00	11.36	**10.17**	8.42	14.00	13.41	**14.02**	**10.52**	15.50	13.074
	10	16.92	18.11	12.21	10.22	9.48	14.67	14.41	14.68	10.66	13.79	13.516
	11	17.69	18.80	13.77	10.91	11.28	16.38	16.07	15.61	12.20	12.62	14.532
	12	18.46	19.95	15.69	12.26	13.05	18.23	18.20	16.94	13.55	**12.36**	15.871

Table 3.1b Minimum Percent Difference (%) to Select Optimum Damping

	Damping Level (%)	Castaic	Tarzana	Llolleo	ElCentro	Kobe	Taft	Seattle	Sendai	Santa Barabara	Hachinohe	Avg. % Diff.
High Seismicity (Girder Depth L/10)	2	17.47	**42.37**	20.14	17.93	33.43	13.78	56.56	43.10	**45.66**	31.09	32.153
	3	14.02	31.61	21.95	21.17	26.08	17.07	39.71	37.40	30.91	31.34	27.125
	4	14.18	23.42	15.82	24.17	21.31	12.88	30.03	31.57	29.74	32.86	23.598
	5	11.74	18.19	13.13	21.78	17.42	8.16	22.54	26.38	30.26	33.66	20.325
	6	10.31	14.61	12.18	17.10	15.31	**6.41**	18.26	20.96	27.69	32.42	17.524
	7	9.51	12.23	13.43	13.87	13.69	6.73	15.38	17.66	20.00	27.95	15.046
	8	8.64	11.30	11.73	11.25	8.29	7.96	13.54	15.33	15.81	23.64	12.748
	9	8.14	**10.88**	10.40	9.64	8.35	9.61	12.07	14.07	13.36	19.87	11.639
	10	7.63	11.28	**9.37**	**9.07**	**7.81**	10.85	10.93	13.45	11.22	16.46	10.806
	11	7.13	11.40	10.33	9.31	8.30	12.32	**10.51**	**13.43**	9.69	14.15	**10.656**
	12	**6.85**	11.66	11.53	10.33	9.50	13.65	11.16	13.55	**9.51**	**13.13**	11.088

Table 3.1c Minimum Percent Difference (%) to Select Optimum Damping

	Damping Level (%)	Castaic	Tarzana	Llolleo	ElCentro	Kobe	Taft	Seattle	Sendai	Santa Barabara	Hachinohe	Avg. % Diff.
Moderate Seismicity (Girder Depth L/12)	2	17.32	31.07	25.97	44.27	32.40	15.80	52.69	35.46	70.17	46.60	37.175
	3	13.20	25.66	24.71	33.06	26.65	14.74	37.26	27.41	53.35	37.87	29.393
	4	11.90	21.93	18.09	25.97	21.51	12.81	27.66	21.58	42.80	30.82	23.507
	5	11.17	20.44	13.93	20.27	17.58	12.87	21.96	17.32	35.25	25.02	19.582
	6	10.46	16.48	**12.06**	15.87	15.69	10.99	17.31	13.68	29.25	19.89	16.170
	7	9.63	14.77	12.14	12.42	14.89	10.65	14.55	11.60	23.91	15.73	14.030
	8	9.00	**14.32**	12.80	10.90	13.48	**10.04**	12.48	**10.53**	19.13	12.31	12.498
	9	8.68	14.55	11.99	9.91	10.93	10.49	**11.70**	10.77	15.18	9.50	11.370
	10	8.40	15.19	12.04	**9.60**	9.34	11.86	11.82	12.11	11.75	7.23	**10.934**
	11	**8.32**	20.59	13.14	10.35	8.21	13.54	12.49	13.59	**9.11**	**6.59**	11.594
	12	8.59	25.93	14.74	12.01	**8.00**	15.59	13.32	15.47	9.41	7.37	13.044

Damping Level (%)	Average % Difference High (L/12)	High (L/10)	Moderate (L/12)	Total Avg. % Diff.
7	14.044	15.046	14.030	14.239
8	**13.286**	12.748	12.498	12.863
9	13.333	11.639	11.370	12.209
10	13.829	10.806	**10.934**	**12.066**
11	14.741	**10.656**	11.594	12.665
12	16.119	11.088	13.044	13.882

Table 3.2a Period Modification Factor Associated w/ Minimum Percent Difference

	Damping Level (%)	Castaic	Tarzana	Llolleo	ElCentro	Kobe	Taft	Seattle	Sendai	Santa Barabara	Hachinohe	Avg.
High Seismicity (Girder Depth L/12)	2	0.68	2.38	0.91	1.05	1.47	1.74	2.03	2.50	2.27	2.56	1.759
	3	2.38	2.38	1.06	1.08	2.28	1.81	2.22	2.50	2.27	2.50	2.048
	4	2.39	2.39	1.05	2.38	2.27	2.23	2.50	2.40	2.38	2.50	2.248
	5	2.38	2.39	1.07	2.38	2.32	2.35	2.35	2.38	2.38	2.50	2.250
	6	2.40	2.39	2.38	2.38	2.19	2.35	2.33	2.39	2.38	2.50	2.368
	7	2.40	2.39	2.38	2.39	1.78	2.38	2.37	2.39	2.38	2.50	2.335
	8	2.40	2.39	2.40	2.40	1.82	2.40	2.40	2.40	2.40	2.50	2.352
	9	2.40	2.40	2.40	2.38	1.83	2.40	2.40	2.40	2.40	2.50	2.354
	10	2.40	2.40	2.40	2.38	1.79	2.40	2.40	2.40	2.40	2.40	**2.340**
	11	2.40	2.40	2.40	2.38	1.84	2.40	2.40	2.40	2.40	2.40	2.344
	12	2.40	2.40	2.40	2.38	1.83	2.40	2.40	2.40	2.40	2.39	2.343

Table 3.2b Period Modification Factor Associated w/ Minimum Percent Difference

	Damping Level (%)	Castaic	Tarzana	Llolleo	ElCentro	Kobe	Taft	Seattle	Sendai	Santa Barabara	Hachinohe	Avg.
High Seismicity (Girder Depth L/10)	2	0.63	2.38	0.89	1.05	1.48	0.99	2.19	1.25	0.98	1.00	1.285
	3	0.63	2.38	1.06	1.08	2.27	1.05	2.20	0.94	0.83	1.00	1.345
	4	2.38	2.38	1.06	1.11	2.38	1.82	2.20	0.94	0.83	1.09	1.619
	5	2.38	2.38	1.25	2.38	2.22	1.87	2.22	2.39	0.90	1.11	1.910
	6	2.38	2.38	1.25	2.40	2.27	1.92	2.28	2.40	1.91	2.70	2.190
	7	2.40	2.40	1.24	2.40	2.31	1.98	2.31	2.40	2.00	2.67	2.212
	8	2.40	2.40	2.33	2.40	1.57	2.00	2.40	2.39	2.00	2.67	2.257
	9	2.40	2.40	2.28	2.40	1.65	2.04	2.40	2.40	2.03	2.61	2.262
	10	2.40	2.40	2.23	2.40	1.62	2.11	2.40	2.40	2.22	2.61	**2.280**
	11	2.40	2.40	2.23	2.40	1.60	2.12	2.40	2.40	2.22	2.61	2.279
	12	2.40	2.40	2.38	2.40	1.60	2.13	2.40	2.40	2.27	2.66	2.306

Table 3.2c Period Modification Factor Associated w/ Minimum Percent Difference

	Damping Level (%)	Castaic	Tarzana	Llolleo	ElCentro	Kobe	Taft	Seattle	Sendai	Santa Barabara	Hachinohe	Avg.
Moderate Seismicity (Girder Depth L/12)	2	1.75	1.91	0.56	2.12	2.13	1.35	1.98	2.13	2.22	2.22	1.837
	3	1.75	1.90	0.57	2.12	2.13	1.43	2.00	2.13	1.82	2.22	1.806
	4	1.75	1.90	0.84	2.13	2.13	1.70	2.00	2.13	1.66	2.22	1.847
	5	1.75	1.90	1.17	2.11	2.13	1.88	2.05	2.13	1.72	2.22	1.907
	6	1.75	2.10	1.17	2.11	2.13	1.88	2.08	2.13	2.00	2.22	1.958
	7	1.74	2.13	1.18	2.12	2.13	2.00	2.08	2.13	2.00	2.22	1.974
	8	1.72	2.13	1.21	2.13	1.47	2.07	2.11	2.13	2.00	2.22	1.919
	9	1.72	2.13	1.91	2.13	1.43	2.11	2.11	2.13	2.00	2.22	1.988
	10	1.72	2.13	1.90	2.13	1.43	2.12	2.11	2.13	2.00	2.22	**1.990**
	11	1.74	2.13	1.91	2.13	1.43	2.13	2.12	2.13	2.00	2.22	1.995
	12	1.75	2.13	1.91	2.13	1.45	2.13	2.13	2.13	2.00	2.22	1.998

Damping Level (%)	Average % Difference High (L/12)	High (L/10)	Moderate (L/12)	Total Avg.
10	2.340	2.280		2.32
10			1.990	1.99

Table 3.3a Approximate Story Stiffness for High Seismicity, Girder Depth = L/12

No. of Stories	Bay Width (ft.)	Story Height (ft.)	Kc Base (kips/in)	Kc Top (kips/in)	Kc Tall (kips/in)	Kg (kips/in)	Story Stiffness Base (kips/in)	Story Stiffness Top (kips/in)	Story Stiffness Tall (kips/in)
5	30	10	317	317		100	2056	2056	
	30	12	356	356		100	1507	1507	
	30	10*	563	563	352	100	2609	2609	2158
	20	10	427	427		28	930	930	
	20	12	356	356		28	625	625	
	20	10*	563	563	352	28	968	968	898
7	30	10	317	317		100	2056	2056	
	30	12	356	356		100	1507	1507	
	30	10*	563	563	352	100	2609	2609	2158
	20	10	427	427		28	930	930	
	20	12	469	469		28	655	655	
	20	10*	563	563	352	28	968	968	898
9	30	10	563	163		100	2609	1406	
	30	12	469	192		100	1694	1084	
	30	10*	728	230	455	100	2833	1738	2411
	20	10	563	427		28	968	930	
	20	12	607	356		28	678	625	
	20	10*	728	427	455	28	997	930	939
11	30	10	563	163		100	2609	1406	
	30	12	607	192		100	1859	1084	
	30	10*	728	230	455	100	2833	1738	2411
	20	10	728	427		28	997	930	
	20	12	607	469		28	678	655	
	20	10*	728	563	455	28	997	968	939
13	30	10	728	230		100	2833	1738	
	30	12	607	192		100	1859	1084	
	30	10*	728	230	455	100	2833	1738	2411
	20	10	728	563		28	997	968	
	20	12	773	469		28	697	655	
	20	10*	928	563	580	28	1020	968	972
15	30	10	928	230		100	3023	1738	
	30	12	773	192		100	2001	1084	
	30	10*	928	230	580	100	3023	1738	2636
	20	10	928	563		28	1020	968	
	20	12	773	607		28	697	678	
	20	10*	928	728	580	28	1020	997	972
17	30	10	1166	317		100	3182	2056	
	30	12	972	264		100	2123	1301	
	30	10*	1166	317	729	100	3182	2056	2834
	20	10	928	728		28	1020	997	
	20	12	773	773		28	697	697	
	20	10*	928	928	580	28	1020	1020	972

K_c = Column Stiffness

K_g = Girder Stiffness

* Tall 1st story (16ft.) with 10-ft. stories above

Table 3.3b Approximate Story Stiffness for Moderate Seismicity, Girder Depth = L/12

No. of Stories	Bay Width (ft.)	Story Height (ft.)	Kc Base (kips/in)	Kc Top (kips/in)	Kc Tall (kips/in)	Kg (kips/in)	Story Stiffness Base (kips/in)	Story Stiffness Top (kips/in)	Story Stiffness Tall (kips/in)
5	30	10	163	163		100	1406	1406	
	30	12	136	136		100	865	865	
	30	10*	163	163	102	100	1406	1406	1012
	20	10	46	46		28	392	392	
	20	12	38	38		28	241	241	
	20	10*	46	46	28	28	392	392	283
7	30	10	230	230		100	1738	1738	
	30	12	192	192		100	1084	1084	
	30	10*	230	230	144	100	1738	1738	1297
	20	10	46	46		28	392	392	
	20	12	38	38		28	241	241	
	20	10*	46	46	28	28	392	392	283
9	30	10	427	163		100	2349	1406	
	30	12	356	136		100	1507	865	
	30	10*	427	163	267	100	2349	1406	1883
	20	10	73	46		28	518	392	
	20	12	61	38		28	325	241	
	20	10*	73	46	46	28	518	392	393
11	30	10	563	230		100	2609	1738	
	30	12	469	192		100	1694	1084	
	30	10*	563	230	352	100	2609	1738	2158
	20	10	111	46		28	635	392	
	20	12	93	38		28	406	241	
	20	10*	111	46	69	28	635	392	505
13	30	10	928	230		100	3023	1738	
	30	12	773	192		100	2001	1084	
	30	10*	928	230	580	100	3023	1738	2636
	20	10	163	46		28	735	392	
	20	12	136	38		28	478	241	
	20	10*	163	46	102	28	735	392	611
15	30	10	1166	317		100	3182	2056	
	30	12	972	264		100	2123	1301	
	30	10*	1166	317	729	100	3182	2056	2834
	20	10	230	73		28	816	518	
	20	12	192	61		28	538	325	
	20	10*	230	73	144	28	816	518	704
17	30	10	1448	427		100	3314	2349	
	30	12	1207	356		100	2225	1507	
	30	10*	1448	427	905	100	3314	2349	3004
	20	10	317	73		28	880	518	
	20	12	264	61		28	587	325	
	20	10*	317	73	198	28	880	518	782

K_c = Column Stiffness

K_g = Girder Stiffness

* Tall 1st story (16ft.) with 10-ft. stories above

Table 3.3c Approximate Story Stiffness for High Seismicity, Girder Depth = L/10

No. of Stories	Bay Width (ft.)	Story Height (ft.)	Kc Base (kips/in)	Kc Top (kips/in)	Kc Tall (kips/in)	Kg (kips/in)	Total Stiffness Base (kips/in)	Total Stiffness Top (kips/in)	Total Stiffness Tall (kips/in)
5	20	10	111	111		58	902	902	
	20	12	136	136		58	703	703	
	20	10*	230	230	144	58	1317	1317	1047
7	20	10	111	111		58	902	902	
	20	12	136	136		58	703	703	
	20	10*	230	230	144	58	1317	1317	1047
9	20	10	111	111		58	902	902	
	20	12	136	93		58	703	558	
	20	10*	230	73	144	58	1317	684	1047
11	20	10	111	111		58	902	902	
	20	12	136	93		58	703	558	
	20	10*	230	73	144	58	1317	684	1047
13	20	10	163	111		58	1117	902	
	20	12	136	93		58	703	558	
	20	10*	317	73	198	58	1492	684	1231
15	20	10	163	73		58	1117	684	
	20	12	264	61		58	968	416	
	20	10*	230	73	144	58	1317	684	1047
17	20	10	230	73		58	1317	684	
	20	12	264	61		58	968	416	
	20	10*	230	73	144	58	1317	684	1047

K_c = Column Stiffness

K_g = Girder Stiffness

* Tall 1st story (16ft.) with 10-ft. stories above

Table 3.4a Average, One Standard Deviation, and COV for Various Damping Levels

			2% Damping			3% Damping			4% Damping			5% Damping		
Earthquake	Seismicity	Girder Depth	average (γi)	one standard deviation	coefficient of variation	average (γi)	one standard deviation	coefficient of variation	average (γi)	one standard deviation	coefficient of variation	average (γi)	one standard deviation	coefficient of variation
Castaic	High	(L/12)	0.910	0.138	0.152	0.946	0.130	0.138	0.970	0.130	0.134	0.992	0.134	0.135
		(L/10)	1.124	0.281	0.250	1.051	0.220	0.210	1.094	0.223	0.204	1.133	0.224	0.198
	Low	(L/12)	0.998	0.216	0.217	1.087	0.213	0.196	0.906	0.113	0.125	0.934	0.110	0.118
Tarzana	High	(L/12)	0.873	0.240	0.275	0.938	0.247	0.263	0.993	0.246	0.247	1.048	0.249	0.238
		(L/10)	0.868	0.220	0.254	0.925	0.218	0.236	0.978	0.214	0.219	1.031	0.215	0.208
	Low	(L/12)	0.744	0.166	0.223	0.796	0.161	0.203	0.844	0.156	0.184	0.890	0.149	0.167
Llolleo	High	(L/12)	1.096	0.464	0.424	1.204	0.485	0.403	0.965	0.224	0.232	0.918	0.122	0.133
		(L/10)	0.979	0.240	0.245	0.966	0.178	0.184	1.051	0.195	0.186	1.114	0.209	0.187
	Low	(L/12)	0.867	0.133	0.153	0.864	0.157	0.182	0.937	0.158	0.169	0.953	0.133	0.139
ElCentro	High	(L/12)	0.715	0.097	0.136	0.774	0.094	0.122	0.816	0.085	0.105	0.859	0.090	0.105
		(L/10)	1.201	0.281	0.234	1.293	0.317	0.245	0.852	0.132	0.155	0.891	0.131	0.147
	Low	(L/12)	1.120	0.261	0.233	1.225	0.321	0.262	1.270	0.313	0.246	0.838	0.116	0.138
Kobe	High	(L/12)	0.777	0.092	0.119	0.814	0.092	0.113	0.852	0.093	0.110	0.887	0.100	0.113
		(L/10)	0.816	0.144	0.176	0.869	0.131	0.151	0.911	0.136	0.149	0.947	0.135	0.142
	Low	(L/12)	0.776	0.136	0.175	0.828	0.140	0.169	0.864	0.138	0.160	0.904	0.140	0.155
Taft	High	(L/12)	1.036	0.179	0.173	1.081	0.185	0.171	1.020	0.185	0.181	1.006	0.168	0.167
		(L/10)	1.016	0.215	0.211	1.069	0.210	0.196	0.995	0.172	0.173	0.982	0.155	0.158
	Low	(L/12)	1.146	0.252	0.220	1.238	0.250	0.202	0.948	0.134	0.142	0.992	0.099	0.100
Seattle	High	(L/12)	0.691	0.157	0.227	0.765	0.149	0.195	0.830	0.149	0.179	0.867	0.132	0.152
		(L/10)	0.795	0.224	0.282	0.838	0.186	0.222	0.883	0.190	0.215	0.947	0.190	0.201
	Low	(L/12)	0.674	0.162	0.241	0.747	0.152	0.203	0.813	0.161	0.198	0.860	0.152	0.177
Sendai	High	(L/12)	0.776	0.133	0.171	0.826	0.129	0.157	0.873	0.128	0.146	0.919	0.128	0.140
		(L/10)	0.782	0.166	0.213	0.835	0.168	0.201	0.886	0.170	0.192	0.934	0.178	0.190
	Low	(L/12)	0.864	0.343	0.397	1.205	0.820	0.680	1.328	0.866	0.653	0.837	0.166	0.198
Santa Barbara	High	(L/12)	0.624	0.119	0.191	0.723	0.206	0.284	0.790	0.232	0.293	0.825	0.223	0.270
		(L/10)	0.712	0.143	0.201	0.770	0.146	0.190	0.805	0.118	0.147	0.848	0.119	0.140
	Low	(L/12)	1.359	1.092	0.804	2.088	1.765	0.845	2.227	1.867	0.838	1.995	1.618	0.811
Hachinohe	High	(L/12)	0.719	0.143	0.199	0.757	0.133	0.176	0.793	0.125	0.158	0.827	0.119	0.144
		(L/10)	0.760	0.285	0.374	0.798	0.273	0.343	0.832	0.264	0.318	0.865	0.256	0.296
	Low	(L/12)	1.435	0.497	0.346	1.535	0.518	0.337	1.482	0.539	0.364	1.526	0.522	0.342
All Earthquakes	All Frames		0.908	0.241	0.250	0.995	0.280	0.249	0.994	0.262	0.227	0.986	0.216	0.194

Table 3.4b Average, One Standard Deviation, and COV for Various Damping Levels

			6% Damping			7% Damping			8% Damping			9% Damping		
Earthquake	Seismicity	Girder Depth	average (γi)	one standard deviation	coefficient of variation	average (γi)	one standard deviation	coefficient of variation	average (γi)	one standard deviation	coefficient of variation	average (γi)	one standard deviation	coefficient of variation
Castaic	High	(L/12)	1.011	0.137	0.136	1.025	0.133	0.130	1.038	0.129	0.124	1.052	0.124	0.118
		(L/10)	1.156	0.225	0.194	1.174	0.223	0.190	1.191	0.223	0.187	1.208	0.222	0.184
	Low	(L/12)	0.955	0.109	0.114	0.967	0.106	0.110	0.983	0.102	0.104	0.997	0.099	0.099
Tarzana	High	(L/12)	0.992	0.172	0.173	1.023	0.158	0.155	1.064	0.156	0.146	1.101	0.153	0.139
		(L/10)	1.079	0.215	0.199	1.124	0.215	0.191	1.166	0.216	0.186	1.195	0.210	0.176
	Low	(L/12)	0.933	0.142	0.152	0.959	0.132	0.137	0.994	0.131	0.132	1.024	0.128	0.125
Llolleo	High	(L/12)	0.976	0.134	0.137	1.035	0.150	0.145	1.072	0.168	0.156	0.972	0.132	0.136
		(L/10)	0.928	0.137	0.148	0.981	0.141	0.144	1.023	0.145	0.142	1.062	0.149	0.140
	Low	(L/12)	1.009	0.139	0.137	1.075	0.148	0.138	0.922	0.104	0.113	0.963	0.109	0.114
ElCentro	High	(L/12)	0.899	0.090	0.100	0.936	0.090	0.096	0.970	0.089	0.092	1.004	0.090	0.089
		(L/10)	0.927	0.130	0.141	0.963	0.130	0.135	0.998	0.130	0.130	1.032	0.134	0.130
	Low	(L/12)	0.873	0.111	0.128	0.905	0.109	0.120	0.938	0.108	0.115	0.971	0.107	0.110
Kobe	High	(L/12)	0.921	0.110	0.120	0.954	0.121	0.127	0.920	0.112	0.122	0.949	0.112	0.118
		(L/10)	0.983	0.138	0.141	0.969	0.106	0.109	1.000	0.101	0.101	1.032	0.098	0.095
	Low	(L/12)	0.942	0.142	0.151	0.979	0.148	0.151	0.960	0.097	0.101	0.991	0.099	0.100
Taft	High	(L/12)	1.054	0.170	0.162	1.023	0.125	0.122	1.032	0.108	0.105	1.047	0.103	0.098
		(L/10)	1.034	0.151	0.146	1.067	0.153	0.143	1.092	0.152	0.139	1.126	0.147	0.131
	Low	(L/12)	1.009	0.088	0.087	1.029	0.083	0.081	1.055	0.086	0.082	1.076	0.092	0.085
Seattle	High	(L/12)	0.913	0.130	0.142	0.952	0.130	0.136	0.990	0.131	0.132	1.022	0.133	0.130
		(L/10)	1.004	0.195	0.194	1.051	0.184	0.175	1.096	0.171	0.156	1.135	0.173	0.152
	Low	(L/12)	0.884	0.132	0.149	0.922	0.132	0.143	0.954	0.136	0.142	0.992	0.143	0.144
Sendai	High	(L/12)	0.961	0.129	0.134	1.000	0.126	0.126	1.036	0.123	0.118	1.069	0.115	0.108
		(L/10)	0.984	0.179	0.182	1.032	0.178	0.173	1.072	0.170	0.159	1.109	0.166	0.150
	Low	(L/12)	0.879	0.166	0.189	0.920	0.168	0.182	0.959	0.166	0.174	0.992	0.158	0.160
Santa Barbara	High	(L/12)	0.810	0.130	0.160	0.850	0.133	0.156	0.890	0.138	0.155	0.929	0.145	0.156
		(L/10)	0.890	0.120	0.135	0.932	0.123	0.132	0.968	0.123	0.127	1.008	0.129	0.128
	Low	(L/12)	0.892	0.270	0.302	0.929	0.235	0.253	0.974	0.248	0.254	1.002	0.244	0.244
Hachinohe	High	(L/12)	0.862	0.113	0.131	0.896	0.107	0.119	0.930	0.103	0.110	0.963	0.100	0.103
		(L/10)	0.897	0.245	0.273	0.929	0.235	0.253	0.961	0.225	0.234	0.993	0.217	0.218
	Low	(L/12)	0.810	0.146	0.180	0.841	0.142	0.169	0.868	0.134	0.154	0.901	0.135	0.150
All Earthquakes	All Frames		0.949	0.150	0.158	0.981	0.145	0.148	1.004	0.141	0.140	1.031	0.139	0.134

Table 3.4c Average, One Standard Deviation, and COV for Various Damping Levels

			10% Damping			11% Damping			12% Damping		
Earthquake	Seismicity	Girder Depth	average (γi)	one standard deviation	coefficient of variation	average (γi)	one standard deviation	coefficient of variation	average (γi)	one standard deviation	coefficient of variation
Castaic	High	(L/12)	1.062	0.121	0.114	1.074	0.118	0.110	1.085	0.117	0.108
		(L/10)	1.224	0.222	0.181	1.241	0.222	0.179	1.257	0.223	0.177
	Low	(L/12)	1.012	0.096	0.095	1.027	0.095	0.092	1.042	0.094	0.090
Tarzana	High	(L/12)	1.135	0.151	0.133	1.159	0.143	0.123	1.182	0.137	0.116
		(L/10)	1.226	0.210	0.171	1.251	0.206	0.164	1.275	0.203	0.159
	Low	(L/12)	1.050	0.126	0.120	1.071	0.123	0.115	1.093	0.123	0.113
Llolleo	High	(L/12)	1.012	0.143	0.141	1.051	0.152	0.145	1.088	0.161	0.148
		(L/10)	1.099	0.155	0.141	1.137	0.162	0.143	1.173	0.171	0.146
	Low	(L/12)	0.992	0.117	0.118	1.029	0.125	0.122	1.050	0.135	0.129
ElCentro	High	(L/12)	1.037	0.090	0.087	1.071	0.091	0.085	1.105	0.093	0.085
		(L/10)	1.065	0.135	0.127	1.098	0.137	0.124	1.131	0.137	0.121
	Low	(L/12)	1.003	0.106	0.105	1.035	0.105	0.101	1.067	0.105	0.098
Kobe	High	(L/12)	0.981	0.113	0.115	1.012	0.114	0.113	1.044	0.116	0.111
		(L/10)	1.065	0.097	0.091	1.097	0.096	0.087	1.130	0.095	0.084
	Low	(L/12)	1.021	0.091	0.089	1.055	0.086	0.081	1.088	0.084	0.077
Taft	High	(L/12)	1.079	0.102	0.094	1.107	0.104	0.094	1.140	0.106	0.093
		(L/10)	1.159	0.145	0.125	1.193	0.146	0.122	1.227	0.148	0.120
	Low	(L/12)	1.091	0.106	0.097	1.117	0.112	0.100	1.146	0.114	0.099
Seattle	High	(L/12)	1.053	0.138	0.131	1.083	0.147	0.136	1.110	0.154	0.139
		(L/10)	1.173	0.178	0.152	1.211	0.187	0.155	1.249	0.199	0.160
	Low	(L/12)	1.028	0.151	0.147	1.063	0.161	0.151	1.098	0.172	0.157
Sendai	High	(L/12)	1.103	0.115	0.104	1.133	0.113	0.100	1.162	0.114	0.098
		(L/10)	1.145	0.164	0.143	1.179	0.164	0.139	1.214	0.165	0.136
	Low	(L/12)	1.027	0.155	0.151	1.058	0.153	0.145	1.090	0.154	0.141
Santa Barbara	High	(L/12)	0.968	0.154	0.160	1.006	0.166	0.165	1.042	0.179	0.171
		(L/10)	1.047	0.134	0.128	1.086	0.140	0.129	1.123	0.145	0.129
	Low	(L/12)	0.980	0.165	0.168	1.020	0.174	0.171	1.044	0.161	0.154
Hachinohe	High	(L/12)	0.995	0.095	0.096	1.027	0.093	0.090	1.059	0.093	0.087
		(L/10)	1.026	0.209	0.204	1.188	0.181	0.153	1.357	0.178	0.131
	Low	(L/12)	0.927	0.126	0.136	0.955	0.118	0.124	0.977	0.104	0.106
All Earthquakes	All Frames		1.060	0.137	0.129	1.094	0.138	0.125	1.128	0.139	0.123

Table 3.5 Average Safety Modification Factor (γ_f) for 10% Damping

Earthquake	Seismicity	Girder Depth	average (γ_i)	one standard deviation	coefficient of variation
Castaic	High	(L/12)	1.062	0.121	0.114
		(L/10)	1.224	0.222	0.181
	Low	(L/12)	1.012	0.096	0.095
Tarzana	High	(L/12)	1.135	0.151	0.133
		(L/10)	1.226	0.210	0.171
	Low	(L/12)	1.050	0.126	0.120
Llolleo	High	(L/12)	1.012	0.143	0.141
		(L/10)	1.099	0.155	0.141
	Low	(L/12)	0.992	0.117	0.118
ElCentro	High	(L/12)	1.037	0.090	0.087
		(L/10)	1.065	0.135	0.127
	Low	(L/12)	1.003	0.106	0.105
Kobe	High	(L/12)	0.981	0.113	0.115
		(L/10)	1.065	0.097	0.091
	Low	(L/12)	1.021	0.091	0.089
Taft	High	(L/12)	1.079	0.102	0.094
		(L/10)	1.159	0.145	0.125
	Low	(L/12)	1.091	0.106	0.097
Seattle	High	(L/12)	1.053	0.138	0.131
		(L/10)	1.173	0.178	0.152
	Low	(L/12)	1.028	0.151	0.147
Sendai	High	(L/12)	1.103	0.115	0.104
		(L/10)	1.145	0.164	0.143
	Low	(L/12)	1.027	0.155	0.151
Santa Barbara	High	(L/12)	0.968	0.154	0.160
		(L/10)	1.047	0.134	0.128
	Low	(L/12)	0.980	0.165	0.168
Hachinohe	High	(L/12)	0.995	0.095	0.096
		(L/10)	1.026	0.209	0.204
	Low	(L/12)	0.927	0.126	0.136
All Earthquakes	All Frames		1.060	0.137	0.129
	Avg.+ 1 standard deviation			1.197	
	Avg.+ 2 standard deviation (γ_f)			1.334	

Table 4.1 Relationship for SDR between Nonlinear and Linear Analysis

Earthquake	Nonlinear SDR / Linear SDR	average	one standard deviation	coeficient of variation (%)
Castaic	Mag. / Mag.	1.41	0.38	0.27
	Loc. / Loc.	1.30	1.07	0.83
Tarzana	Mag. / Mag.	1.64	0.64	0.39
	Loc. / Loc.	1.52	0.94	0.62
Llolleo	Mag. / Mag.	1.18	0.22	0.19
	Loc. / Loc.	1.41	0.89	0.63
ElCentro	Mag. / Mag.	1.57	0.42	0.26
	Loc. / Loc.	1.50	0.90	0.60
Kobe	Mag. / Mag.	1.24	0.32	0.26
	Loc. / Loc.	1.14	0.81	0.71
Taft	Mag. / Mag.	1.33	0.24	0.18
	Loc. / Loc.	1.78	1.05	0.59
Seattle	Mag. / Mag.	1.40	0.70	0.50
	Loc. / Loc.	0.98	0.61	0.62
Sendai	Mag. / Mag.	1.42	0.66	0.46
	Loc. / Loc.	1.12	0.85	0.75
Santa Barbara	Mag. / Mag.	1.53	0.72	0.47
	Loc. / Loc.	1.22	0.67	0.55
Hachinohe	Mag. / Mag.	1.85	0.75	0.41
	Loc. / Loc.	1.37	0.80	0.59
All Earthquakes	Mag. / Mag.	1.46	0.51	0.35
	Avg.+ 1 standard deviation		1.962	
	Avg.+ 2 standard deviation		2.467	
	Loc. / Loc.	1.34	0.86	0.64
	Avg.+ 1 standard deviation		2.195	
	Avg.+ 2 standard deviation		3.054	
All minus SEN, SAB, & HAC	Mag. / Mag.	1.40	0.42	0.30
	Avg.+ 1 standard deviation		1.813	
	Avg.+ 2 standard deviation		2.230	
	Loc. / Loc.	1.38	0.90	0.65
	Avg.+ 1 standard deviation		2.272	
	Avg.+ 2 standard deviation		3.167	

Table 5.1 Average Percent Difference (%) for Each Method

Earthquake	Warden	Iwan		Lepage
		Girder	Column	
Castaic	15.51	24.09	23.67	25.77
Tarzana	16.28	38.52	29.32	41.48
Llolleo	11.10	19.63	26.35	24.93
ElCentro	10.92	32.70	26.84	39.54
Kobe	11.23	33.52	31.16	29.32
Taft	12.27	30.51	23.41	24.31
Seattle	12.53	63.45	83.14	65.85
Sendai	14.12	35.86	36.60	37.27
Santa Barbara	11.01	40.90	39.76	55.49
Hachinohe	18.81	38.32	46.86	60.83
Average	13.38	35.75	36.71	40.48
Standard Deviation	2.58	11.16	17.04	14.63

FIGURES

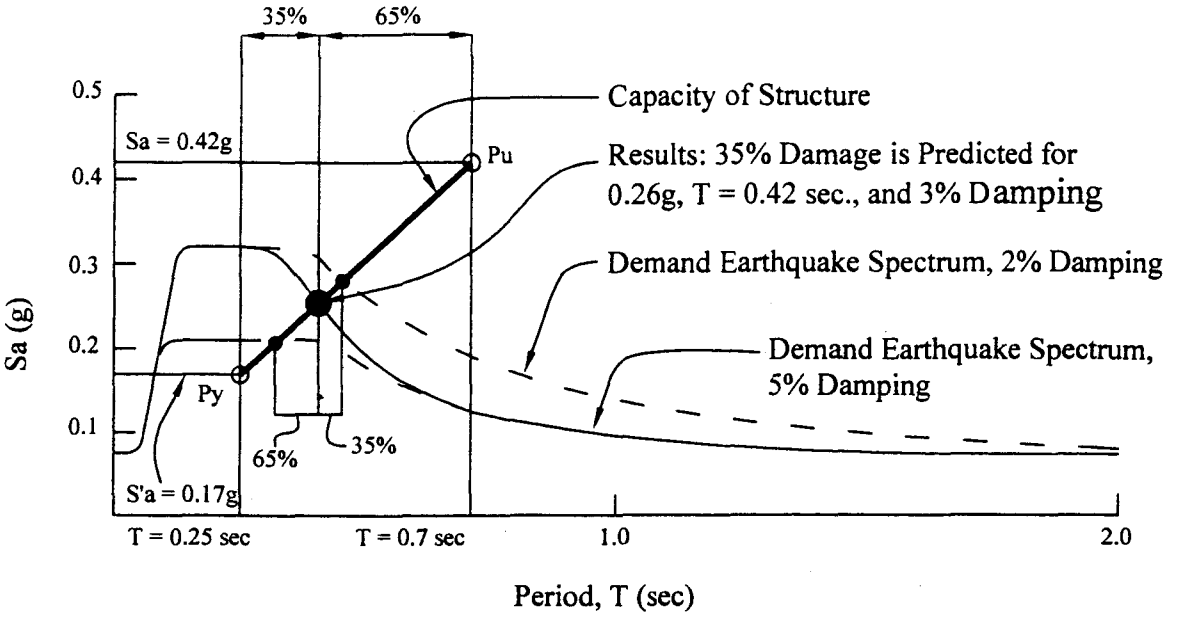

Py = Yield Limit (Initial Yield Capacity of the Structure)
S'a = The Acceleration Corresponding to the Yield Limit
Pu = Ultimate Limit (Ultimate Capacity of the Structure)
Sa = The Acceleration Corresponding to the Ultimate Limit

Fig 1.1 Capacity Spectrum Method Proposed by Freeman (1979)

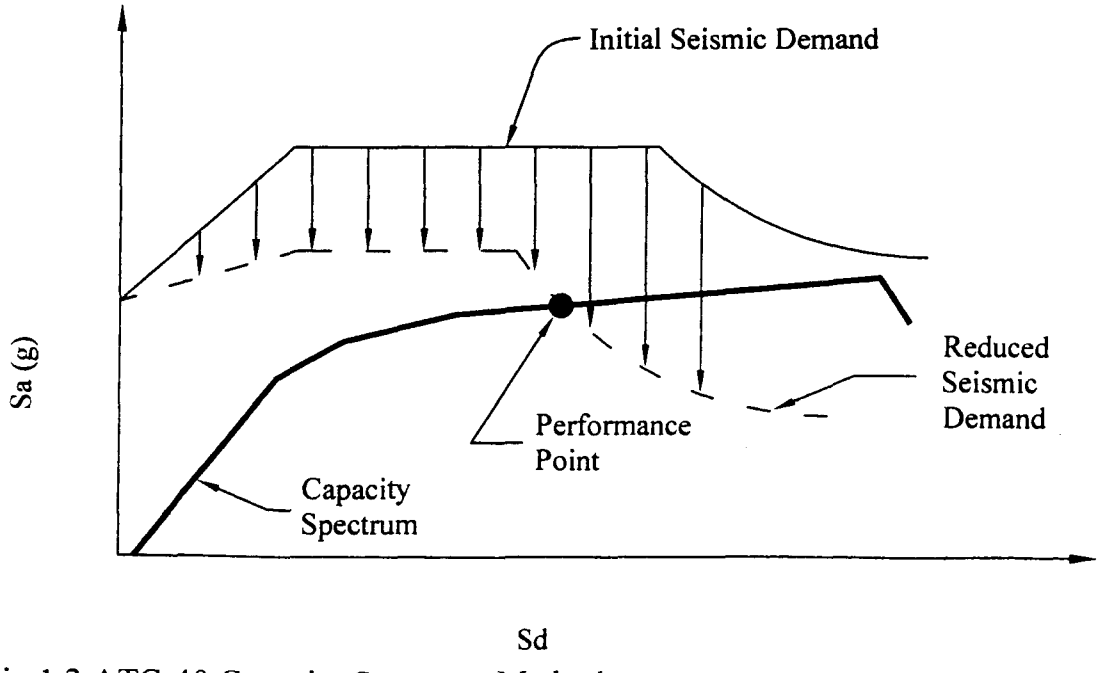

Fig 1.2 ATC-40 Capacity Spectrum Method

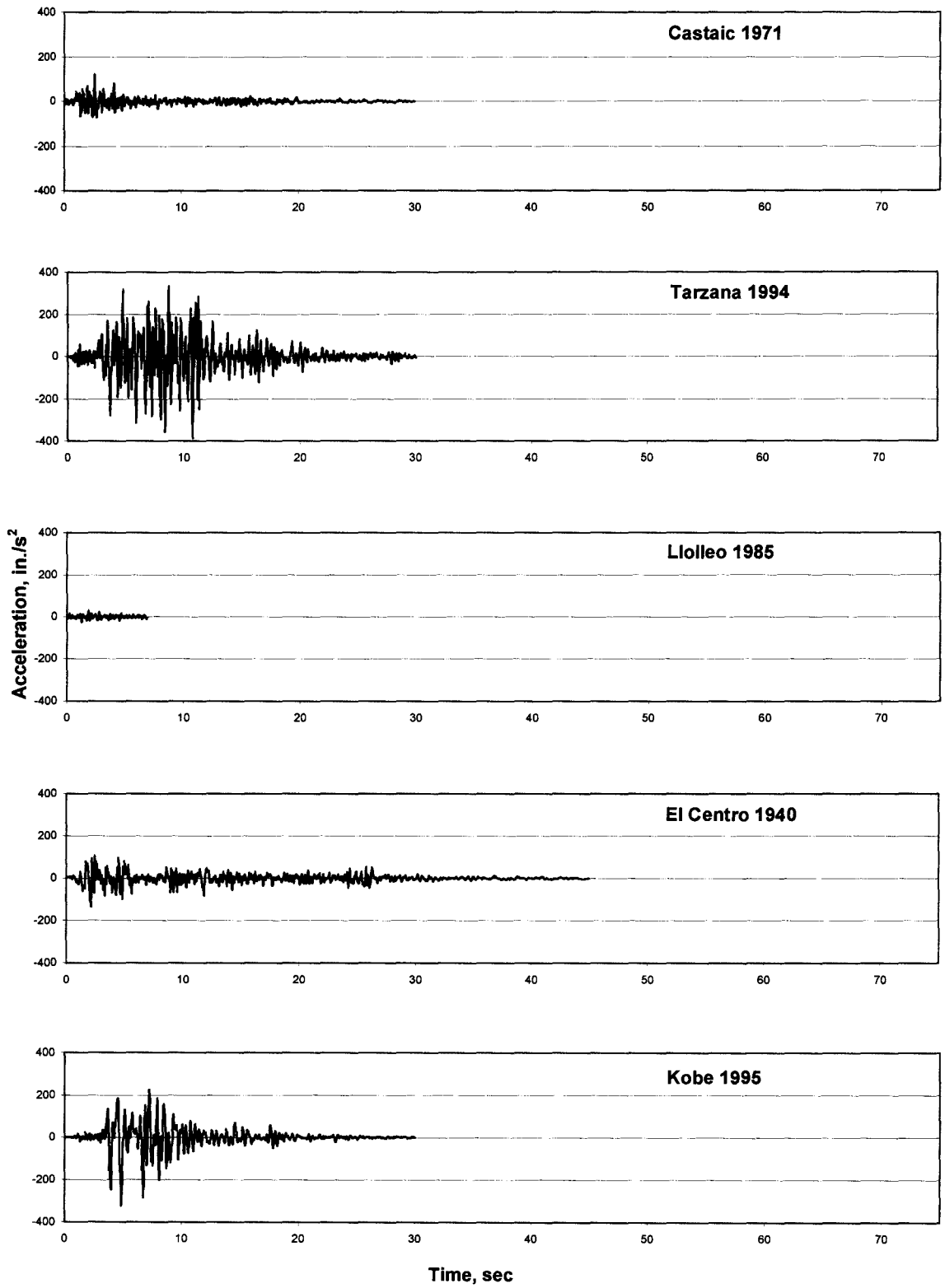

Figure 2.1 Ground Motions Used in Analysis